

Garcia Center for Polymers at Engineered Interfaces



AT STONY BROOK UNIVERSITY



Summer 2017

“The program has no set time limits. Research is a lifelong experience and we hope to remain a resource to our students long after ‘graduation’ ”



The Garcia Center for Polymers at Engineered Interfaces was founded in 1996 and is named after the late Queens College professor Narciso Garcia, who was a pioneer in the integration of education and research. The Center focuses on the integration of materials research with tissue engineering, biomaterials, drug delivery systems, sustainable energy, nanocomposites, and recently, additive manufacturing. The Center also supports innovation through entrepreneurship and has multiple collaborations with industry and national laboratories, both in the US and abroad. For information on the numerous programs that are available please see our website at: <http://polymer.matscieng.stonybrook.edu>



The research scholar program offers the opportunity for high school teachers and students to perform research on the forefront of polymer science and technology together with the Garcia faculty and staff. Students work as part of focus research teams and are taught to make original contributions of interest to the scientific community. In addition to entering national competitions, the students are encouraged to publish in refereed scientific journals, present their results at national conferences, and develop patents to protect their intellectual property. Our goal is to convey to the students the excitement we enjoy daily in research and provide for them a supportive network within the scientific community. Research is a lifelong experience and we hope to remain a resource to our students long after “graduation”.

Miriam Rafailovich Jonathan Schulz
8/8/2017





Garcia: Polymers at Engineered Interfaces-2017 Summer Scholar Program Schedule of Activities




EVERY DAY STARTS WITH A GROUP MEETING

CHECK SCHEDULE DAILY!

	MONDAY	TUESDAY	WEDNESDAY	THURSDAY	FRIDAY
	6/26	6/27	6/28	6/29	6/30
Week of 6/26	<p>10:00am -10:30 Intro to Garcia Miriam Rafailovich</p> <p>10:30-11:15 Madeline Augustine, BOEING</p> <p>11:30am-1:30pm ID cards at SAC and lunch at East Side Dining</p> <p>1:30pm-2:15pm Jacob Trevino, CUNY Nanocenter</p> <p>2:15pm-3:00pm Jessica Rouge, University of Connecticut</p> <p>3:00pm-3:45pm Gordon Taylor, SOMAS, SBU</p>	<p>10:00am General meeting</p> <p>10:30am Mandatory Lab Safety Training w/ EH&S</p> <p>12:45pm-1:45pm Lunch</p> <p>1:45pm-4:00pm Facilities Tour: AFM - Zhenhua Yang FTIR - Harry Shan He LB trough - Yuchen Zhou 3D printer - Yuval Shmueli Cell Lab - Kuan-Che Feng Rheology - Clement Marmorat Electrospinning - Kao LI, Ya-chen Chuang Fuel cells - Likun Wang Hands on safety training specific to Garcia labs - Linxi Zhang Tensile - Xianghao Zuo Brands ender - Yuan Xue IZOD - Yichen Guo Spinner/ Oven Ellipsometer - Jonathan Sokolov Confocal microscope - Vincent Ricotta UV vis and DLS - Fan Yang</p>	<p>10:00am Welcome to Garcia Dr. Fotis Sotiropoulos, Dean CEAS 10:15-10:25 General organizational meeting</p> <p>10:30am-12:30pm Library Resources and Intro to Excel Courses (2 Groups)</p> <p>12:30pm-1:30pm Lunch</p> <p>1:30pm-2:15pm Lab Safety and Facilities Quiz</p> <p>2:15pm-3:00pm Amy Marshilok Battery Technology - Stony Brook University</p> <p>3:00pm-3:45pm Ping Liu, DFT Calculations modeling catalytic processes - BNL</p>	<p>10:00am General meeting DOIT Counselors to help with SOLAR/NetID questions</p> <p>10:15am-11:00am Chang Yon Nam - BNL Hydrogen Fuel Cells</p> <p>11:00am-11:45am Dr. Steven Schwarz - Department of Physics, Queens College</p> <p>11:45am-12:45pm Lunch</p> <p>12:45pm-1:30pm Dennis Galanakis, MD The story of Blood Stony Brook University</p> <p>1:30pm-2:30pm Jonathan Sokolov - Stony Brook University; DNA</p> <p>2:30pm-4:00pm Ms. Rebecca Isseroff, Lawrence HS Science Research Coordinator (i) Magic of Graphene (ii) Keeping a Laboratory Notebook</p>	<p>10:00am General meeting</p> <p>10:05am Greg Filiano- Media relations</p> <p>10:30am-11:30am Michael Hadjiargyrou - NYIT</p> <p>11:30 Bloodborne Pathogen safety training course</p> <p>12:00-12:40 PIZZA (Hunkis) Herb Weiss/ISEF Ethics regulations</p> <p>12:40pm-2:00pm Graduate students presentations--research projects</p> <p>John Mikhails Clement Marmorat Linxi Zhang Kuan-Che Yuchen Zhou Yichen Guo Shan He</p>

<p>Week of 7/3</p> <p>HOMEWORK for 7/3</p> <p>Prepare ppt for journal club.</p> <p>a. Choose a research paper of interest to you.</p> <p>b. Prepare a 5 minute Power Point presentation summarizing the paper.</p> <p>Slides:</p> <ol style="list-style-type: none"> 1. your name, school, title of paper, reference 2. Hypothesis 3. Materials/Methods 4. Results and Discussion 5. Conclusion and evaluation 	<p>7/3</p> <p>10:00-10:15 am General Meeting</p> <p>Devinder Mahajan: Energy Policy</p> <p>10:15am-12:30pm Divide into groups for Journal Club Student Presentations</p> <p>12:30pm-1:30 pm Lunch</p> <p>1:30pm-2:00 pm Garry Halada - Nano scale characterization</p> <p>2:00-2:30 PM Steve Walker: Microbiology</p> <p>2:30-3:15 PM Marcia Simon: Biology of cells on surfaces/projects</p> <p>REMEMBER: appropriate laboratory dress on Wednesday</p>	<p>7/4</p> <p>Happy 4th of July</p> 	<p>7/5</p> <p>10:00am General Meeting</p> <p>Statistics part I Dr. Miriam Rafailovich</p> <p><u>Distribution of boxes</u></p> <p>10:15 -4:00 Group Experiment: Polymer Thin Film Processing:</p> <p>Recycling, Rheology, Determination of Mw Si Single Xtals Lab Data Analysis</p> <p>Dr. Jonathan Sokolov The ellipsometer: coherent and incoherent light--a hands on experience</p> <p>Proper Laboratory Attire</p>	<p>7/6</p> <p>10:00am General Meeting</p> <p>Data Analysis and Statistics Part II Dr. Miriam Rafailovich</p> <p>10:15 am-3:00pm Group Experiment Cont: Polymer Thin Film Processing:</p> <p>Recycling Rheology Determination of Mw Si Single Xtals Lab Data Analysis</p> <p>Dr. Jonathan Sokolov The ellipsometer: coherent and incoherent light--a hands on experience</p> <p>3:00pm-4:00pm Preparation of group ppt and lab reports.</p> <p>Proper Laboratory Attire</p>	<p>7/7</p> <p>10:00am General meeting</p> <p>10:15 PPT presentations by the 7 spin casting groups</p> <p>11:30pm Pizza Lunch</p> <p>11:30-2:00 Graduate student talks and selection of projects</p> <p>Likun Wang Yuval Shmueli Yuan Xue Vincent Ricotta Harry Shan He</p>
<p>Week of 7/10</p> <p>Homework</p> <p>Each student must submit a lab report by Midnight on Monday Morning.</p> <p>Remember to give proper acknowledgements</p>	<p>7/10</p> <p>10:00am General meeting</p> <p>10:20-11:00 Gabor Balazsi- Laufer Center</p> <p>11:00am-11:40 am Dilip Gersappe -Theory and modelling</p> <p>11:40am-12:20 pm Adriana Pinkas-Sarafova -</p>	<p>7/11</p> <p>10:00am General meeting</p> <p>10:10-10:20 Oren Rotman: Heart valve technology</p> <p>10:30 How to write your SOP (Dr. Ying Liu and EH&S staff)</p> <p>11:00am Discussion of research topics</p>	<p>7/12</p> <p>10:00am General meeting</p> <p>10:15 am WORK!</p> <p>12:30pm Lunch</p> <p>1:30pm WORK!</p> <p>Trip to City College Nanocenter meet at 10:00</p>	<p>7/13</p> <p>10:00am General meeting</p> <p>10:30am WORK!</p> <p>12:30pm Lunch</p> <p>1:30pm WORK!</p>	<p>7/14</p> <p>10:00-10:30 am: Prof. Brooke Ellison Broader Impact of Engineering Ethics</p> <p>General meeting</p> <p>10:30 Group Meeting: research updates</p> <ol style="list-style-type: none"> 1. Rose Hong: Update on cells in shear 2. Yuval's group: Nanocomposite <p>11:30 pm</p>

<p>to your group partners, REUs, Grads.</p>	<p>Dental Pulp Stem Cells</p> <p>12:20-1:20 pm Lunch</p> <p>1:20 pm-4:00pm Discussion of research topics</p> <p>Selection of Projects</p>	<p>12:30pm-1:30pm Lunch</p> <p>1:00pm Continue Discussion of research topics</p> <p>Submission of SOPs with student signatures Official date for ISEF/Regeneration project paper work</p> 	<p>promptly</p> <p>Proper Laboratory Attire</p>	 <p>4:00 Softball game</p> <p>Meet in room 145 and we will walk to baseball fields. Dr. Jerome-Manager</p>	<p>BBQ--Veggie grill selections available</p> <p>2:00pm End of Day</p> <p>BBQ: Rain or shine</p>  <p>Proper Laboratory Attire</p>
<p>Week of 7/24</p>	<p>7/24</p> <p>10:00am General meeting</p> <p>10:30am WORK!</p> <p>12:30pm Lunch</p> <p>1:30pm WORK!</p> <p>Proper Laboratory Attire</p>	<p>7/25</p> <p>10:00am General meeting</p> <p>12:00pm Vanderbilt museum</p> 	<p>7/26</p> <p>10:00am General meeting</p> <p>10:30am WORK!</p> <p>12:30pm Lunch</p> <p>1:30pm WORK!</p> <p>3:30pm liquid nitrogen Ice Cream and student presentations</p> <p>Proper Laboratory Attire</p>	<p>7/27</p> <p>10:00am General meeting</p> <p>10:30am WORK!</p> <p>12:30pm Lunch</p> <p>1:30pm WORK!</p> <p>Proper Laboratory Attire</p>	<p>7/28</p> <p>10:00am General meeting</p> <p>12:30pm Pizza Lunch</p> <p>2:00pm End of Day</p> <p>Proper Laboratory Attire</p>

<p>July 30th BNL trip: NSLS II</p> <p>Week of 7/31</p>	<p>7/31</p> <p>10:00am General meeting</p> <p>10:30am WORK!</p> <p>12:30pm Lunch</p> <p>1:30pm WORK!</p> <p>3:30pm Ice Cream and Student Presentations</p> <p>Proper Laboratory Attire</p>	<p>8/1</p> <p>10:00am General meeting</p> <p>10:30am WORK!</p> <p>12:30pm Lunch</p> <p>1:30pm WORK!</p> <p>3:30pm Ice Cream and Student Presentations</p> <p>Proper Laboratory Attire</p>	<p>8/2</p> <p>10:00am General meeting</p> <p>10:30am WORK!</p> <p>12:30pm Lunch</p> <p>1:30pm WORK!</p> <p>3:30pm Ice Cream and Student Presentations</p> <p>Proper Laboratory Attire</p>	<p>8/3</p> <p>10:00am General meeting: Adriana Sarafova: Performing RT/PCR</p> <p>10:30am WORK!</p> <p>12:30pm Lunch</p> <p>5:00 Student presentations</p> <p>5:45 Buses to PJ marina</p> <p>6:30-8:30 Dinner and Fishing cruise</p> 	<p>8/4</p> <p>11:00am General meeting Abstract preparation instructions Student Presentations</p> <p>12:30pm Pizza Lunch</p> <p>2:00pm End of Day</p> <p>Proper Laboratory Attire</p>
<p>Week of 8/7</p> <p>Abstracts due at 5 PM on Sunday 8/6</p>	<p>8/7</p> <p>10:00am General meeting: Science moment by Dr. Young Soo-Seo</p> <p>Abstract review Student presentations: All remaining presentations</p> <p>10:30am WORK!</p> <p>12:30pm Lunch</p> <p>1:30pm WORK!</p> <p>Proper Laboratory Attire</p>	<p>8/8</p> <p>10:00am General meeting</p> <p>10:30am WORK!</p> <p>12:30pm Lunch</p> <p>1:30pm WORK!</p> <p>REUs: FINAL PROGRAM DUE AT 8:00 PM</p> <p>Proper Laboratory Attire</p>	<p>8/9</p> <p>Garcia Program Symposium</p> <p>SAC Ballroom A Stony Brook Wing Wan of West Hempstead Catering Musical production, Dr. John Luckner Jerome, conductor</p> <p>9:30 am - 2:00 pm</p> 		 <p>Keep in Touch—you're now part of the Garcia Family!!</p>

Faculty Mentors



Adriana Pinkas-Sarafova



Gabor Balaszi



Marcia Simon



Dennis Galanakis



Stephen Walker



Dilip Gersappe



John Luckner



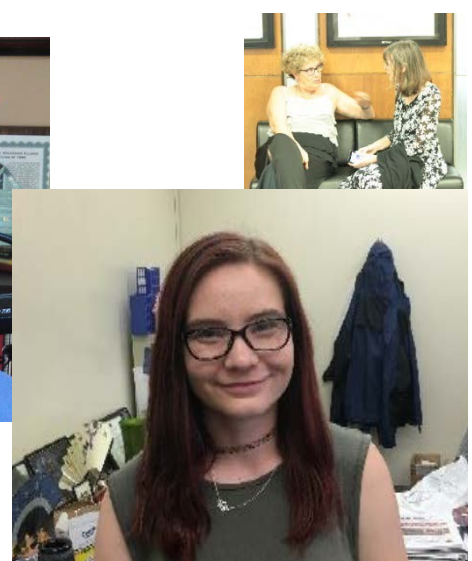
Jerome Jacob Trevino



Maria Rodriguez and Katherine Vorvolakos



Brooke Ellison

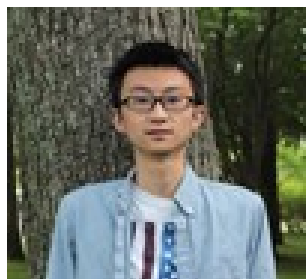


Zoe Auletta

Graduate and Post-Graduate Students



Kuan-Che Feng



Juyi Li



Zhenhua Yang



Harry Shan He



Linxi Zhang



Yichen Guo



Fan Yang



Kao Li



Yuan Xue



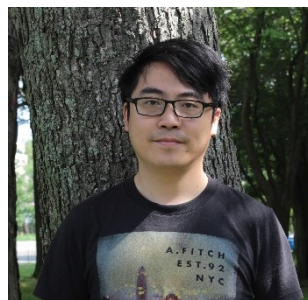
Vincent Ricotta



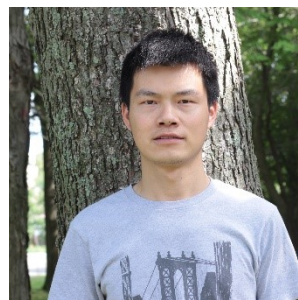
Ya-Chen Chuang



Yuval Shmueli



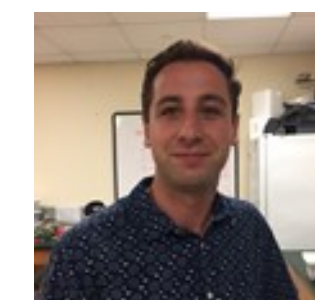
Yuchen Zhou



Likun Wang



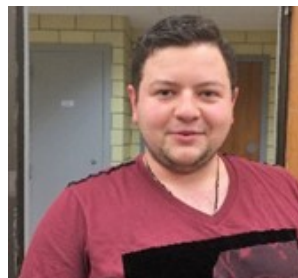
Donald Liu



Clement Marmorat



Carmen Hung



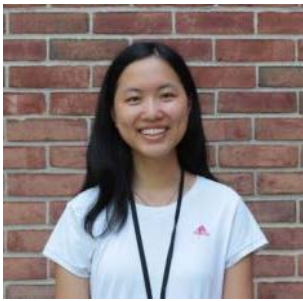
Vladimir Morareu



Joshua Weinstein



Research Experience for Undergraduates (I)



Grace Hu



Karena Etwaru



Carolyn Wong



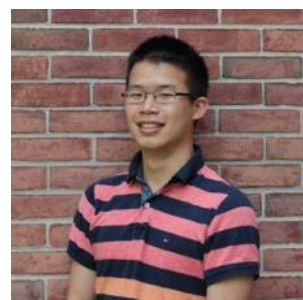
Anyerlin Mora



Allen Green



Indeeep Singh



Bill Chen



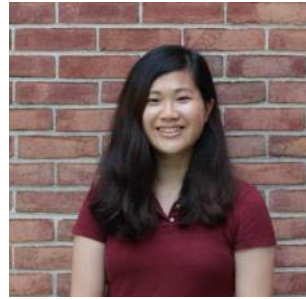
Sam Plaut



Levy Sominsky



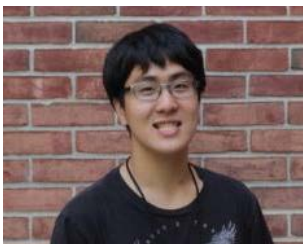
Marci Gottlieb



Christy Siu



Simon Lin



Jeremy Wang



Shamilah Faria

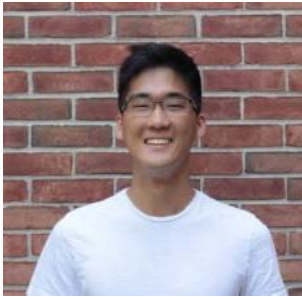


Nathan Sandler



Oliver Xu

Research Experience for Undergraduates (II)



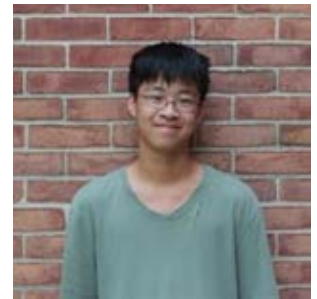
Luke Shin



Tianai Ye



Maira Khan



Peyrin Kao



Rahat Ullah



Research Experience for Teachers



Rebecca Isseroff
Lawrence HS



Herbert Weiss
Southside HS

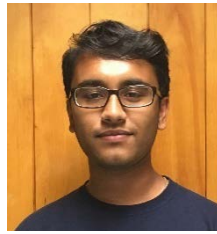


Michael Vaccariello
Sachem HS East

High School Students



Adavi, Anirudh



Akhter, Atif



Angoura, Konstantina



Appel, Natan



Chavre, Bharvi



Chen, Justin



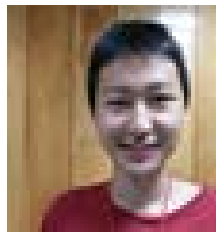
Chen, John



Chen, Kenneth



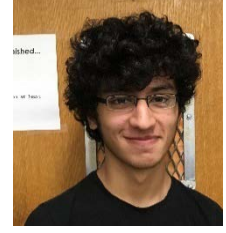
Chen Sophia



Chen, Thomas



Dave, Nupur



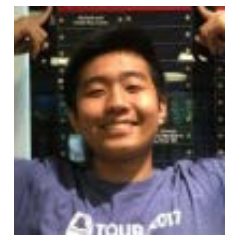
Del Valle, Anthony



Dhinojwala, Maria



Edsparr, Isabella

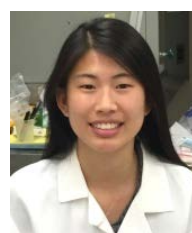


Franqueiro, Angelina

Gao, Kevin



Guha, Anoushka



Hong, Rose



Hou, Karly



Howell, Thomas



Hsu, Ian



Johnston, Emma



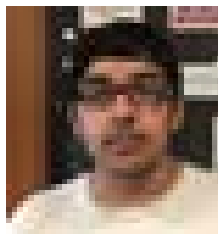
Kao, Michael



Katz, Zachary



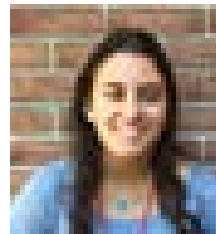
Kelly, Danielle



Khan, Zaiff



Kurlander, Jason



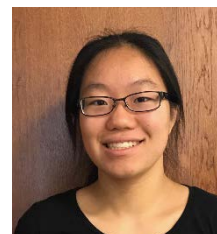
Laks, Yael



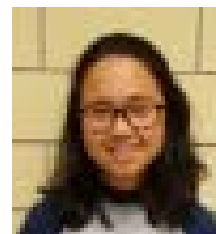
Li, Jack



Li, Jarrad



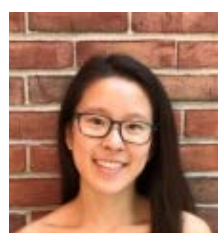
Li, Rachel



Liu, Yingyue



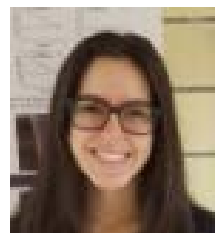
Liu, Yuqing



Lo, Savannah



Lu, Ruoxin



Luntz, Danielle



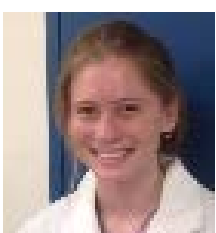
Ma, Jiaming
(Maggie)



Ma, Zifan
(Emily)



Martinez, Pastor



Milan, Siobhan



Patel, Rushikesh



Pedley, Taylor



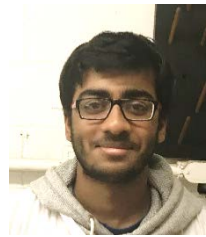
Pennisi, John



Porter, Max



Rao, Kavya



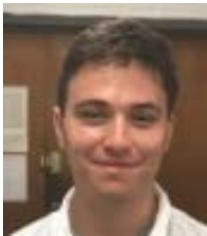
Reddy, Roshan



Reguyal, Sabrina



Reyes, Jerry



Rizzo, Daniel



Rulin, Yin



Sahith, Vadada



Schneider, Gemma



Seligson, Daniel



Shen, Ke



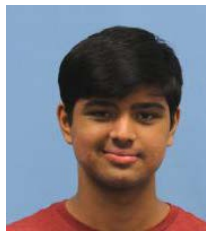
Shine, Audrey



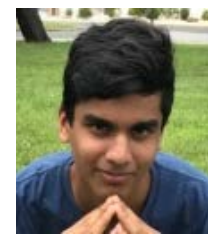
Shtilianova, Mariya



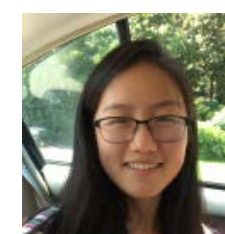
Singer, Aaron



Singh, Vedant



Soni, Neal



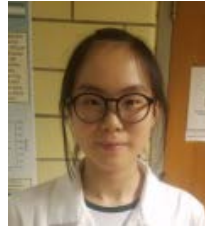
Sui, Margaret



Sullivan, Leeba



Sutaria, Jainil



Tang, Jinghan (Effy)



Than, Luigia



Tian, Albert



Waitman, Dana



Wang, Alexander



Wang, Andrew



Wang, Chelsea



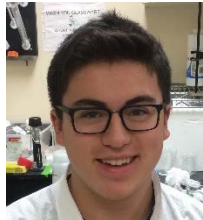
Wang, Emily



Wang, Michael



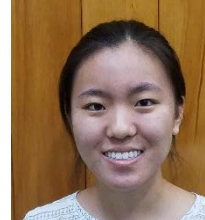
Waquar, Kasim



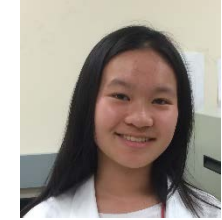
Weiss, Brandon



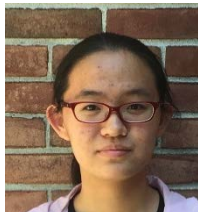
Williams, Nicholas



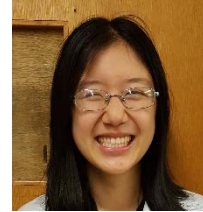
Yang, Eunice



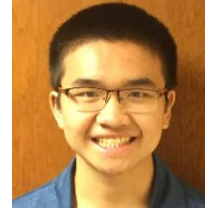
Ye Angela



Yu, Feiyang



Zhang, Helen



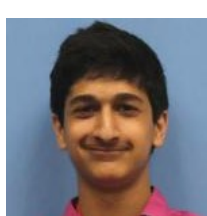
Zhu, Richard



Zumba, Nicholas



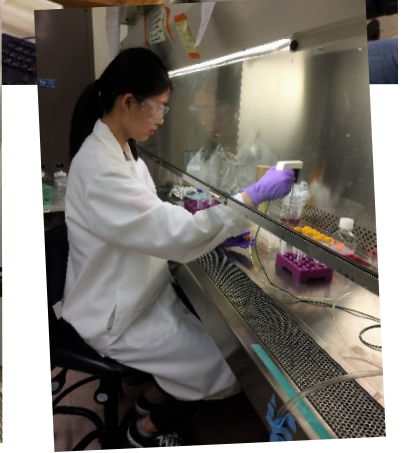
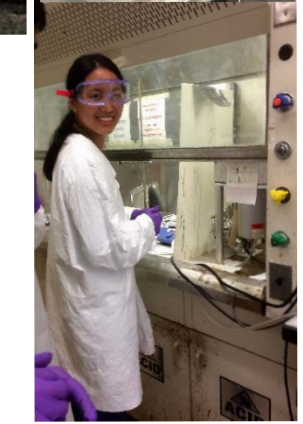
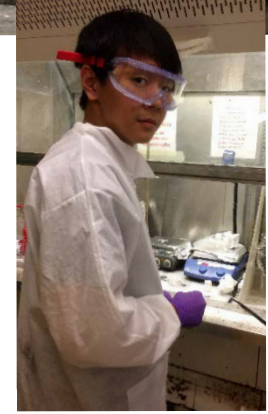
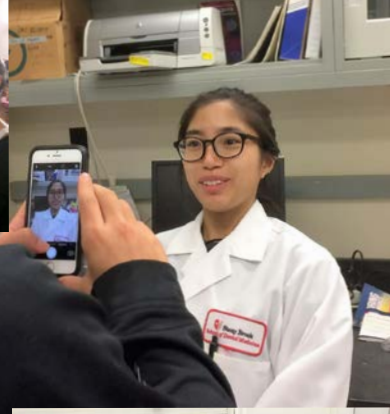
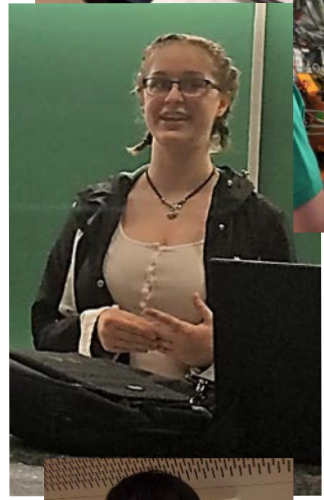
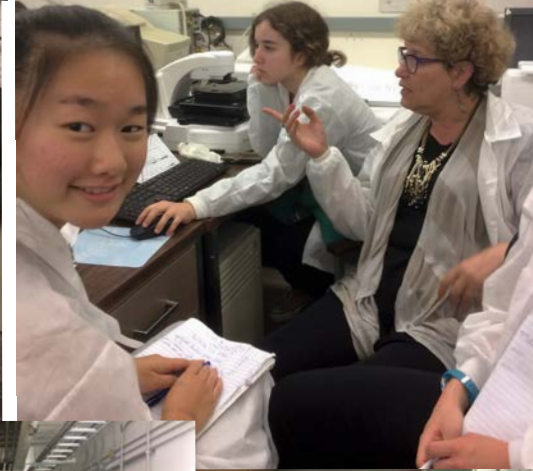
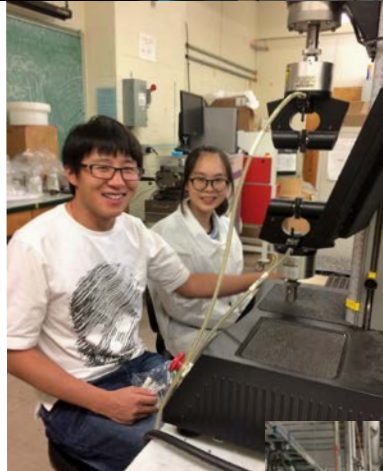
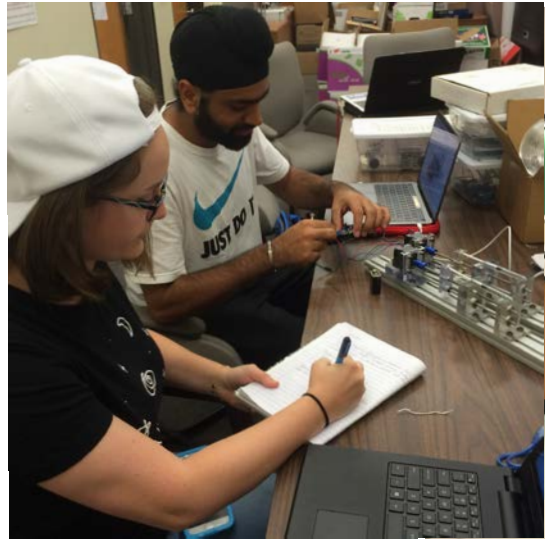
Panday, Abishrant

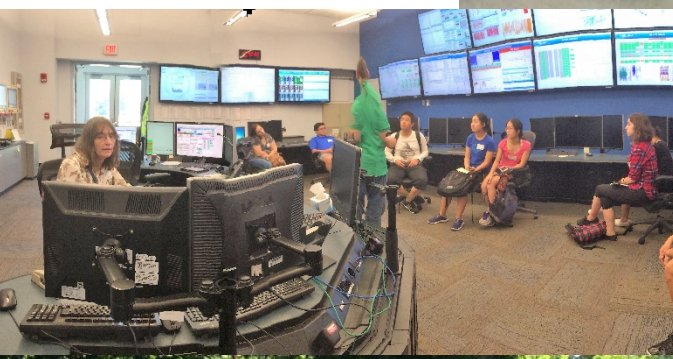


Wadhwa, Varun



Julia, Pandolfo

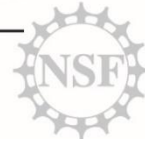




Garcia Center for Polymers at Engineered Interfaces



AT STONY BROOK UNIVERSITY



*The students of the Garcia Research Scholar Program
cordially invite you to attend
The Annual Summer Research Symposium and Luncheon
Wednesday, August 9th, 2017,*

9:30am — 2:00pm

Student Activities Center, Ballroom A

Opening Address: Dr. Elaine DiMasi, Physicist

Musical Arrangement by Garcia Students

conducted by Dr. John Luckner Jerome

Student Research Presentations

Sponsored in part by the National Science Foundation and the

Morin Foundation Trust

catered by Wing Wan of West Hempstead

Garcia Center for Polymers at Engineered Interfaces

Summer 2017 Student Research Symposium-1



AT STONY BROOK UNIVERSITY



Wednesday, August 9, 2017 SAC Ballroom A

9:30 Light Breakfast and Musical Arrangement by the Garcia Student Musicians,
Dr. John Luckner Jerome, conductor

9:45 Guest Speaker: **Dr. Elaine DiMasi**

10:00 Student Research Symposium

10:00-10:30 Session 1: **Energy Generation and Storage**

10:00 - 10:15 A. Photovoltaics and Batteries

Chairs: **Shamila Faria** and **Tianai Ye**, *Stony Brook University, Stony Brook, NY*, **Luke Shin**, *Cornell University, Ithaca, NY*

Enhancing Inorganic-Organic Lead Halide Perovskite Solar Cell Efficiency via Polymer-Templated Nucleation and Stabilizing Additives

Michael Kao, *Troy High School, Fullerton CA*, **Jack Li** *St. George's School, Vancouver, Canada*,
Neal Soni, *Staples High School, Westport CT*, **Ke Shen**, *Sunset High School, Portland OR*, **Andy Wang**, *Clark High School, Las Vegas ND*, **Varun Wadhwa**, *Rye Country Day High School, Rye NY*

Optimizing the Morphology of the P3HT:PCBM Polymer Solar Cell Active Layer Using PEG and PMMA as Additives

Abishrant Panday and **Sabrina Reguyal**, *Hunter College High School, New York, NY*

Optimization of Polymer Solar Cells' Efficiency Using Molecular Dynamics simulation

Ruilin Yin, *Saint Anthony's High School, South Huntington, NY*, **Karly Hou**, *Henry M. Gunn High School, Palo Alto, CA*
Isabella Edsparr, *James Allen's Girls' School, 144 East Dulwich Grove, London, United Kingdom*

Lattice Boltzmann Modeling of the Prevention of Dendrite Formation in Lithium-Ion Batteries

Feiyang Yu, *Shenzhen Middle School, Shenzhen, Guangdong, PRC* **Luigia Than**, *Earl L. Vandermeulen High School, Port Jefferson, NY*

10:15 - 10:30 B. Hydrogen as a Fuel

Chairs: **Peyrin Kao**, *University of California, Berkeley, Berkeley, CA*, **Samuel Plaut**, *SUNY Binghamton, Binghamton, NY*, **Allen Green**, *Brown University, Providence, RI*,

Effects of Incorporating Graphene Oxide into Nafion on a Polymer Electrolyte Membrane Fuel Cell

Jerry Reyes and **Daniel Rizzo**, *Lawrence High School, Cedarhurst, NY*

Optimizing Molar Ratios of Au-Ag Alloy Nanoparticles to Enhance the Performance of PEM Fuel Cells

Jarrad Li, *Syosset High School, Syosset, NY*, **Ruoxin Lu**, *Plainview-Old Bethpage John F. Kennedy High School, Plainview, NY*, **Helen Zhang**, *General Douglas MacArthur High School, Levittown, NY*

Summer 2017 Student Research Symposium-2

Application of Graphene Oxide onto Polymer Electrolyte Membranes (PEM) and Electrodes to Optimize Hydrogen Fuel Cell Performance

Danielle Kelly, *Friends Academy, Locust Valley, NY*, **Audrey Shine**, *Plainview Old-Bethpage JFK High School, Plainview, NY*, **Mariya Shtilyanova**, *Concord-Carlisle High School, 500 Walden St, Concord MA*

Utilizing ALD-Coated Titanium Dioxide on Nafion Membrane to Increase Efficiency of Proton Exchange Membrane Fuel Cells

Angela Ye *Basis Independent Silicon Valley, San Jose, CA*, **Kenneth Chan** *Island Trees High School, Levittown, NY*, **Pastor Martinez**, *Brentwood High School, Brentwood, NY*

10:30- 11:05 Session II: Scaffolds for Tissue Engineering

10:30 - 10:50 A. Engineering 3-D Constructs

Chairs: **William Chen**, *Columbia University, New York, NY*, **Carolyn Wang**, *Harvard University, Cambridge, MA*, **Grace Hu**, *Stanford University, Stanford, CA*

Effects of Mechanical Stress Generated by Laminar Fluid Flow and Rapid Environmental Viscosity Transitions on Human Dermal Fibroblast, Dental Pulp Stem Cell, and Squamous Cell Carcinoma Suspensions Sheared in Polyethylene Glycol Solutions

Rose Hong, *Del Norte High School, San Diego,*

2D vs 3D — The Effect of the Morphology of P4VP Scaffolds on Dental Pulp Stem Cell Differentiation

Jiaming Ma, *The High School Affiliated to Renmin University, International Curriculum Center, Beijing, China*

Evaluating the Effect of Graphene-Loaded Poly(4-vinylpyridine) Electrospun Fibrous Scaffolds and Spun-cast Thin Films on the Proliferation and Differentiation of Dental Pulp Stem Cells

Sahith Vadada, **Rushikesh Patel**, *Herricks High School, New Hyde Park, NY*, **Vedant Singh**, *The Wheatley School, Old Westbury, NY*

Use of Gelatin mTG Crosslinked Gel to Study Mesenchymal Epithelial Interaction in Dentin and Enamel Synthesis

Margaret Sui, *Bethlehem Central High School, 700 Delaware Ave, Delmar, NY*, **Sophia Chen**, *Palm Harbor University High School, Palm Harbor, FL*, **Konstantina Angoura**, *Hellenic-American Educational Foundation Athens College, 15 Stephanou Delta, Street, Athens 154 52, Greece*

Characterizing *In Situ* mTG Crosslinked Gelatin Hydrogels with Encapsulated Dental Pulp Stem Cells for Cell Delivery in Applications of Regenerative Medicine

Jason Kurlander, *North Shore Hebrew Academy High School, Great Neck, NY*, **Yael Laks** and **Leeba Sullivan**, *Yeshiva University High School For Girls, Hollis, NY*

Investigating the Effects of Cell Plating Density and Surface Topography on Dental Pulp Stem Cell Response to 3D-Printed and Molded Scaffolds

Eunice Yang, *Mountain View High School, Mountain View, CA*, **Maria Dhinojwala**, *Archbishop Hoban High School, Akron, OH*, **Ian Hsu**, *Mission San Jose High School, Fremont, CA*

10:50 – 11:05 B: Nanocomposite scaffolds

Chairs: **Oliver Xu**, *UCLA, Los Angeles, CA*, **Simon Lin**, *Stony Brook University, Stony Brook, NY*, **Jeremy Wang**, *Cornell University, Ithaca*

Summer 2017 Student Research Symposium-3

The Influence of Titanium Dioxide Nanoparticles Underlying Polybutadiene on Differentiation Properties of Dental Pulp Stem Cells

Emily Ma and **Zachary Katz**, *Paul D. Schreiber High School, Port Washington, NY*

Utilizing Magnetic Graphene Oxide/Iron Carbonyl thin films to Promote Dental Pulp Stem Cell Differentiation

Anoushka Guha, **John Chen**, and **Zaiff Khan**, *Lawrence High School, Cedarhurst, NY 11581*, ²State University of New York at Stony Brook, Stony Brook, NY, 11794, ³Department of Material Science and Engineering, State University of New York at Stony Brook, Stony Brook, NY, 11794

Investigating the Differentiation and Proliferation of Human Dental Pulp Stem Cells Regulated by TiO₂ Nanoparticles Added Before and After Substrate Recognition

Richard Zhu *Edina High School, Edina, MN*, **Michael Wang**, *Aragon High School, San Mateo, CA* **Yuqing Liu**, *Texas Academy of Math and Science*

Investigating the Effects of Addition of Resorcinol Bis(Diphenyl Phosphate) and Clay on Capacity of Polystyrene Molds to Facilitate Human Dental Pulp Stem Cell Proliferation and Differentiation

Anirudh Adavi, *DuPont Manual High School, Louisville, KY*, **Nicholas Zumba**, *George W. Hewlett High School, Hewlett, NY*

Assessing the modulus of the cellular and extracellular matrices and the motility of MDA-MB-231, MDA-MB-4175, MCF-7, and MCF-10A normal and cancerous ductal breast cells

Angelina Franqueiro, *Sachem High School North, 212 Smith Rd., Ronkonkoma, NY*, **Gemma Schneider**, *Roslyn High School, 475 Round Hill Rd, Roslyn Heights, NY*, **Siobhan Milan**, *Southside High School, 140 Shepherd St, Rockville Centre, NY*

11:05- 11:15 Session III: Graphene Nanocomposites

Chairs: **Rahat Ulah**, *Stony Brook University, Stony Brook, NY*, **Marc Gottleib**, *Cooper Union, New York*,

Enhancing the Mechanical Properties of Polymers with Graphene Nanocomposites

Danielle Luntz, **Kasim Waqar**, and **Kavya Rao**, *Half Hollow Hills High School East, Dix Hills, NY*

Thermal Conductivity of Nanocomposites in the FDM 3D Printing Process

Justin Chen, *Arcadia High School, Arcadia, CA*, **Thomas Howell**, *Ward Melville High School, East Setauket, NY*
Max Porter *Hollis Brookline High School, Hollis, NH*

Thermal Enhancement of PBAT/Graphene Composites by Applying PLA as Second Phase Controller

Jinghan (Effy) Tang, *Mater Dei High School, Santa Ana, CA*

11: 15-11:30 Session IV: DNA and Proteins on Surfaces

Chairs: **Christy Siu**, *Stony Brook University, Stony Brook, NY*, **Anyerlin Mora**, *Suffolk Community College*, **Nathan Sandler**, *Tufts University, Medford, MA*

Utilizing microwells and microchannels to improve the efficiency of lithographic enzymatic fragmentation of surface-adsorbed DNA for use in Next Generation Sequencing (NGS)

Albert Tian, *Ward Melville High School, NY, 11790*, **Dana Waitman**, *The Frisch School, NJ*, **Aaron Singer**, *Davis Renov Stahler Yeshiva High School for Boys, NY*

Synthesis of a water-soluble thin-film for absorption of DNA and subsequent removal

Anthony Del Valle *Ward Melville High School, New York, 11790*

Summer 2017 Student Research Symposium-4

Investigating the Viability of PCL and xSIBS As Polymers for Heart Valves and Blood Vessels

Emma Johnston, *Harborfields High School, Greenlawn, NY*

Examining the Effect of Varying Surface Chemistries and Its Influence on the Growth of Fibers

Nupur Dave, *John Foster Dulles High School, Sugar Land, TX*, **Yingyue Liu**, *General Douglas MacArthur High School, Levittown, NY*

P12 Peptide's Effects on Inhibiting Fibrinogen Fiber Formation in Blood Coagulation and Application of Machine Learning in Fiber Counting

Thomas Chen *Mission San Jose High School, Fremont, CA*, **Kevin Gao**, *Amador Valley High School, Pleasanton, CA*, **Alexander Wang**, *Dougherty Valley High School, San Ramon, CA*

11:30 - 11:40 V. Hydrogel Materials

Chairs: **Levy Sominsky**, *Vanderbilt University, Nashville, TN*, **Karena Etwaru**, *Cornell University, Ithaca, NY*

Examining the Integrity of Pluronic® F127 for use in Drug Delivery

Atif Akhter, *St. Mary's High School, 51 Clapham Ave, Manhasset, NY*, **Bharvi M. Chavre** and **Brandon Weiss**, *G.W. Hewlett High School, Hewlett, NY 11557*,

The Integration of Graphene Oxide and Reduced Graphene Oxide to Strengthen and Expand Elastic Modulus in F-127 Pluronic Acid Gels

Nicholas Williams, **Roshan Reddy**, *Lawrence High School, Cedarhurst, NY*,

Synthesis and Characterization of Gelatin and Pluronic F127 Hybrid Hydrogels for Cell Barrier Layer Applications

Rachel Li, *Spackenkill High School, New York, NY*, **Jainil Sutaria**, *Ardsley High School, Ardsley, NY*, **Chelsea Wang**, *Fossil Ridge High School, Fort Collins, CO*

11:40 – 12:00 VI. Sensors and Detectors

Chairs: **Maira Kahn**, *Harvard University, Cambridge Mass*, **Indeep Singh**, *Stony Brook University, NY*

Developing a Prototype Home Automation System Using Arduino Microcontrollers

Taylor Pedley, *Smithtown High School East, Saint James, NY*;

Utilizing Natural Patterns from Polymer Blend Phase Separation with Argon Etching to Create Gold Patterned Silicon Wafers

Daniel Seligson, *Ramaz Upper School, New York, NY*, **Emily Wang**, *The Wheatley School, Old Westbury, NY*
Savannah Lo, *South Side High School, Rockville Centre, NY*

Analyzing the Antibacterial Properties of Bismuth Oxyhalides When Exposed to Light¹

Daniel Seligson, *Ramaz Upper School, New York, NY*, **Emily Wang**, *The Wheatley School, Old Westbury, NY*
Savannah Lo, *South Side High School, Rockville Centre, NY*

Optimizing and Testing the specificity and accuracy of a bio sensor

Neil Appel, *Rambam Mesivta, Lawrence, NY, 11559*

Examining the Digestion of Polystyrene by *Tenebrio molitor*

John Pennisi *South Side High School, Rockville Centre, NY 11570*

Engineering Electrospun Microfibers Capable of Trapping Termites

Julia Pandolfo, *South Side High School, Rockville Centre, NY 11570*

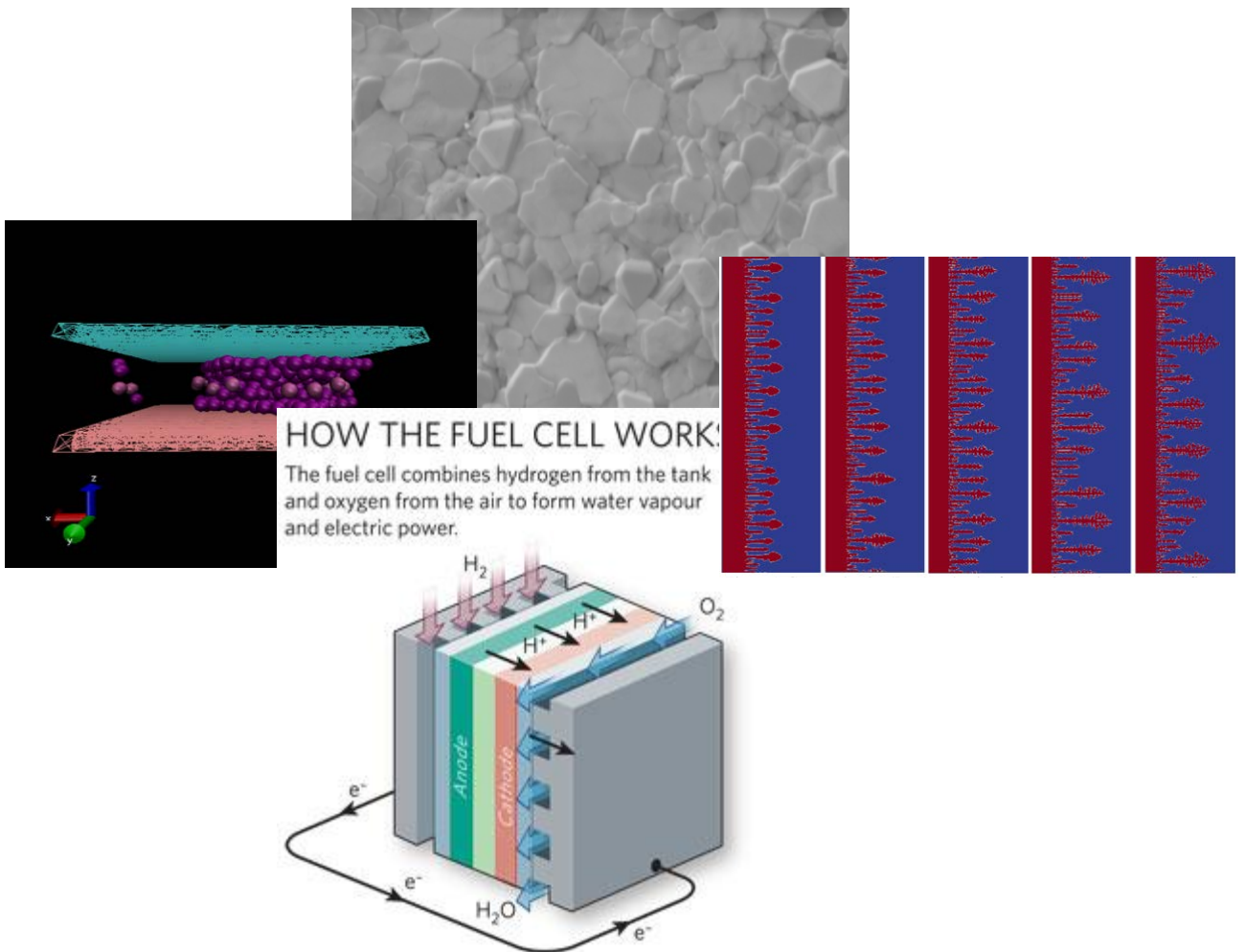
12:00-1:30 Formal Luncheon
Catered by Wing Wan

of West Hempstead



Session I: Energy Generation and Storage

**Graduate Student Mentors:
Likun Wang, Yuchen Zou
Zhenhua Yang**



Enhancing Inorganic–Organic Lead Halide Perovskite Solar Cell Efficiency via Polymer-Templated Nucleation and Stabilizing Additives

Michael Kao¹, Jack Li², Neal Soni³, Ke Shen⁴, Andy Wang⁵, Varun Wadhwa⁶, Yuchen Zhou⁷, Miriam Rafailovich⁷

¹Troy High School, Fullerton CA ²St. George's School, Vancouver, Canada ³Staples High School, Westport CT

⁴Sunset High School, Portland OR ⁵Ed W. Clark High School, Las Vegas ND ⁶Rye Country Day High School, Rye NY

⁷Department of Materials Science and Engineering, Stony Brook University, Stony Brook NY

A dramatic rise in global energy demands has spurred interest in renewable alternatives and the advent of photovoltaics. In particular, perovskite solar cells (PSCs) offer an efficient and cost-effective method of energy generation; PSC power conversion efficiency (PCE) has increased sevenfold in a decade, making them the fastest growing photovoltaic technology to date¹. Limited only by polar solvent degradation and relative instability compared to inorganic multijunction photovoltaics, PSCs are substantially cheaper to fabricate². Perovskite hybrid solar cells composed of CH₃NH₃PbI₃ (MAPbI₃) [Figure 1] inorganic-organic lead trihalide perovskite films are promising due to high bandgap energies and wide absorption range. Our work attempts to optimize surface morphology and increase perovskite PCE by utilizing polylactic acid (PLA), PCDTBT, and PEG additives chosen to analyze their impacts on PSC performance - PLA's effect on grain size, PCDTBT's effect on photoabsorption and lead passivation, and PEG's ability to retard crystal aggregation and improve stability.

Functional perovskite planar architectures were fabricated with polymer-doped perovskite active layers sandwiched between hole-transporting material Spiro-OMeTAD and electron-transporting material TiO₂ to promote carrier mobility. Layers were spin-coated onto ozone-treated fluorine-doped tin oxide glass substrates and activated via oxygen-doping in a desiccator. All devices were tested for efficiency and MAPbI₃ thin-film morphology was analyzed for surface quality. Scanning electron microscopy (SEM) was conducted to analyze grain size alterations as a function of polymer doping and Weibull distribution curves of grain sizes were subsequently created to statistically analyze morphological changes.

Thermoplastic semi-crystalline PLA was added at 0.1, 0.3, 0.6, and 1.0 mg/mL to aid in crystal formation via polymer-templated nucleation and growth (PTNG). γ -butyrolactone (GBL) and dimethyl sulfoxide (DMSO) solvents mixed at a 7:3 ratio acted as solvents for PLA and added to a spin-coated layer of MAI and PbI₂ precursor solution. SEM surface imaging of the active layer at 20,000x showed a positive correlation between grain size and PLA concentration [Figure 3], though surface defects and pinhole size also increased. UV-VIS spectra absorbance showed a positive relationship between concentration and absorbance. PCDTBT was added at the same concentrations to understand implications using chlorobenzene solvent instead to promote crystal aggregation and uniformity; PCDTBT passivates uncoordinated lead ions

and decrease trap state probability and is thus useful in this process. At lower concentrations (0.1, 0.3 mg/mL), PCDTBT slightly increased grain size but significantly decreased prevalence of grain boundaries. However, it was unable to diffuse into crystals at higher concentrations and was thus left on surface, preventing crystal growth altogether [Figure 4] due to formation of additive clusters disrupting surface uniformity.

Nevertheless, UV-VIS spectra absorbance showed a particularly strong positive relationship between concentration and absorbance. Lastly, PEG was added at different molecular weights (100, 1000, and 4000 kDa) to increase interfacial tension to alter viscosity of perovskite precursor solution to improve crystal growth. PEG was not found to have a significant advantageous effect on grain size or effect grain boundaries.

Ongoing PSC developmental work includes use of perovskite-grade PbI₂ in the active layer, enabling easier dissolution during solution preparation and smoother film morphology. Solution preparation and device fabrication will be performed in an argon gas environment to reduce humidity and the rate of film degradation. X-ray diffraction (XRD) analysis and atomic force microscopy (AFM) tests will be conducted to visualize chemical changes during device degradation and surface topography to further understand morphology. PCE tests will run continuously and molecular dynamics simulations via LAMMPS will be conducted to model perovskite interactions with additives.

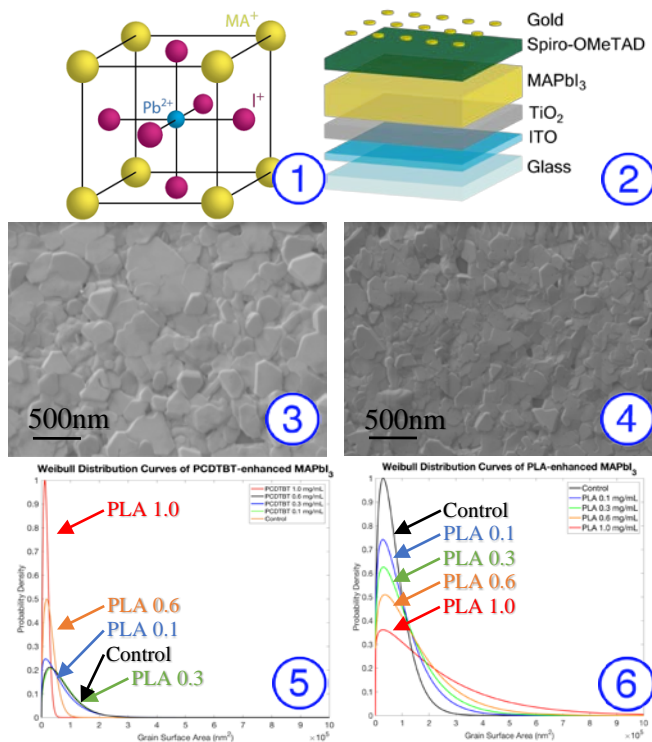


Fig. 1: Perovskite molecule **Fig. 2:** Device Architecture

Fig. 3,4: 1.0 and 0.1 mg/mL PLA SEM Images

Fig. 5,6: PLA/PCDTBT Grain Size Distribution

¹ Miyasaka, T. Perovskite photovoltaics: Rare functions of organo lead halide in solar cells and optoelectronic devices. Chem. Lett. 44, 720–729 (2015).

² Kojima, A., Teshima, K., Shirai, Y.. Organometal halide perovskites as visible-light sensitizers for photovoltaic cells. J. Am. Chem. Soc. 131, 6050–6051 (2009).

Optimizing the Morphology of the P₃HT:PCBM Polymer Solar Cell Active Layer Using PEG and PMMA as Additives

Abishrant Panday¹, Sabrina Reguyal¹, Zhenhua Yang², and Miriam Rafailovich

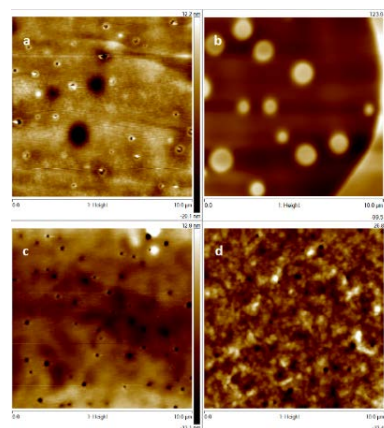
¹Hunter College High School, New York, NY 10128, ²Department of Materials Science, SUNY Stony Brook, Stony Brook, New York 11790

Polymer solar cells are a promising photovoltaic technology with useful and advantageous characteristics such as low cost, optical transparency, ability for manufacture at ambient temperature and pressure using roll-to-roll fabrication techniques, and use in novel applications [1]. The current standard blend for bulk heterojunction (BHJ) solar cells is poly (3-hexylthiophene):1-(3-methoxycarbonyl) propyl-1-phenyl [6, 6] C₆₁ (P₃HT:PCBM) [2].

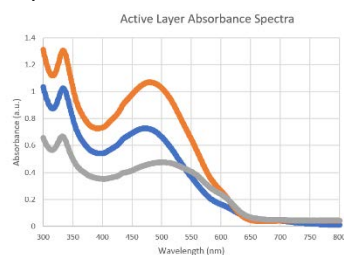
In order to improve the power conversion efficiency (PCE) of BHJ solar cells, the electron-hole recombination rate can be reduced, the absorption window can be broadened, or the energy levels of the polymers can be adjusted. A way to address these problems is to add a third polymer to the active layer blend [3]. In this project, we aimed to improve PCE with enhanced active layer morphology through addition of poly (ethylene glycol) (PEG) and poly (methyl methacrylate) (PMMA).

Initially, PEG of molecular weights 100K and 4,000K were tested as additives, as it was hypothesized that their high crystallinity would allow for them to serve as nucleation sites, thus improving crystal structure, charge transfer performance and hence the PCE. PEG:P₃HT:PCBM solutions were created at 1:20:20 mg/mL ratios and spin cast at 1000 rpm for absorbance and morphology analysis using UV-Vis spectroscopy and atomic force microscopy (AFM), and at .2:20:20 mg/mL ratios for device fabrication and PCE analysis.

As shown in Figure 1, the ternary blends containing PEG at lower molecular weights tended to form rough films with small, shallow valleys, and at higher molecular weights failed to form a cohesive structure. However, UV-Vis results showed that the absorbance of 4000K PEG is significantly greater than that of 100K PEG, which is evident in the PCE data collected for the PEG devices: the PEG(4000K):P₃HT:PCBM blend achieved a PCE of 1.58%, as opposed to the PEG(100K):P₃HT:PCBM, which attained a PCE of 1.14%. However, the P₃HT:PCBM control had a PCE of 1.57%. Therefore, PEG as an additive offers no substantial improvement over the standard active layer blend.



AFM images of (a) PEO:P₃HT:PCBM, (b) PMMA:P₃HT:PCBM, (c) PEG(100K):P₃HT:PCBM, (d) PEG(4000K):P₃HT:PCBM



UV-Vis absorption spectrum of active layers containing PEG (100K, 4000K) and PMMA.

For this reason, we shifted our focus to optimizing the concentration of the PMMA:P₃HT:PCBM active layer blend. As shown in Figure 1, the PMMA additive induces the formation of tall columns on the surface, which significantly reduce the electron-hole recombination rate and have the added benefit of promoting internal reflectance, which increases the external quantum efficiency (EQE). Preliminary tests have returned values of 2.10%, a 33.7% increase from the control.

In the future, we aim to further optimize the morphology of PMMA:P₃HT:PCBM by varying polymer concentrations, calculate the EQE of the devices, and use molecular dynamics to model the columnar structure of the active layer and determine the impact of

light refraction on the PCE.

[1] Søndergaard, R., H'osel, M., Angmo, D., Larsen-Olsen, T., Krebs, F. "Roll-to-roll fabrication of polymer solar cells." *Materials Today*. 15(2), 36-49. [https://doi.org/10.1016/S1369-7021\(12\)70019-6](https://doi.org/10.1016/S1369-7021(12)70019-6)

[2] Dennler, G., Scharber M., Brabec, C. "Polymer-Fullerene Bulk-Heterojunction Solar Cells." *Advanced Materials*. 21, 1323-1338. <https://doi.org/10.1002/adma.200801283>

[3] Zhang, L., and Ma, W. "Morphology optimization in ternary organic solar cells." *Chinese Journal of Polymer Science*. 35(2), 184-197. <https://doi.org/10.1007/s10118-017-1898-5>

Optimization of Polymer Solar Cells' Efficiency Using Molecular Dynamics simulation Rulin Yin¹, Karly Hou², Isabella Edsparr³, Dilip Gersappe⁴, Miriam Rafailovich⁴

¹ Saint Anthony's High School, South Huntington, NY 11747

² Henry M. Gunn High School, Palo Alto, CA 94306

³ James Allen's Girls' School, 144 East Dulwich Grove, London, United Kingdom SE22 8TE

⁴ Department of Materials Science and Engineering, Stony Brook University, Stony Brook, NY 11794

The need for renewable energy is becoming increasingly more important as the supply of fossil fuels diminishes and their damaging effects on the environment increase. Organic polymer solar cells are relatively inexpensive to produce and flexible, making them an attractive means of producing clean energy. However, inorganic solar cells have a relatively high efficiency, with an upper limit reaching 29%^[3], whereas most organic solar cells have only shown 3-5% efficiency and can only be used in small devices^[4]. This low efficiency is largely due to the convoluted structure of the active layer polymer blend; the long conjunction path results in recombination of electron and hole pairs. As shown in Figure 1^[5], adding a non-photoactive third polymer helps to form column nanostructures between the electrodes, allowing the electrons to move faster and more directly, thus increasing efficiency.

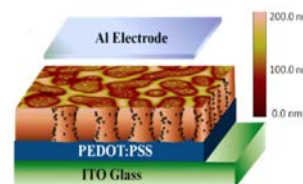


Fig.1 | Column nanostructures in a ternary blend polymer solar cell (figure adapted from ^[3])

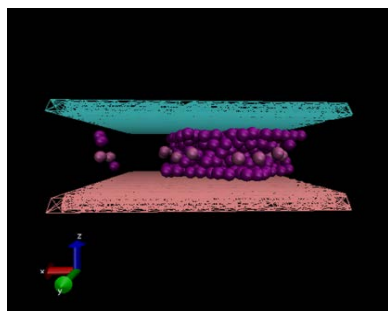


Fig.2 | Internal structure study simulation. The purple represents the photoactive polymer, the flesh color represents the nanofiller particles, and the top and bottom lattice represents the wall. The other polymer (nonphotoactive) is not shown for clarity.

The aim of this study is to use computer simulations to improve our understanding of the interactions in the ternary polymer blend and predict column stability while trying to increase the thickness of the solar cell. We used the Large Atomic/Molecular Massively Parallel Simulator (LAMMPS) to process molecular dynamics (MD) simulations. Using fixed x-y systems, we observed the internal structure and column quality while varying the system size, polymer interactions, polymer-filler interactions, and polymer-wall interactions.

We began the simulation study investigating the internal column structure formation process. By changing the modified Lennard-Jones potential and FENE potential parameters, we carefully monitored the results in many aspects: temperature, volume, entropy, and column morphology. Figure 2 is an example of an ideal column structure, as the active polymer forms a single large stable column through the cell. This gave us an intuitive and thorough understanding of the polymer column in the solar cell. We carried out several further trials to investigate how changing the height and the potential parameter of the solar cell in the simulation affected column formation and stability. At the moment, we can manage to form columns when the initial dimensions are set to no larger than 12:12:7, and learned that the more immiscible between the two polymers and stronger bonding between the polymers and the fillers can help to form better column.

For future research, we plan to simulate the system on a larger scale, while controlling different parameters and increasing the height of the solar cell in the simulation. Future research will also include combined the simulation data with polymer solar cell experimental data to guide future polymer selection, have a better understanding of the internal structure, and achieve possible improvement of the cell efficiency.

[1] Zhao J, Wang A, Green MA. 24.5% Efficiency silicon PERT cells on MCZ substrates and 24.7% efficiency PERL cells on FZ substrates. *Progress in Photovoltaics: Research and Applications* 1999; 7:471-4.

[4] Lai, Y.; Higashihara, T.; Hsu, J.; Ueda, M.; Chen, W.-C. "Sol. Energy Mater. Sol. Cells" 2012, 97, 164-170.

[5] Pan, Cheng, Hongfei Li, Bulent Akgun, Sushil K. Satijia, Yimei Zhu, Di Xu, Joseph Ortiz, Dilip Gersappe, and Miriam H. Rafailovich. "Enhancing the Efficiency of Bulk Heterojunction Solar Cells via Templated Self-Assembly." *Macromolecules* 46.5 (2013): 1812-819.

Lattice Boltzmann Modeling of the Prevention of Dendrite Formation in Lithium-Ion Batteries

Feiyang Yu¹, Luigia Than², Luke Shin³, Tianai Ye⁴, Dilip Gersappe⁵

¹Shenzhen Middle School, Shenzhen, Guangdong, ²Earl L. Vandermeulen High School, Port Jefferson, NY, 11777, ³Cornell University, Ithaca, NY, 14850, ⁴Stony Brook University, Stony Brook, NY, 11790, ⁵Department of Material Sciences and Chemical Engineering, Stony Brook University, Stony Brook, NY, 11790

Lithium-ion batteries are widely used in electrical vehicles and portable devices. Improving their performance depends on minimizing dendrite formation, which occurs during the charging process[1]. These dendrites increase the risk of internal short-circuiting and decrease battery capacity[2]. Our objective in this study is to prevent dendrite formation by altering the anode surface and the charging process.

Our study has two parts: simulations of lithium-ion batteries and analysis of the dendrites' solid fraction data. In the simulations, we used the model designed by Ning Sun, which employs the Lattice Boltzmann Method to create a mesoscopic model of the electrolyte and electrode-electrolyte domains of lithium-ion batteries[1]. We also altered four parameters: curvature constant (which indicates roughness), current density, the ratio of the duration of the battery being on to off (pulse time), and the length of time the battery stayed on within one pulse. To analyze the data we developed models that monitored the height of the dendrites (as a function of time) and also utilized a cluster counting algorithm to



Figure 1. Current density and pulse frequencies are kept constant; figure shows the morphologies when curvature constant $K=1, 2, 3, 4, 5$ (from left to right); as curvature constant increases, the dendrites' mass and height and number of dendrite branches increase.

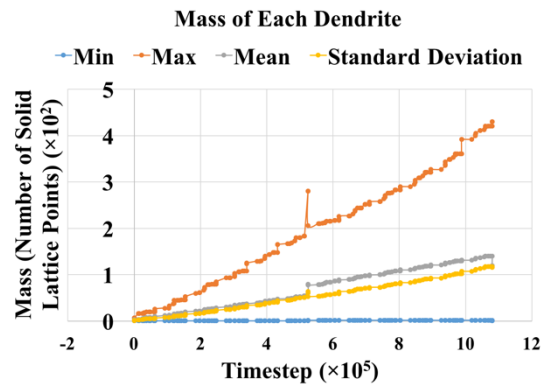


Figure 2. The minimum, maximum, mean and standard deviation of mass for dendrites versus timestep in simulation with curvature constant=5, current density=10 mA/cm², and frequency on-off=1-

follow the evolution of the mass of the dendrites. Both approaches estimated a similar number of dendrites, and we utilized these models to analyze dendrite growth in terms of height, total number, and mass.

We discovered that the number of dendrites increased dramatically at first, then decreased and remained relatively constant, throughout the simulations. Only the larger dendrites showed significant growth. As the curvature constant increased, dendrites' height and mass of the larger dendrites increased; the total number of dendrites slightly increased.

At current densities below 20 mA/cm² (with $K=5$ and frequency on-off=1-0.5), no dendrite is formed. As current density increased, dendrites' height increased and they had fewer branches. The mean mass of dendrites seemed unaffected.

Pulse time did not seem to exert strong effects on dendrite formation. As the ratio of the battery being on to off increased, dendrites' height and the mass of larger dendrites increased, while the total number of dendrites and mean mass seemed unaffected. As the battery stayed on longer within one pulse, dendrites' height increased. The total number of dendrites and mean mass seemed unaffected.

Our future plans include using more sets of parameters in simulations, comparing the results with experimental data, conducting deeper analyses of dendrite growth in height, total number, and mass, and improving the measurement of dendrite growth.

[⁶] Sun, Ning. *Application of Lattice Boltzmann Methods in Complex Mass Transfer Systems*. Dissertation, State University of New York at Stony Brook. Ann Arbor: ProQuest/UMI, 2016 (Publication No. [AAT 10144803]).

[2] Li, Zhe, et al. *A review of lithium deposition in lithium-ion and lithium metal secondary batteries*. Journal of Power Sources, Volume 254, (168-182). 15 May 2014.

Effects of Incorporating Graphene Oxide into Nafion on a Polymer Electrolyte Membrane Fuel Cell

Jerry Reyes¹, Daniel Rizzo¹, Rebecca Isseroff¹, Allen Green², Miriam Rafailovich³

¹Lawrence High School, Cedarhurst, NY, 11581

²Brown University, Providence, RI, 02912

³Department of Material Science and Engineering, State University of New York at Stony Brook, Stony Brook, NY, 11794

Previous research has constantly involved modifying the platinum coated carbon electrodes and coating the membrane of the polymer electrolyte membrane fuel cell (PEMFC) with metallized graphene oxide (GO)¹. However, no one has ever been able to incorporate the GO into the Nafion membrane itself. This research chemically combines graphene oxide with liquid nafion in water to coat a 50 μm nafion membrane (FuelCellsEtc, Nafion 212) of a PEMFC. An increase in wattage produced in the fuel cell would tell if GO increased the proton flow of the nafion membrane. Different concentrations of solutions made of GO and Nafion in water were made to determine the ideal concentration of GO. The ratio of these solutions were, by mass, 1:99, and 1:249.

GO was synthesized using a modified Hummer's method which involved dissolving graphite in sulfuric acid (H_2SO_4) and oxidizing it with potassium permanganate (KMnO_4) and sodium nitrate (NaNO_3)². Once the graphene oxide was extensively washed and then dried into flakes, a 1 mg/ml solution was made in distilled water, sonicated and then centrifuged to remove impurities. This supernatant was combined with a solution of liquid Nafion (Chemours, D1021) to create the ratios indicated above and were left to stir overnight. Each solution was poured onto one of two Nafion membranes in a clean glass plate that allowed the solution to make contact with all points of the Nafion membrane. The two samples were left to dry in a vacuum oven overnight at 50°C. The GO-Nafion membranes were cut from the glass plates and were hydrated in petri dishes. Both were tested in the hydrogen fuel cell and were compared to a regular Nafion membrane of the same thickness.

Results showed that the 1:249 ratio solution applied on the Nafion had a higher output power than that of the control and the 1:99 ratio solution. The peak wattage of the control was 0.18 Watts whereas that of the membrane treated with the 1:99 solution was 0.20 Watts, an increase of 11% over the control. The peak wattage of the fuel cell with the membrane treated with the 1:249 solution was 0.21 Watts. This is an increase of 17% compared to the control. (**Figure1**).

Further work will include more tests between the 1:99 ratio and 1:249 ratio solutions; creating and testing different concentrations, and testing the samples in a hydrogen gas feed contaminated with carbon monoxide to determine the modified fuel cells resistance to contaminants.

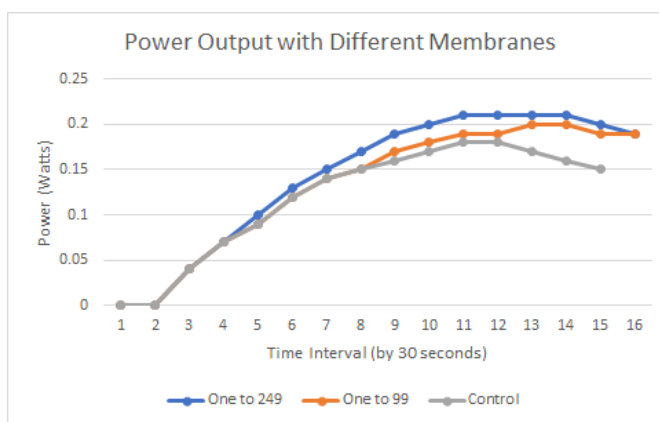


Figure 1: The graph above shows that of the three Nafion membranes tested on, the one treated with 1:249 solution made the hydrogen fuel cell perform the best.

¹Green, A., Isseroff, R., Lin, S., Wang, L., & Rafailovich, M. (2017). Synthesis and characterization of iron nanoparticles on partially reduced graphene oxide as a cost-effective catalyst for polymer electrolyte membrane fuel cells. *MRS Communications*, 7(02), 166-172. doi:10.1557/mrc.2017.14

²Hummers, W. S., & Offeman, R. E. (1958, September 25). Preparation of Graphitic Oxide. *J. Am. Chem. Soc. Journal of the American Chemical Society*, 80(6), 1339-1339. doi:10.1021/ja01539a017

Optimizing Molar Ratios of Gold-Silver Alloy Nanoparticles to Enhance the Performance of Proton Exchange Membrane Fuel Cells

Jarrad Li¹, Ruoxin Lu², Helen Zhang³, Samuel Plaut⁴, Peyrin Kao⁵, Likun Wang⁶, Miriam Rafailovich⁶

¹Syosset High School, Syosset, NY 11791; ²Plainview-Old Bethpage John F. Kennedy High School, Plainview, NY 11803;

³General Douglas MacArthur High School, Levittown, NY 11756; ⁴Binghamton University, Binghamton, NY 13902; ⁵University of California, Berkeley, Berkeley, CA 94720; ⁶Department of Materials Science and Chemical Engineering, Stony Brook University, Stony Brook, NY 11794

As the world continues to deplete nonrenewable energy sources, proton exchange membrane (PEM) fuel cells have recently become a topic of interest in the field of alternative energy, as they operate at a favorably low temperature, are able to produce a relatively high power density, are mechanically stable, and their emissions are almost completely pollution-free with water being the only byproduct¹. However, ambient operation leads to carbon monoxide (CO) poison formation via the reverse water-gas shift reaction. CO adsorbs onto the active sites of platinum and blocks its ability to catalyze hydrogen oxidation and oxygen reduction reactions that power the fuel cell, causing decreased power output, cell efficiency, and platinum durability¹³. It has been discovered that gold nanoparticles can mitigate platinum catalyst degradation and improve efficiency by over 50%¹¹.

Utilizing a modified two-phase method devised by Brust³, thiol-functionalized gold-silver alloy nanoparticles were synthesized at molar ratios of 1:1, 3:1, and 7:1. A KSV 3000 Langmuir-Blodgett trough was used to coat Nafion 117 membranes with gold-silver alloy nanoparticles at different target surface tensions, which were determined from isothermal curves generated from the nanoparticles. 1:1 gold-silver alloy nanoparticles were coated at surface tensions of 1mN/m, 3mN/m, and 8mN/m. The 8mN/m coating generated a multilayer of nanoparticles on the Nafion while the 1mN/m and 3mN/m coatings produced a monolayer. Both the 3:1 and 7:1 gold-silver alloy nanoparticles were coated onto the Nafion membranes at surface tensions of 1mN/m, 3mN/m, and 5mN/m, producing monolayers.

The coated Nafion membranes and an uncoated control Nafion membrane were assembled into a H-Tec Demonstration Kit single stack hydrogen fuel cell connected to a multimeter and BK 8600 software to measure current, voltage, and power output. A list was run in which current increased by .05A increments starting from 0A and ending at .7A. 3 trials were run for each different Nafion membrane. Power-current curves (Figure 1) and polarization curves (Figure 2) were generated.

The Nafion membrane coated with 3:1 AuAg nanoparticles exhibited the highest maximum average power output, reaching .219 W, an 64.6% increase over the control (Figure 1). Overall, 3:1 AuAg nanoparticles produced a greater enhancement in power output than 1:1 AuAg nanoparticles. All 3:1 AuAg nanoparticles generated maximum power outputs significantly greater than the control.

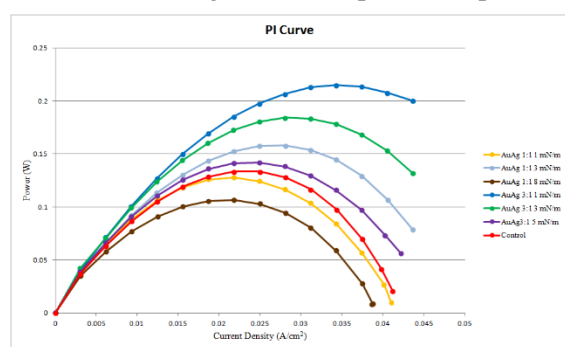


Figure 1: Graph of power output v. current density for all measured surface tensions on Nafion membranes.

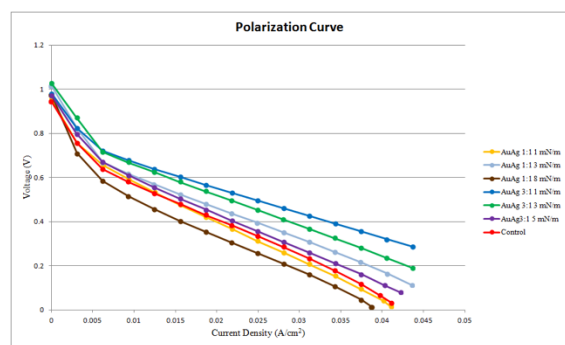


Figure 2: Graph of voltage output v. current density for each measured surface tension on Nafion membrane.

[1] Li, H., Pan, C., Zhao, S., Liu, P., Zhu, Y., & Rafailovich, M. H. (2016). Enhancing performance of PEM fuel cells: Using the Au nanoplatelet/Nafion interface to enable CO oxidation under ambient conditions. *Journal of Catalysis*, 339, 31-37.

[2] Baschuk, J.J., & Li, X. (2001). Carbon monoxide poisoning of proton exchange membrane fuel cells. *International Journal of Energy Research*, 25(8), 695-713.

[3] Brust, M., Walker, M., Bethell, D., Schiffrin, D. J., & Whyman, R. (1994). Synthesis of thiol-derivatized gold nanoparticles in a two-phase liquid-liquid system. *Journal of the Chemical Society, Chemical Communications*, (7), 801.

Application of Graphene Oxide onto Polymer Electrolyte Membranes (PEM) and Electrodes to Optimize Hydrogen Fuel Cell Performance

Danielle Kelly¹, Audrey Shine², Mariya Shtiliyanova³, Peyrin Kao⁴, Likun Wang⁵, Miriam Rafailovich⁵

¹Friends Academy, Locust Valley, NY; ²Plainview Old-Bethpage JFK High School, Plainview, NY; ³Concord-Carlisle High School, Concord MA; ⁴University of California, Berkeley, Berkeley, California; ⁵Department of Materials Science & Engineering, Stony Brook University, NY⁵

From 300 years ago to modern day, fossil fuels have remained the primary source of energy, threatening the fragile balance on our planet through ever increasing carbon emissions. Standing at the cutting edge of material science, Polymer Electrolyte Membrane Fuel Cells (PEMFCs) provide an alternative source of clean energy through the reduction-oxidation reaction of hydrogen and oxygen gas. Highly efficient and effectively pollution less, the operation of PEMFCs in theory produces only one byproduct: H₂O. However, in reality, the conversion of naturally occurring CO₂ → CO, poisons the platinum catalyst, blocking active sites, and in turn reducing the efficiency of the cell¹. This study investigates the mechanisms by which graphene oxide (GO) may increase PEMFC efficiency, including the potential for GO to reduce CO poisoning, improve proton conductivity, and inhibit crossover impedance².

To accomplish this, GO was first sprayed onto microporous carbon electrodes in a catalyst ink blend of isopropanol, liquid Nafion, and carbon-supported platinum nanoparticles combined with GO in DI water ranging from 0.05 mg/mL to 0.8 mg/mL. The electrodes were spray coated with the catalyst ink to achieve a Pt loading of around 0.100 mg/cm². Second, various loadings of GO were directly bladed onto a Nafion 117 membrane. The GO bladed membranes and non-GO electrodes and the GO coated electrodes with an uncoated Nafion membrane were tested in an H-tech PEMFC kit with both pure oxygen and an open-air environment at the cathode and pure hydrogen fed into the anode.

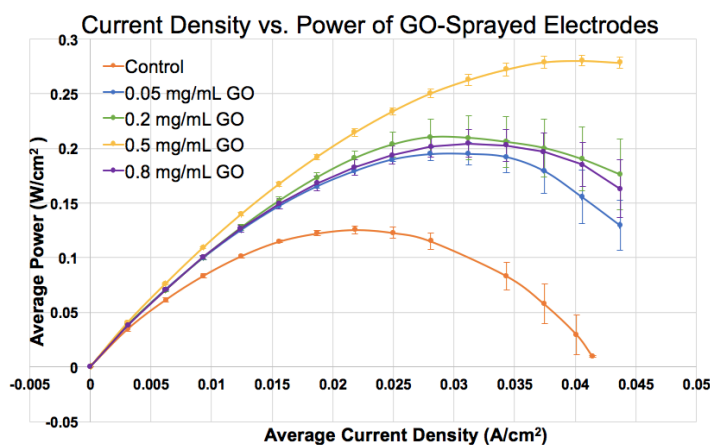


Figure 3: Power performance curves of PEMFCs with electrodes of all different GO loadings

The test results indicate overall that GO enhanced fuel cell efficiency. 0.5 mg/mL GO sprayed on the electrodes led to the greatest max power output, 132% higher than the control (Figure 1). GO-bladed membranes facing the anode increased power output by roughly 80%, regardless of GO loading, while membranes facing the cathode saw greater performance as GO loading increased. This data supports the theory that GO reduces CO poisoning, a process which begins at the cathode and would be better reversed by the GO lodged in the electrodes. Tests where pure oxygen was aimed towards the cathode on non-GO and GO electrodes showed a decreased gap in performance compared to open-air tests, further substantiating the conclusion that GO decreases CO poisoning, in addition to other mechanisms of increasing efficiency.

Future work includes tests to ascertain whether GO affects the hydrogen oxidation reaction at the anode; pure CO tests and prolonged open-air tests to determine a more precise mechanism by which GO reduces CO poisoning; and platinum wires added to electrodes to determine how catalyst shape affects fuel cell performance.

¹Kwon, Kyungjung, et al. "Experimental Factors That Influence Carbon Monoxide Tolerance of High-Temperature Proton-Exchange Membrane Fuel Cells." *Journal of Power Sources*, vol. 185, no. 1, 15 Oct. 2008, pp. 202–206. EBESCO

²Tseng, Chi-Yung, et al. "Sulfonated Polyimide Proton Exchange Membranes with Graphene Oxide Show Improved Proton Conductivity, Methanol Crossover Impedance, and Mechanical Properties." *Advanced Energy Materials*, WILEY-VCH Verlag, 4 Oct. 2011

Utilizing ALD-Coated Titanium Dioxide on Nafion Membrane to Increase Efficiency of Proton Exchange Membrane Fuel Cells

Angela Ye¹, Kenneth Chan², Pastor Martinez³, Peyrin Kao⁴, Likun Wang⁵, Miriam Rafailovich⁵
¹Basis Independent Silicon Valley, San Jose, CA 95126; ²Island Trees High School, Levittown, NY 11756;
³Brentwood High School, Brentwood, NY 11717; ⁴University of California, Berkeley, Berkeley, CA 94720; ⁵Department of Materials Science and Engineering, SUNY Stony Brook, Stony Brook, NY 11794

Due to increasing fossil fuel consumption and the resulting environmental impact, there is a high demand for new energy sources, especially proton exchange membrane fuel cells (PEMFC)⁷. However, when carbon monoxide (CO) is introduced to PEMFCs through hydrogen gas impurities and air, it bonds to platinum catalysts, reducing efficiency. Gold nanoparticles can catalyze CO oxidation at low temperatures, and titanium dioxide (TiO₂) is an effective catalytic support⁸. Thus, we investigated the effects of coating the Nafion membrane with titanium dioxide and gold nanoparticles.

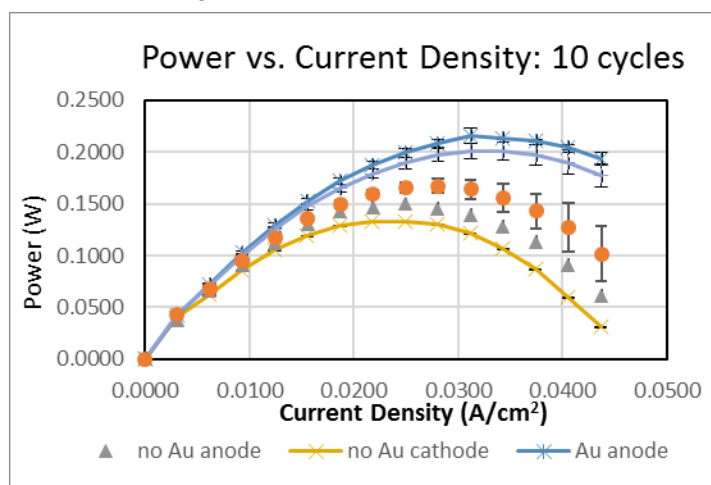


Figure 4: PI curve of 10 cycle ALD

Nafion membranes were the control, generating a maximum power of 0.1671W. When the 10 cycles ALD membrane was coated with TiO₂, the maximum power decreased to 0.1332 when facing the cathode and 0.1497 for the anode. When gold nanoparticles were coated on top of TiO₂, the maximum power increased to 0.2009 for cathode and 0.2161 for anode. Similar results were obtained for 20 cycles, while for 30 and 40 cycles the TiO₂-only power outputs were unexpectedly high; we attribute this to an unpredicted beneficial effect or to error. Few tests were done for 5 and 50 cycles; more will be done later. We theorize the TiO₂ layer decreases Nafion pore size, reducing proton conductivity. However, the gold nanoparticle coating on TiO₂ catalyzes CO oxidation, overcoming the adverse effects of TiO₂ alone.

Future work includes scanning electron microscopy (SEM) will be done to observe the thickness of the TiO₂ layer. Membranes with both sides coated will be created and tested to determine the cumulative effect of the catalysts on each side. Additional cycles will be tested to find the optimal thickness of TiO₂.

Atomic layer deposition (ALD) of TiO₂ was done on one side of Nafion membranes at 80°C using precursors of titanium tetraisopropoxide (TTIP) and water from 5 to 50 cycles⁹. Gold nanoparticles were synthesized through the Brust method. A Langmuir-Blodgett (LB) trough was used to coat a gold nanoparticle monolayer onto the TiO₂-coated Nafion. The membranes were tested in a fuel cell test station (BK Precision 8601 DC Electronic Load single stack) with 4cm x 4cm electrodes of 0.1 g/cm² Pt/C. Tests were run with currents from 0.000A to 0.700A at 0.050A intervals to determine voltage and power output.

As shown in Figure 1, uncoated

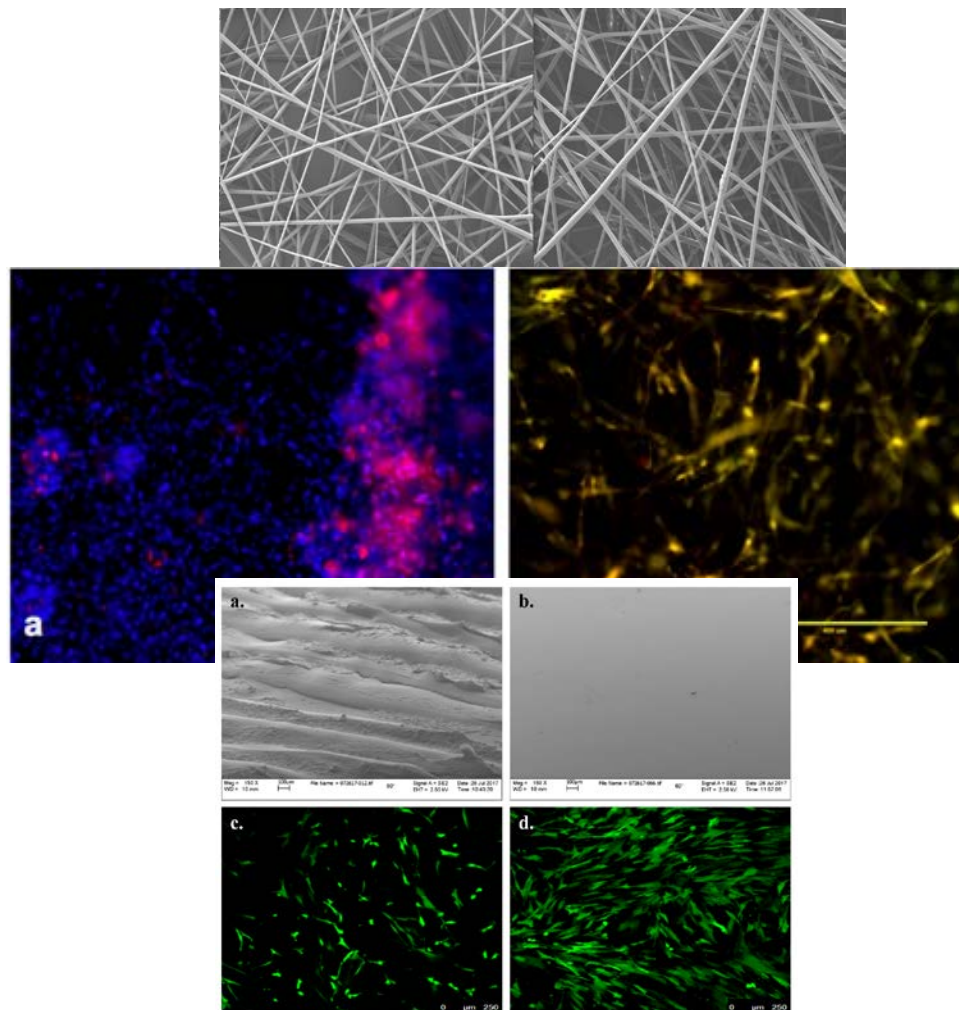
⁷ Cusick, Daniel. "Fossil Fuel Use Continues to Rise." *Scientific American*, Springer Nature. Web. 5 Oct. 2013.

⁸ Haruta, M. "Nanoparticulate Gold Catalysts for Low-Temperature CO Oxidation." *ChemInform*, vol. 35, no. 48, 2004, doi:10.1002/chin.200448226.

⁹ Aghaee, Morteza, et al. "Low Temperature Temporal and Spatial Atomic Layer Deposition of TiO₂ Films." *Journal of Vacuum Science & Technology A: Vacuum, Surfaces, and Films*, vol. 33, no. 4, 2015, p. 041512., doi:10.1116/1.4922588.

Session III: Scaffolds for Tissue Engineering

**Graduate Mentors: Kuan-Che Feng,
Fan Yang, Clement Marmorat, Juyi Li,
Linxi Zhang, Ya-Chen Chuang, Kao Li**



Effects of Mechanical Stress Generated by Laminar Fluid Flow and Rapid Environmental Viscosity Transitions on Human Dermal Fibroblast, Dental Pulp Stem Cell, and Squamous Cell Carcinoma Suspensions Sheared in Polyethylene Glycol Solutions

Rose Hong¹, Bill Chen², Carmen Hung³, Maria Rodriguez⁴, Clement Marmorat⁵, Marcia Simon³, Miriam Rafailovich⁵

¹Del Norte High School, San Diego, CA 92127, ²Columbia University, New York, NY 10027, ³Stony Brook University School of Dental Medicine, Stony Brook, NY 11794, ⁴U.S. Food and Drug Administration, Silver Spring, MD 20993, ⁵Stony Brook University Department of Materials Science and Engineering, Stony Brook, NY 11794

Bioprinting, an emerging technology in the field of tissue engineering, creates complex, viable tissue constructs for the restoration of biological function.¹ However, dispensing mechanisms used place cells under large amounts of shear stress, thereby influencing cell signaling and protein expression.² Understanding cellular responses to these forces, therefore, is paramount, especially when considering bioprinting for drug delivery, organ replacement, *in vivo* research models, and other medical applications.¹ As a result, we researched the effects of shear stress on human dermal fibroblasts (HDFs), dental pulp stem cells (DPSCs), and squamous cell carcinoma (SCC) in polyethylene glycol (PEG) solutions in order to aid in the comprehension and development of functional, engineered tissue structures. PEG, a versatile polymer, was chosen in this study for its variable viscosity and biological inertness, which allowed it to serve as an appropriate cell delivery vehicle to model the effects of shear stress independent of biochemical cell-substrate interactions.³

PEG solutions 300K-3%, 1000K-2%, and 4000K-0.8%, where 300K-3% denotes a molecular weight of 300,000 amu and a concentration of 3%, were dissolved in phosphate-buffered saline (PBS). Specific concentrations from literature were chosen for the 1000K and 4000K solutions to achieve viscosities on the same order of magnitude as that of the 300K-3% so that the effects of polymer chain lengths could be compared.⁴ Rheology (Malvern Bohlin Gemini II) was then performed to determine the actual viscosities of the 3 solutions so that shear stress values could later be calculated from flow rate. A 300K-3.8% solution was also created, in accordance with literature, to have a viscosity double that of the 300K-3%, and rheology will be performed on that sample as well.⁴

In 2 separate experiments, HDFs (MT Pass 4) and DPSCs (AV3) were suspended in 1:10 dilutions with PEG 300K-3% or PBS. Cell solutions were then sheared with a syringe pump (NE-1000 Programmable Single) in 5 mL syringes (BD Luer-Lok™) connected with 0.35 mm radius × 700 mm tubing (Zeus Industrial Products, Inc) at flow rates 1.5, 4.5, and 22.5 mL/min, which corresponded to shear stress levels 1700, 5200, and 25600 Pa (Fig. 1); cells prepared without shear in either PEG or PBS served as positive controls. HDFs were also either pre-suspended by inversion in a conical tube before being sheared in the pump or directly sheared into PEG or PBS solutions at 22.5 mg/mL. Significant reductions in cell counts existed in all 22.5 mL/min HDF-PBS samples, as well as HDF-PEG without pre-inversion at 22.5 mL/min (Fig. 2), demonstrating that the rapid low to high viscosity transition into PEG 300K-3% adversely affected HDFs. Meanwhile, no significant differences in DPSC cell counts were noted on Day 4, indicating that DPSCs could tolerate at least 25600 Pa of shear. In another experiment, HDFs were passed 5, 10, or 20 times through the tubing at 4.5 mL/min and compared against the controls to evaluate whether the length of time under shear affected cell viability and proliferation. No significant differences in cell counts were observed between the different numbers of passes, indicating that HDFs were able to tolerate 5200 Pa of shear for up to 400 s. A similar procedure will be used to shear SCC, which has been genetically altered to produce lecithin-retinol acyltransferase (SCC +LRAT) and can be compared against the SCC -LRAT control to determine whether cancer cells with distinctive mechanical properties respond differently to shear. Later, HDFs will also be sheared in 1000K-2%, 4000K-0.8%, and 300K-3.8% to determine the effects of molecular weight and viscosity on sheared cells, and endpoint analysis by SEM and RT-PCR will be conducted on Day 28 to determine the effects of shear stress on the differentiation lineage of DPSCs.

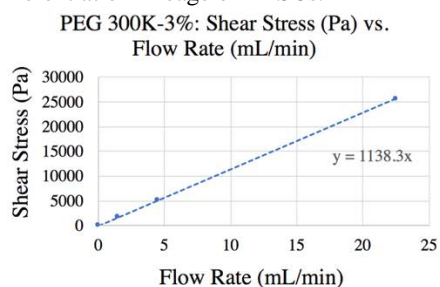


Fig. 1: Graph of PEG 300K-3% Shear Stress (Pa) vs. Flow Rate (mL/min). Linear relationship graphed through 3 rates tested (1.5 mL/min, 4.5 mL/min, 22.5 mL/min) and corresponding calculated shear stress values (1700, 5200, and 25600 Pa).

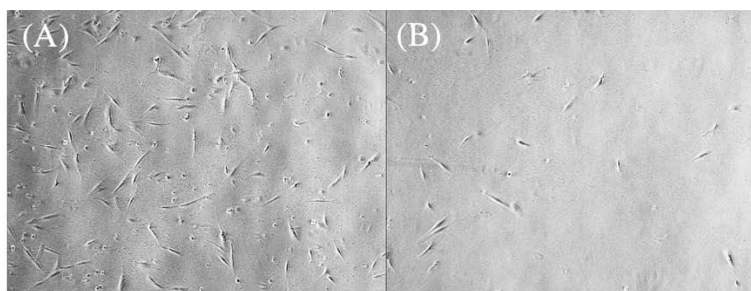


Fig. 2: Optical microscope images of HDFs plated in PEG 300K-3% after (A) pre-inversion in a conical tube, and (B) no pre-inversion followed by rapid suspension and shearing in the pump at 22.5 mL/min, or 25600 Pa.

¹Nair, K., Gandhi, M., Khalil, S., Yan, K. C., Marcolongo, M., Barbee, K., & Sun, W. (2009). Characterization of cell viability during bioprinting processes. *Biotechnology journal*, 4(8), 1168-1177.

²Blaeser, A., Duarte Campos, D. F., Puster, U., Richtering, W., Stevens, M. M., & Fischer, H. (2016). Controlling shear stress in 3D bioprinting is a key factor to balance printing resolution and stem cell integrity. *Advanced healthcare materials*, 5(3), 326-333.

³Bailon, P., & Berthold, W. (1998). Polyethylene glycol-conjugated pharmaceutical proteins. *Pharmaceutical Science & Technology Today*, 1(8), 352-356.

⁴Ebagninin, K. W., Benchabane, A., & Bekkour, K. (2009). Rheological characterization of poly (ethylene oxide) solutions of different molecular weights. *Journal of colloid and interface science*, 336(1), 360-367.

2D vs 3D — The Effect of the Morphology of P4VP Scaffolds on Dental Pulp Stem Cell Proliferation and Differentiation

Jiaming Ma¹, Grace Hu², Carolyn Wong³, Linxi Zhang⁴, Miriam Rafailovich⁴

¹The High School Affiliated to Renmin University, International Curriculum Center, Beijing, China

²Stanford University, Stanford, CA 94305

³Harvard University, Cambridge, MA 02138

⁴Stony Brook University, Stony Brook, NY 11790

Dental pulp stem cells (DPSCs) are increasingly becoming a focus in research due to its multi-lineage differentiation capacity and its relative accessibility. Specifically, DPSCs are capable of differentiating into adipocytes, neural-like cells, osteoblasts and odontoblasts^[1]. Research has shown that poly-4-vinyl pyridine (P4VP) is a biocompatible polymer material^[2] and is potential to be used as a substitutional material for traditional tissue culture plastic of Polystyrene.

This research evaluates the different morphology of the P4VP scaffolds on the proliferation and differentiation of the DPSCs. The 2-dimensional thin film scaffolds were prepared by spin casting 5mg/ml P4VP solution in DMF at 2500rpm for 30s. The nano-size and micro-size 3-dimensional fiber scaffolds were fabricated by electrospinning 17% and 25% P4VP solution in DMF/Ethanol (1:5), with feeding rate at 5 μ l/min and voltage at 15kV. DPSCs were cultured in 24-well plates (5,000 cells per well) and 6-well plates (20,000 cells per well) and incubated at 37°C and 5% CO₂ for 2, 4, 7, 14, and 28 days for cell behavior analysis.

AFM and SEM were utilized to characterize the morphology of the scaffold the results show that a uniform thin film had been successfully fabricated by spin casting. SEM images of fiber scaffolds were taken and the fiber diameters were also measured. The difference of average fiber diameter of nanofibers (0.456 \pm 0.152 μ m) and microfibers (2.244 \pm 0.485 μ m) were statistically significant, from which can be concluded that the two kinds of fibers are two different kinds of scaffolds. At day 2, day 4, and day 7, the cells were fixed with formaldehyde and then stained with Alexa Fluor 488 and DAPI for confocal microscopy. The confocal images (Figure 1) shows that cells actin filament are more stretched on fiber surfaces, where the cells grow along the fibers. The confocal images were used to conduct cell counting, from which the doubling time and cell attachment rate can be calculated and cell growth curve can be obtained. Results show that on day 2, DPSCs attach more on the flat surface, and attach less on fibers. The fiber scaffolds reduce the effective attachable surface area, which might have led to the decrease in attachment rate. The doubling time of DPSCs are the longest on flat surfaces, which reveals that the fiber scaffolds might have made the cell growth directional, thus making the DPSCs proliferate faster. The MF scaffold had significantly less cells than the other two kinds of scaffolds, which may have resulted from the reaching of cell confluency during the period of 7 days.

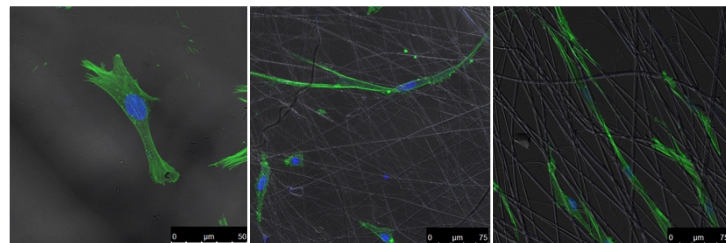


Figure 1. Confocal Image of DPSCs.
Left to right: flat, nanofiber, microfiber

the

Results show that on day 2, DPSCs attach more on the flat surface, and attach less on fibers. The fiber scaffolds reduce the effective attachable surface area, which might have led to the decrease in attachment rate. The doubling time of DPSCs are the longest on flat surfaces, which reveals that the fiber scaffolds might have made the cell growth directional, thus making the DPSCs proliferate faster. The MF scaffold had significantly less cells than the other two kinds of scaffolds, which may have resulted from the reaching of cell confluency during the period of 7 days.

After 28 days of incubation of the cells, RT-PCR will be conducted to evaluate the expression of the relative differentiation gene markers. Confocal microscopy will also be conducted by staining the osteocalcin proteins to obtain data on the expression of the proteins. SEM and EDX will be utilized to examine the deposition of mineralization of DPSCs on different scaffolds.

^[1] Gronthos, S., Brahim, J., Li, W., Fisher, L.W., Cherman, N., Boyde, A., Besten, P. D., Robey, P. G., & Shi, S. Stem Cell Properties of Human Dental Pulp Stem Cells. *Journal of Dental Research*, **81(8)**, 531-535 (2002).

^[2] Apostol, M., Mironava, T., Yang, N., Pernodet, N., & Rafailovich, M. H. Cell sheet patterning using photo-cleavable polymers. *Polymer Journal*, **43**, 723-732 (2011).

Evaluating the Effect of Graphene-Loaded Poly(4-vinylpyridine) Electrospun Fibrous Scaffolds and Spun-cast Thin Films on the Proliferation and Differentiation of Dental Pulp Stem Cells

Sahith Vadada¹, Rushikesh Patel¹, Vedant Singh², Grace Hu³, Carolyn Wong⁴, Linxi Zhang⁵, Miriam Rafailovich⁵

¹Herricks High School, New Hyde Park, NY 11040; ²The Wheatley School, Old Westbury, NY 11568; ³Stanford University, Stanford, CA 94305; ⁴Harvard University, Cambridge, MA 02138; ⁵Department of Materials Science and Engineering, Stony Brook University, Stony Brook, NY 11790

As research in biomedical engineering continues to peak interest of many scientists, studies in dental pulp stem cells (DPSCs) have started to play a major role in the development of scaffolds. Along with having multilineage differentiation potential, DPSCs are prime examples of a cost-efficient way to retrieve stem cells¹. The polymer scaffold being used in this experiment consists of poly(4-vinylpyridine), rather than the more commonly used polystyrene(PS)-based tissue culture plastic. Although the two are very similar in chemical structure, P4VP has a nitrogen atom on the benzene ring rather than a carbon one. This slight difference may make P4VP a biocompatible, photocleavable polymer.² Adding a material like graphene, which holds many unique mechanical, chemical, and electrical properties, can have a powerful affect on how the cells behave on biocompatible scaffolds.

The primary goal of our research was to test the impact of graphene in our electrospun scaffolds on the differentiation and proliferation of DPSCs. However, within this project lies an ulterior motive in seeking to replace polystyrene-based tissue culture plastic with P4VP. To initiate the experiment, we created six different solutions of varying concentrations of P4VP and graphene. Two samples of 17% wt P4VP/DMF:ethanol solution and 25% wt P4VP/DMF:Ethanol solutions, both 3 mL, were created for electrospinning. These samples were reproduced with the addition of 3% graphene into the solutions. The two varying solutions will allow for the synthesis of two separate electrospun fibers: nanofibers and microfibers. Additionally, P4VP thin film substrates with and without graphene were spun-cast at 2500 rpm for 30 seconds each. Fibers were electrospun on silicon wafers or glass slides at 15 microliters/minute and 15kV. After electrospinning and spincasting were completed, DPSC cultures were prepared for a 28-day analysis to study cell proliferation and differentiation.

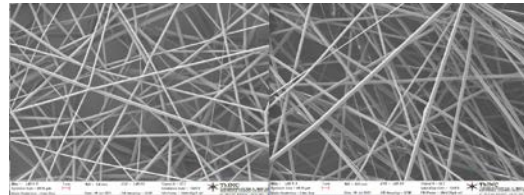


Figure 1: SEM of Fiber Scaffolds

Scaffolds were characterized by SEM images. After determining the diameter of the P4VP fibers from Figure 1 SEM images, we discovered graphene had nearly no effect on diameter and had a high dispersion rate. According to Figure 2, doubling time from days 2, 4, and 7 displayed that thin films initially have increased the proliferation of DPSCs due to the larger surface area. Graphene also increased the doubling time of all three samples. Confocal microscopy was performed to view cell morphology, and 40x magnification images displayed that cells grew linearly along nano- and microfibers. Microfiber scaffolds had the least cells, indicating a possible cell confluency on day 7.

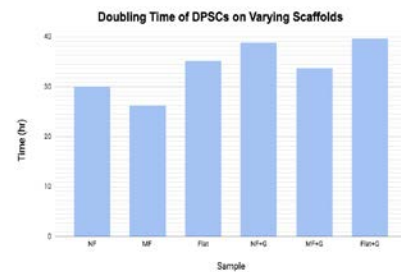


Figure 2: Doubling Time of DPSCs

On days 7, 14, and 28, RT-PCR, SEM/EDX, ROS, and additional confocal microscopy will be conducted in order to measure the differentiation and biomineralization of DPSCs. While the microscopy will determine if the deposits and proteins display differentiation, PCR will measure how differentiation gene markers of DPSCs. Lastly, ROS will measure how cells are reacting to the electrospun P4VP fibers with and without graphene.

[1] Mabel M Cordeiro, Tomoatsu Kaneko, Zhihong Dong, Zhaocheng Zhang, Marta Miyazawa, Songtao Shi, Anthony J. Smith, Jacques E Nor. Dental Pulp Tissue Engineering with Stem Cells from Exfoliated Deciduous Teeth. *Journal of Endodontics*, Volume 34, Issue 8, 962 - 969.

[2] Apostol, M., Mironava, T., Yang, N., Pernodet, N., & Rafailovich, M. H. Cell sheet patterning using photocleavable polymers. *Polymer Journal*, 43, 723-732 (2011).

Use of Gelatin mTG Cross-linked Gel to Study Mesenchymal Epithelial Interaction in Dentin and Enamel Synthesis

Margaret Sui¹, Sophia Chen², Konstantina Angoura³, Juyi Li⁵, Vladimir Moraru⁴, Kuan-che Feng⁵, Miriam Rafailovich⁵, Marcia Simon⁴, Adriana Pinkas-Sarafova^{4,5}

¹Bethlehem Central High School, Delmar, NY, ²Palm Harbor University High School, Omaha St, Palm Harbor, FL, ³Hellenic-American Educational Foundation Athens College, 15, Athens, Greece, ⁴Department of Oral Biology and Pathology, School of Dental Medicine, Stony Brook, NY, ⁵Department of Materials Science and Chemical Engineering, Stony Brook University, Stony Brook, NY

Despite current advances in technology and research, tooth regeneration from adult human stem cells has proven difficult. Adult damaged dentin can be renewed by odontoblasts differentiated from dental pulp stem cells (DPSCs), but enamel cannot be renewed because the ameloblasts differentiated from epithelial cells disappear after tooth eruption¹. Previous studies concerning *in vitro* ameloblast differentiation required the co-culturing of DPSCs and epithelial cells, where at least one of the cell lines was from an embryonic source². Human embryonic stem cells are difficult to access. Thus, it is pertinent to design a scaffold model for mesenchymal-epithelial interaction that encourages ameloblast differentiation and enamel production, using only adult stem cells lineages.

Gelatin is a product of collagen hydrolysis that adequately mimics the chemistry of the extracellular matrix. Our goal is to use a microbial transglutaminase (mTG) cross-linked gelatin gel model to co-culture adult DPSCs (mesenchymal origin) and adult gingival cells (epithelial origin) to study the viability of enamel production *in vitro* through epithelial mesenchymal interactions.

This experiment utilized AV3 DPSCs transduced with green fluorescent protein (GFP) and gingival cell lines, both isolated from waste tissue. Cells were expanded in KGM and α MEM+10% FBS media. DPSCs (2×10^5 cells/mL) or gingival cells (10^6 cells/mL) and 2.6 mg/mL of mTG, were added to a 10% gelatin solution, mixed, and transferred to plates resulting in soft gels. Once plated, the media was switched to a 1:1 ratio of DMEM, 10% FBS and 3:1 Keratinocyte media, 5% FBS. On 4th day after plating β -glycerol phosphate and ascorbic acid were added to the media for the induction of biomineralization. The media was changed every other day.

Cell behavior was monitored by EVOS fluorescent microscope, after adding blue life dye for nuclear staining, and xylenol orange for Ca⁺ detection. Encapsulated cells from both cell lines have shown viability and mobility in a drop test (Fig.1). One week after induction, gingival cells plated on mTG gelatin gel formed clusters with large Ca⁺ deposits, while DPSC had a strong overlapping of red and green signals, suggesting high intracellular Ca⁺ accumulation (Fig.2). The fastest interaction between the two cell lines was observed in the co-culture of non-encapsulated gingival cells and DPSCs, separated by a thin gel layer. The gingival cells formed clusters and were able to penetrate the barrier

layer (Fig 3). For end point analysis hydroxyapatite mineralization formation will be analyzed at day 40 using Scanning Electron Microscopy (SEM) and Raman spectroscopy. RT qPCR will be performed at day 7, 21 and 40 for detection of the differentiation profile.

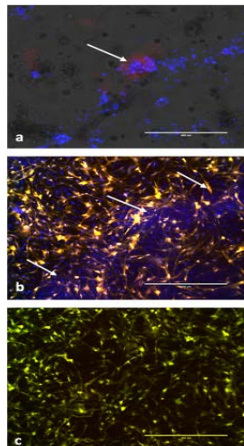


Figure 3: Fluorescent microscope pictures; (a) gingival cells on top of gel, arrow shows calcium; (b) middle gel area, arrow shows nuclear clusters; (c) bottom DPSC on plate

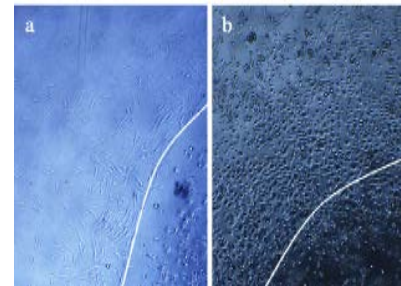


Figure 1: Phase contrast microscope pictures of cells encapsulated in a drop of gelatin mTG gel—white line defines the drop border; (a) DPSC; (b) gingival cells

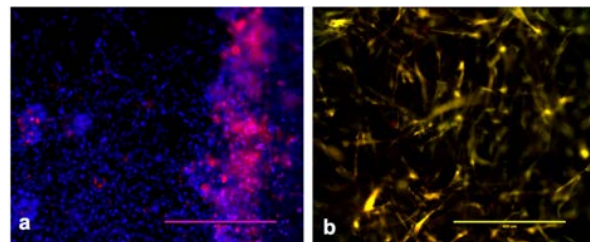


Figure 2: Fluorescent microscope pictures of day 7 cultured cells on mTG gelatin gel; (a) gingival cells; (b) DPSC

References

- ¹Young CS, Terada S, Vacanti JP, Honda M, Bartlett JD, Yelick PC. Tissue engineering of complex tooth structures on biodegradable polymer scaffolds. *J Dent Res.* 2002 Oct;81(10):695-700.
- ²Chatzistavrou, Xanthippi et al. "Innovative Approaches to Regenerate Enamel and Dentin." *International Journal of Dentistry* 2012 (2012): 856470. *PMC. Web.* 6 Aug. 2017.

Characterizing *In Situ* mTG Crosslinked Gelatin Hydrogels with Encapsulated Dental Pulp Stem Cells for Cell Delivery in Applications of Regenerative Medicine

Jason Kurlander¹, Yael Laks², Leeba Sullivan², Juyi Li³, Kuan-Che Feng³, Clement Marmorat³, Vlad Moraru⁴, Marcia Simon⁴, Adriana Pinkas-Sarafova^{3,4}, Miriam Rafailovich³

¹North Shore Hebrew Academy High School, Great Neck, NY 11020; ²Yeshiva University High School For Girls, Hollis, NY 11423;

³Department of Materials Science and Engineering, State University of New York at Stony Brook, Stony Brook, NY 11794 ⁴Department of Oral Biology and Pathology, State University of New York at Stony Brook, Stony Brook, NY 11794

Dental pulp stem cells (DPSC) are on the forefront of tooth regeneration technology due to their proliferative and differentiative abilities as well as their easy accessibility¹. One way to implant the cells *in vivo* is to encapsulate them within a scaffold or gel. Gelatin is natural, biocompatible, and biodegradable making it an ideal cell scaffold for tissue regeneration. The gel must polymerize *in vivo* at body temperature and therefore must be crosslinked. One method is enzymatic crosslinking using microbial transglutaminase (mTG)². Since cell encapsulation does not allow for the inactivation of mTG, characterization of these gels and DPSCs' response is critical in order to attain a gelatin hydrogel for injectable stem cell therapy.

In this study, hydrogels were created by mixing 10% gelatin into PBS (phosphate buffered saline), and were then crosslinked with various concentrations of mTG (Ajinomoto Transglutaminase): 12.5, 6.25, 3.13, and 1.56 mg/mL. Gels were divided into three groups, which were soaked in PBS, α MEM (Minimum Essential Medium Eagle), or α MEM with DPSC (AV3 GFP). DPSC encapsulation was achieved by simultaneously mixing gelatin solution with 2×10^5 cells/mL, and corresponding amounts of mTG.

The time of polymerization was measured for gels with the various concentrations of mTG, and was shown to be inversely proportional to the concentration of mTG. Accordingly, the 1.56 mg/mL mTG gel polymerized slowly (approximately 72 min), and would therefore not be suitable for the overall goal.

In order to determine how long the mTG enzyme would remain active, and whether or not the cells would degrade the gel, elastic modulus of the gels were measured by rheology over a period of 14 days. As seen in Fig. 1, the elastic modulus reached its peak between days 3 and 6, showing that the mTG was no longer active. Additionally, by day 3 there was no significant difference between the 6.25 mg/mL and the 12.5 mg/mL mTG. The gels soaked in media with and without DPSC were also observed to be softer than those soaked in PBS. This was likely due to the proteins present in the media interfering with the crosslinking. The gels with encapsulated cells were also seen to degrade slightly compared to those without cells between days 6 and 14. Based on collective results, concentrations of 6.25 and 3.13 mg/mL were used for characterization of DPSC behavior.!

Proliferation of the DPSC in the hydrogel was measured between days 1 and 7 via fluorometry using alamar blue dye. The cells in the 3.13 mg/mL of mTG gels had more cells than the 6.25 mg/mL gels, but the cells had a doubling time of 2.3 days and 1.8 days, respectively, in the gels.!

A drop of gel was deposited on a cell culture plate and then observed under a microscope in order to measure the motility of the cells. After 24 hours very few cells left the gel. On day 5, the 3.13 mg/mL concentration shows a lot more cells migrating out of the gel than the 6.25 mg/mL, and on day 8 even more cells left the gel as can be seen in Fig. 2.!

The morphology of encapsulated cells was observed using an EVOS fluorescence microscope over a span of multiple days. By day 8, the cells began to appear elongated on the top of both gels, but with a different distribution (Fig.3). This could be reflecting the different networks of each gelatin/mTG gel.

Future work includes testing the encapsulated cells for differentiation gene expression by RT qPCR and for biomineralization using SEM on days 21 and 40.

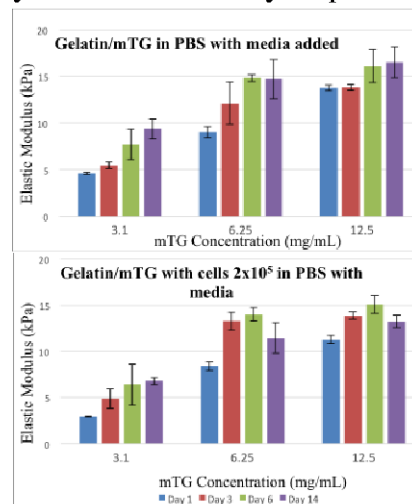


Figure 1: Rheology data of various mTG concentrations over time in media (top) and in media with cells (bottom)

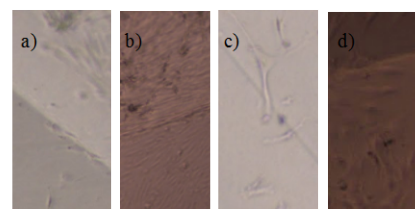


Figure 2: Microscope images of DPSC in gel. a) 3.13 mg/mL mTG day 5 b) 3.13 mg/mL mTG day 8 c) 6.25 mg/mL mTG day 5 d) 6.25 mg/mL mTG day 8

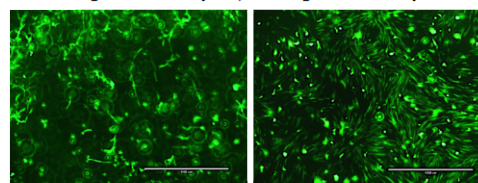


Figure 3: Fluorescent microscope images of DPSC on day 8 in 3.13 mg/mL mTG gel (left) and 6.25 mg/mL mTG gel (right)

References:

¹Kabir, Ramchandra, et al. "Imperative Role of Dental Pulp Stem Cells in Regenerative Therapies: A Systematic Review." *Nigerian Journal of Surgery: Official Publication of the Nigerian Surgical Research Society*, Medknow Publications & Media Pvt Ltd, 2014

²Paguirigan, Amy L, and David J Beebe. "Protocol for the Fabrication of Enzymatically Crosslinked Gelatin Microchannels for Microfluidic Cell Culture." *Nature News*, Nature Publishing Group, 12 July 2007

Investigating the Effects of Cell Plating Density and Surface Topography on Dental Pulp Stem Cell Response to 3D-Printed and Molded Scaffolds

Eunice Yang¹, Maria Dhinojwala², Ian Hsu³, Kuan-Che Feng⁴, Adriana Pinkas-Sarafova⁴, Miriam Rafailovich⁴
¹Mountain View High School, Mountain View, CA 94040; ²Archbishop Hoban High School, Akron, OH 44306;
³Mission San Jose High School, Fremont, CA 94539; ⁴Department of Materials Science and Engineering, Stony Brook, NY 11794

Dental pulp stem cells (DPSCs) are multipotent stem cells that exhibit a large potential for regenerative medicine due to their ability to undergo odontogenic and osteogenic differentiation.¹ Certain features of stem cell microenvironment, such as initial cell plating density and surface topography, have been shown to influence DPSC behavior.² 3D printing is a very promising technique in the field of tissue regeneration, as it creates scaffolds with specific surface topographies. To correlate the effects of cell plating density and surface topography on DPSC behavior, we plated DPSCs of 3 varying densities on 3D printed and molded poly(lactic acid) (PLA) scaffolds.

PLA filament was used to create circular molded and 3D printed scaffolds, each with a diameter of 1.2 cm. We used DPSCs AV3-eGFP cell line in α -MEM medium with 10% FBS and Pen/Strep. On Day 2, the medium was changed to α -MEM medium with 10% FBS, Pen/Strep, 200 μ M ascorbic acid, and 10 μ M β -glycerol phosphate; this media was then changed every other day until the end of the experiment. We used an Alamar Blue[®] cell viability assay each day to determine the cell number by the optical density.

An SEM analysis revealed that the 3D printed surfaces were rougher than molded surfaces, with sharkskin pattern³ ranging from the nanoscale to the milliscale (Fig. 1 a and b). The contact angle analysis of the scaffolds indicated that the 3D printed scaffolds are more hydrophilic than the molded scaffolds, as the 3D printed scaffold had an average contact angle of 44.53°, while the molded scaffolds had an average contact angle of 56.68°.

Further, human DPSCs (hDPSCs) were plated on the scaffolds placed on 2% agarose gel coated plates at 3 concentrations: 3000, 6000, and 9000 cells/mL. Our early stage data showed that the molded scaffolds had a higher cell population than their 3D printed counterparts but had similar doubling times, indicating that DPSCs do not attach as well to the 3D printed scaffolds. Interestingly, after calculating cell plating efficiencies, we found that the 3D printed and molded scaffolds had similar plating efficiencies at a plating density of 6,000 cells/mL (Fig.2). This suggests that there is a relation between surface topography and optimal plating density. Laser scanning confocal microscopy was used to further analyze cell attachment, as the images show a larger population of cells well spread out across the molded scaffolds, as compared to the sparser configuration of the DPSCs on the 3D printed scaffolds (Fig. 1,c and d).

RT-PCR, SEM, and confocal microscopy analysis will be conducted after Day 28 and Day 35 to study the differentiation and biomineralization of DPSCs in late stage. Additionally, because the DPSCs were not attaching as well onto the 3D printed scaffold as the molded scaffold, a second cell plating trial will be performed with higher cell concentrations: 6000, 9000, and 12000 cells/mL.

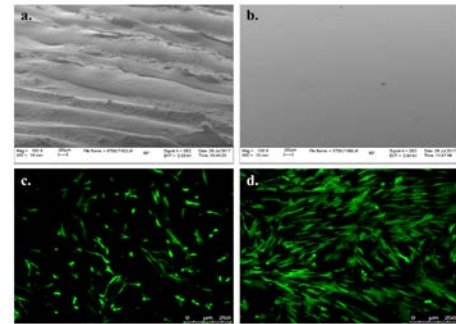


Fig. 1 | a. SEM image of 3D printed PLA, b. SEM

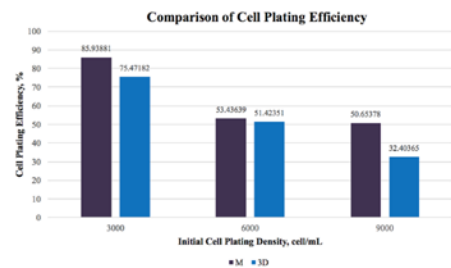


Fig. 2 | Graph of cell plating efficiency for 3D and molded scaffolds at each density

¹Cao, Y., Song, M., Kim, E., Shon, W., Chugal, N., Bogen, G., Kang, M. (2015). Pulp-dentin Regeneration. *Journal of Dental Research*, 94(11), 1544-1551. doi:10.1177/0022034515601658

²Kanafi, M. M., Pal, R., & Gupta, P. K. (2013). Phenotypic and functional comparison of optimum culture conditions for upscaling of dental pulp stem cells. *Cell Biology International*, 37(2), 126-136. doi:10.1002/cbin.

³Kanev, D., Takacs, E., Vlachopoulos, J. (2007). Rheological Evaluation and Observations of Extrusion Instabilities of Biodegradable Polymers. *International Polymer Processing Journal of the Polymer Processing Society*, 22(5), 395-401. doi: 10.3139/217.2053

The Influence of Titanium Dioxide Nanoparticles Underlying Polybutadiene on Differentiation Properties of Dental Pulp Stem Cells

Emily Ma¹, Zachary Katz¹, Ya-Chen Chuang², Oliver Xu³, Miriam Rafailovich²

¹Paul D. Schreiber High School, Port Washington, NY 11050, ²Department of Materials Science and Engineering, SBU, Stony Brook 11794, ³University of California, Los Angeles, Los Angeles, CA 90095

Millions of Americans receive dental or joint implants annually, and researchers project that this number will only grow as life expectancy increases.¹ However, problems arise with current types of implants since the surgeries are highly invasive and scientists have difficulty modeling the natural tissue. Thus, regenerative stem cell therapies have gained prominence in recent years as an alternative to traditional implants. Dental pulp stem cells (DPSCs) are a promising stem cell source since they are easy to extract, are biocompatible, and can differentiate into both odontoblasts and osteoblasts. Currently, titanium and its alloys are among the most common substrates used in dental and bone implants. Unfortunately, titanium implants erode in the human body and create titanium dioxide nanoparticles (TiO₂ NPs). Previously, Hou et al. found that cellular uptake of TiO₂ NPs had a negative impact on stem cell proliferation, adhesion, and differentiation.² The purpose of the present study was to investigate whether embedded and exposed TiO₂ NPs in polybutadiene (PB) have an adverse effect on DPSC modulus, proliferation, and differentiation.

To create growth substrates for DPSCs, silicon wafers were spun cast to produce three types of thin films. Thus, three spin casting solutions were created: 2 mg/mL PB and 0.1 mg/mL TiO₂ (group 1); 5 mg/mL PB and 0.1 mg/mL TiO₂ (group 2); and 3 mg/mL PB (control). After spin casting, the films were characterized using atomic force microscopy (AFM), scanning electron microscopy (SEM), and energy dispersive x-ray spectroscopy (EDS). AFM and SEM scans revealed that the 2 mg/mL PB & 0.1 mg/mL TiO₂ film had many small TiO₂ NPs distributed on top of and embedded within its surface. In contrast, there were a small number of TiO₂ NP aggregates observed on top of the 5 mg/mL PB & 0.1 mg/mL TiO₂ film. Thus, the 2 mg/mL PB film better represented a degraded implant.

DPSCs (line AX3, passage 5) were grown on the spun cast wafers in microtiter plates. The cells were supported by an osteogenic medium with an α -MEM base. On days 1, 4, and 8 after plating, the DPSCs were analyzed using confocal microscopy and AFM. For the confocal microscope, cells were fixed with 10% formalin and then stained with DAPI and AF488 dyes to show nuclei and actin, respectively. DPSC morphology was imaged, and cell stretching indicated that they were healthy. On day 8, group 1 appeared to be almost fully confluent and demonstrated cell stretching (Figure 1 h). Cell proliferation was also calculated using confocal microscopy. Using a one-tailed t-test, a statistically significant increase ($p < 0.05$) was found when comparing group 1 and the control on day 8 (Figure 1 a). The AFM was used in low-force contact mode to determine the shear modulus (hardness) of the DPSCs. Cell modulus increased over time for almost all cases.

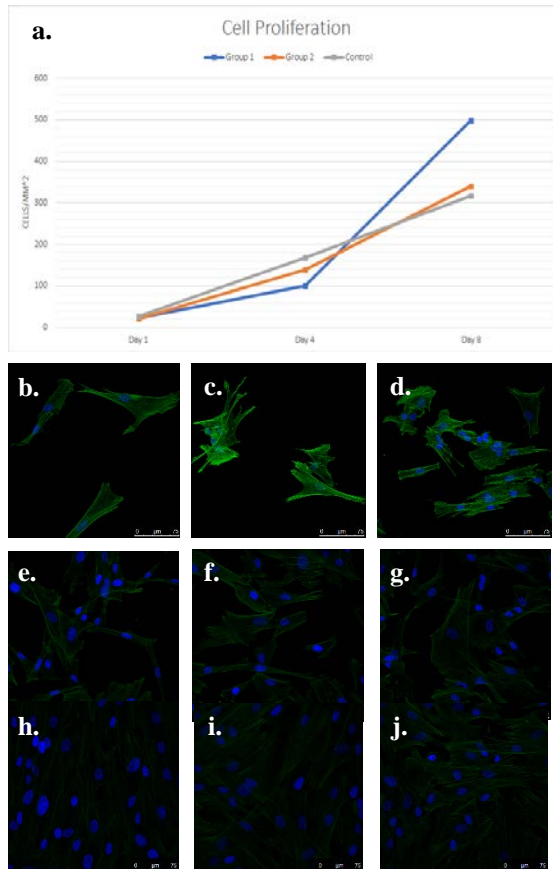


Fig. 1 | a. Graph of cell proliferation on each film group; b. confocal image of group 1 on day 1; c. confocal image of group 2 on day 1; d. confocal image of control on day 1; e. confocal image of group 1 on day 4; f. confocal image of group 2 on day 4; g. confocal image of control on day 4; h. confocal image of group 1 on day 8; i. confocal image of group 2 on day 8; j. confocal image of control on day 8

¹ Kremers, Hilal Maradit, Dirk R. Larson, Cynthia S. Crowson..., and Daniel J. Berry. "Prevalence of Total Hip and Knee Replacement in the United States." *The Journal of Bone and Joint Surgery-American* Volume 97.17 (2015): 1386-397. Web.

² Hou, Yanhua, Kaiyong Cai, Jinghua Li, Xiuyong Chen, Yan Hu..., and Min Lai. "Effects of titanium nanoparticles on adhesion, migration, proliferation, and differentiation of mesenchymal stem cells." *International Journal of Nanomedicine* (2013): 3619. Web.

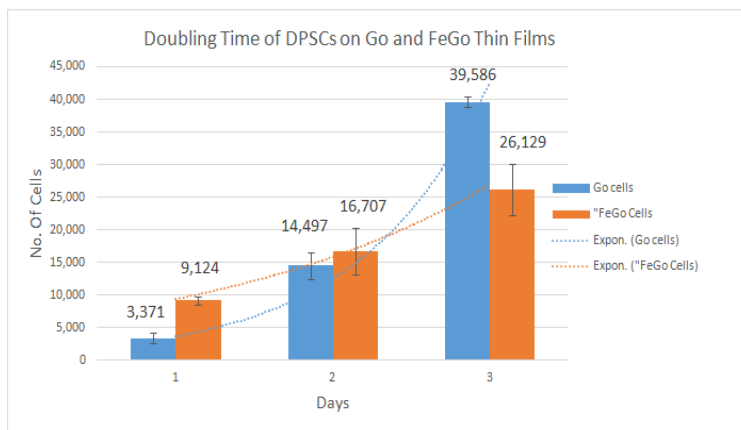
Utilizing Magnetic Graphene Oxide/Iron Carbonyl thin films to Promote Dental Pulp Stem Cell Differentiation

Anoushka Guha¹, John Chen¹, Zaiff Khan¹, Rebecca Isseroff¹, Simon Lin², Juyi Li³, Dr. Miriam Rafailovich³

¹Lawrence High School, Cedarhurst, NY 11581, ²State University of New York at Stony Brook, Stony Brook, NY, 11794, ³Department of Material Science and Engineering, State University of New York at Stony Brook, Stony Brook, NY, 11794

Dental pulp stem cells(DPSCs) are known to proliferate and differentiate into various types of cells such as bone cells, neural cells, dentin, odontoblasts, and osteoblasts which shows hope in the area of bone and tissue regeneration.¹ On different surfaces, the DPSCs may differentiate into numerous cells due to substrate mechanics which include many factors such as topography and cell modulus.² A substrate such as graphene oxide(GO) and iron pentacarbonyl/graphene oxide(FeGO) has the potential to stimulate differentiation in a magnetic field. This experiment compares GO, FeGO, and FeGO with a magnetic field all combined with PLA as substrates on a silicon wafer to plate DPSCs using tests such as doubling time, cell modulus, RT-PCR, scanning electron microscope(SEM) and the confocal microscope to analyze each substrate.

In order to spin-cast a thin film of PLA/GO and PLA/FeGO, a solution of pure PLA was created using chloroform as the solvent(3.5mg/mL-50 to 80nm). Next, graphene oxide solution was made by dissolving GO flakes in water (1mg/mL) which was sonicated and then centrifuged. The resulting GO supernatant was dried in a vacuum oven which made GO flakes. 1% of GO was added to the PLA/chloroform solution, sonicated for 30 minutes and then stirred overnight. Once the GO was suspended in the PLA/chloroform, it was spin-casted onto clean silicon wafers and annealed for three days(40-50°C). This process was repeated to make a thin film of FeGO/PLA. 15,000 DPSCs were plated onto each silicon wafer to grow for 28 days in the incubator. The three groups plated were PLA/GO, PLA/FeGO and PLA/FeGO with magnets. The first test was doubling time on days 1,2 and 3(Figure 1). This test showed that GO had a faster doubling time than FeGO while FeGO had a steady growth rate.



Future work includes analyzing the silicon wafers which continue to grow on the 28-day process while 4 more groups are added to the cell plating process including pure PLA as the control group and reduced GO, reduced FeGO, and reduced FeGO with magnets which will be analyzed and prepared with the same methods and tests. Each of these surfaces will be compared in their abilities to promote DPSC differentiation

to be used for bone regeneration.

¹Yun-Jong Park, Seunghee Cha, and Young-Seok Park, "Regenerative Applications Using Tooth Derived Stem Cells in Other Than Tooth Regeneration: A Literature Review," Stem Cells International, vol. 2016, Article ID 9305986, 12 pages, 2016. doi:10.1155/2016/9305986

²Nuti, N., Corallo, C., Chan, B.M.F. et al. Stem Cell Rev and Rep (2016) 12: 511. <https://doi-org.proxy.library.stonybrook.edu/10.1007/s12015-016-9661-9>

Investigating the Differentiation and Proliferation of Human Dental Pulp Stem Cells Regulated by TiO₂ Nanoparticles Added Before and After Substrate Recognition

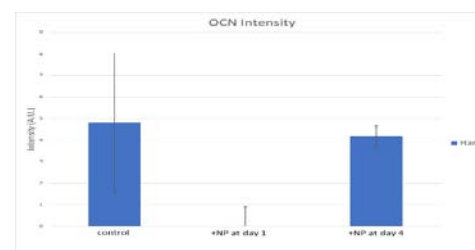
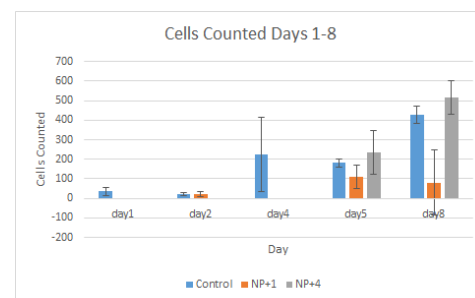
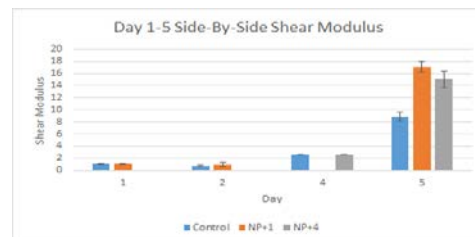
Richard Zhu¹, Michael Wang², Yuqing Liu³, Ya-Chen Chuang⁴, Oliver Xu,¹ Dr. Miriam Rafailovich⁴, Dr. Adriana Pinkas-Sarafova⁴

¹Edina High School, Edina, MN; ²Aragon High School, San Mateo, CA; ³Texas Academy of Math and Science, Denton, TX; ⁴Department of Materials Science and Engineering, Stony Brook, NY

Stem cells have the distinct ability to proliferate and differentiate into a multitude of different cell types. Dental pulp stem cells (DPSCs) in particular are interesting because of their accessibility and multipotent differentiation. Titanium Dioxide nanoparticles (TiO₂ NPs) are cytotoxic but useful due to many factors, including their low cost, strength, chemical inertness, and antibacterial properties. This study aims to combine DPSCs and TiO₂ NPs by investigating the effects of adding the particles at different time points on DPSC viability, proliferation, and differentiation, which can be extended to include other nanoparticles and cells³ and has applications in many fields including drug delivery.

Hard polybutadiene (PB) films were prepared by spin casting a solution into 20 nm thin films on Si wafers. Cells were placed over many samples, with three groups of samples: TiO₂ NPs added to DPSCs on days 1 (NP-1) and 4 (NP-4) as well as the control group with no NPs added. The concentration of 0.1 mg/mL for the TiO₂ was chosen for its lack of significant toxicity², and the day 4 time frame was chosen because of the large increase in shear modulus and difference in mechanical properties after that day, which is seen in the control bars in Figure 1. Contact mode AFM was used to measure the shear modulus of the samples at key days, and certain samples were given actin, nuclei, and osteocalcin stains (AF488, DAPI, and OCN antibody, respectively) to be viewed under the confocal and fluorescent microscopes to be counted and have the intensity measured. Focused Ion Beam Scanning Electron Microscopy (FIB-SEM) was performed on days 2 and 5, marking 1 day after adding the nanoparticles to obtain the cross section of the cell samples. Scanning Electron Microscopy (SEM) was performed on day 21 to examine the biomineralization of the samples.

As shown in Figure 2, the proliferation of the NP-4 cells was very similar to the Control, and Figure 3 shows that the NP-4 cells did not have its biomineralization or osteocalcin expression significantly affected while the NP-1 cells were suppressed almost completely. The suspected reason for this difference is a different uptake mechanism, which was illustrated in the cross-section SEM and Figure 1. NP-1 cells viewed on day 2 showed particles individually permeating the membrane, while NP-4 cells viewed on day 5 had large aggregates seemingly taken in vesicles, targeting specific intracellular locations while leaving the DPSCs unharmed.



³ Shakeel, Muhammad, et al. "Toxicity of Nano-Titanium Dioxide (TiO₂-NP) Through Various Routes of Exposure: a Review." *Biological Trace Element Research*, vol. 172, no. 1, Nov. 2015, pp. 1–36., doi:10.1007/s12011-015-0550-x.

² Pan, Zhi, et al. "Adverse Effects of Titanium Dioxide Nanoparticles on Human Dermal Fibroblasts and How to Protect Cells." *Small*, vol. 5, no. 4, 2009, pp. 511–520., doi:10.1002/sml.200800798.

Assessing the modulus of the cellular and extracellular matrices and the motility of MDA-MB-231, MDA-MB-4175, MCF-7, and MCF-10A normal and cancerous ductal breast cells

Angelina Franqueiro, Sachem High School North, 212 Smith Rd., Ronkonkoma, NY

Gemma Schneider, Roslyn High School, 475 Round Hill Rd, Roslyn Heights, NY 11577

Siobhan Milan, Southside High School, 140 Shepherd St, Rockville Centre, NY 11570

Jeremy Wang, Cornell University

Miriam Rafailovich, Kao Li, Department of Material Sciences and Chemical Engineering, Stony Brook University, Stony Brook NY 11794

It is of great importance that we understand the progression of cancer as it approaches a metastatic state, as 90% of cancer-related deaths are a result of metastasis^[1]. While some studies focus on the genetics of cancer development^[2], our research places an emphasis on the material science and biophysical aspects of the disease. Previous studies have shown that the softness/rigidity of a cancer cell and its extracellular matrix (ECM) are inversely proportional. We hypothesized that the more aggressive the cancer cell line, the softer the cellular matrix and the stiffer its ECM and, consequently, the higher the cell's motility. By means of atomic force microscopy (AFM), we intend to establish an association between the cells' modularity and metastatic properties.

In our study, we focused specifically on four ductal breast cancer lines: MCF-10A, MCF-7, MDA-MB-231, and MDA-MB-4175. We plated the cells on sulfonated polystyrene (SPS) coated silicon wafers at a density of 5,000 cells/cm². Four microwells were then layered with 300µl of melted 2% agarose-PBS; thereafter, a cell-plated SPS wafer chip was added to each well. Following a 48 hour period of CO₂ incubation, AFM was used to observe the ECM and cell moduli of MDA-MB-231 and MDA-MB-4175 cells that were plated on both SPS wafers and tissue culture plastic. The experimental control used was an SPS coated wafer that forwent cell plating. It was found that both the MDA-MB-231 and MDA-MB-4175 were softer than the SPS surface, and that their moduli were similar with relatively small values of deviation. Interestingly, the ECMs of both cell lines were undetectable.

In the future, we plan to perform AFM trials that incorporate the usage of a media-coated SPS chip (control) and all four (MCF-10A, MCF-7, MDA-MB-231, and MDA-MB-4175) cell lines. We also intend to use AFM to investigate the moduli of dermal fibroblasts; we hypothesize that their physical makeup will be quite similar to that of the MCF-10A cells. Additionally, we will use agarose droplets and sequential imaging techniques to aid in an investigation of cell migration. Through this migration assay, we hope to gain insight on the connection between cell modularity and migratory tendencies. Moreover, in an effort to better understand the foundation of the observed biophysical differences among cells (specifically rigidity and motility), we plan to study the composition of the cellular matrix and ECM via confocal microscopy and Alexa Fluor staining procedures.

1. Weiss, Marissa C. "U.S. Breast Cancer Statistics." Breastcancer.org. N.p., n.d. Web. 4 Aug. 2017.

2. Lekka, Malgorzata. "Discrimination Between Normal and Cancerous Cells Using AFM." BioNanoSci. (2016): 1-16.

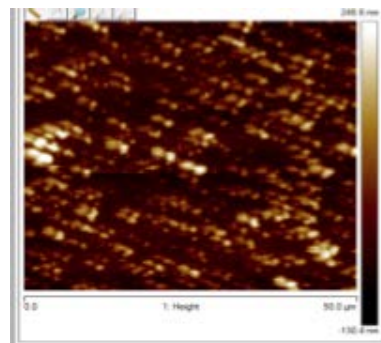


Figure 1. AFM analytics: topography of MDA-MB-231 ECM

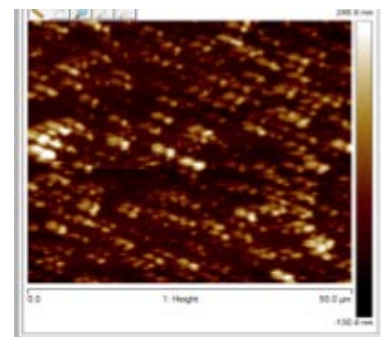
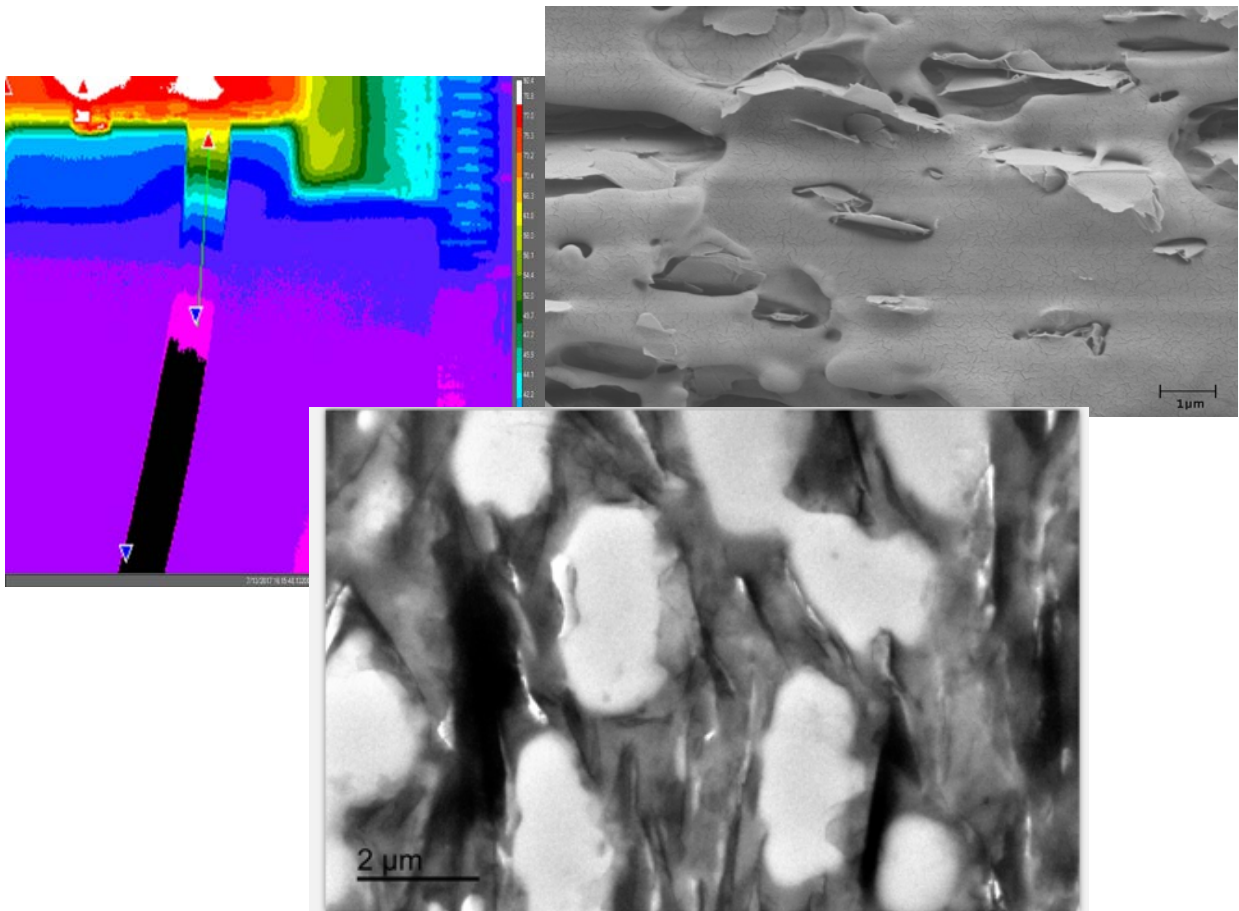


Figure 2. AFM analytics: topography of MDA-MB-4175 ECM

Session III : Graphene Nanocomposites

**Graduate Student Mentors: Yuval
Schmueli, Yichen Guo, Xianghao Zuo,
Yuan Xue, Joshua Weinstein**



Enhancing the Mechanical Properties of Polymers with Graphene Nanocomposites

Danielle Luntz¹, Kasim Waqar¹, Kavya Rao¹, Marc Gottlieb², Rahat Ullah³, Effy Tang⁴, Yichen Guo⁵, Yuan Xue⁵, Miriam Rafailovich⁵

¹Half Hollow Hills High School East, Dix Hills, NY

²Cooper Union, Manhattan, NY

³State University of New York at Stony Brook, Stony Brook, NY

⁴Mater Dei High School, Santa Ana, CA

⁵Department of Material Science and Engineering, State University of New York at Stony Brook, Stony Brook, NY

Graphene is currently the strongest, thinnest, lightest and most thermally conductive material discovered¹. This material has the potential to improve the properties of other popular materials, especially plastics. The plastics market will be valued at \$654 billion by 2020 and can be enhanced using graphene nanocomposites². Polymer blends may offer many benefits over alternative materials due to their flexibility, cost efficiency, and non-corrosive properties. This experiment aimed to bolster the strength and thermal conductivity of various polymer blends by incorporating graphene H-5.

Samples of PP/PMMA, PP, PS/PMMA, and PS with varying graphene concentrations were created using a CW Brabender, and were then molded with a Carver Hot Press to perform mechanical tests. Tensile tests were conducted five times for each sample in order to determine stress versus strain capabilities for each blend. Izod impact tests were performed five times per sample and the average of the impact strength was calculated for each copolymer blend. Thermal conductivity was tested to measure the heat flow through each sample.

The thermal conductivity results show that graphene-loaded samples of PP-PMMA conducted heat better than pure PP due to the percolation of graphene at a lower concentration (Figure 1). Addition of graphene to the samples significantly improved thermal conductivity for all polymer blends tested. Izod impact test show the pure PP sample had an impact strength above 25 J/m (Figure 2). However, as graphene concentration increased, a gradual decrease in strength was observed. We observed that the addition of any amount of graphene to PP increased the tensile strength to about the same value near 25 MPa compared to the control being at around 15 MPa, hence, improving flexibility (Figure 3).

Future work includes testing and evaluating rheology and dynamic mechanical properties of the copolymer blends. Analysis by transform electron microscopy (TEM) could explain differences in the observed properties of the copolymer blends. Also, further testing could compare the effect of GNP size (H-5 versus H-25) on mechanical properties of polymers.

¹Fuente, Jesus de La. "Article." Graphenea. N.p., n.d. Web.

²Research, Inc. Grand View. "Plastics Market Worth \$654.38 Billion By 2020: Grand View Research, Inc." PR Newswire: news distribution, targeting and monitoring. PRNewswire, 06 Aug. 2017. Web.

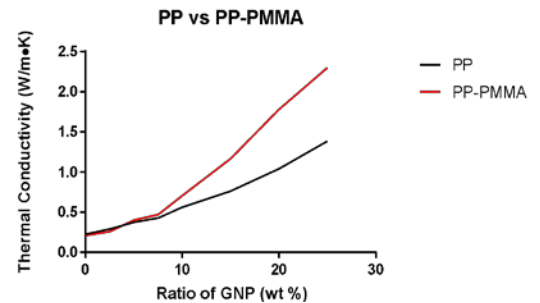


Figure 1: Thermal
PP

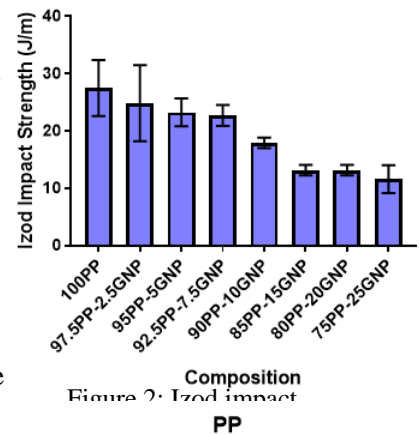
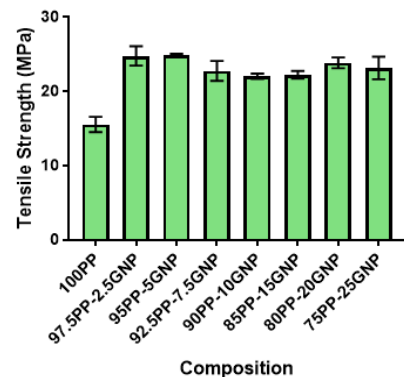


Figure 2: Izod impact
PP



Composition

Thermal Conductivity of Nanocomposites in the FDM 3D Printing Process

Justin Chen¹, Thomas Howell², Max Porter³, Joshua Weinstein⁴, Yuval Shmueli⁴, Miriam Rafailovich⁴

¹Arcadia High School, Arcadia, CA 91007; ²Ward Melville High School, East Setauket, NY 11733; ³Hollis Brookline High School, Hollis, NH 03049; ⁴Department of Materials Science and Chemical Engineering, Stony Brook University, Stony Brook, NY 11794

3D Printing is an emerging technology with applications for rapid prototyping, industrial manufacturing, and hobbyist use. A common and affordable method of 3D printing is fused deposition modeling (FDM), in which filament is melted and layered via extrusion through a nozzle.¹ Currently, bond strength between the deposited filaments suffers as a result of the poor thermal properties of available printing materials, leading to poor mechanical properties in printed product.² Furthermore, the poor thermal properties exhibited by 3D printing materials limit the method's usefulness, as many engineered systems, such as heat exchangers and thermal management devices, require materials with high thermal conductivities to effectively transfer heat from one medium to another.

Polylactic acid (PLA) and polypropylene (PP) are two thermoplastic polymers that have gained attention in recent years as increasingly popular materials for FDM printing, but neither polymer exhibits high thermal conductivity. Graphene nanoplatelets (GNP), nanoparticles made from several small layers of graphene, inherit many properties of two-dimensional graphene, including high thermal and electrical conductivity. Boron nitride (BN) has a hexagonal lattice structure similar to that of graphene and a similar high thermal conductivity. Due to the favorable thermal properties of these nanoparticles, a polymer nanocomposite with GNP or BN will also have improved thermal conductivity.

In the present study, we fabricated composite materials of the polymers, PP and PLA, with the additives, GNP and BN, in concentrations of 5%, 10%, and 20% of the nanoparticles, and then extruded filaments of each material for use in FDM printing. Using a FLIR A300C thermal camera, we analyzed the effect of the additives on the thermal properties of the pure plastics (Fig. 1) and observed that the nanoparticles vastly improved thermal conductivity, in some cases threefold (Fig. 2).

Using an Ultimaker FDM printer, we then created oriented printed samples for testing. Thermal conductivity tests on these printed samples showed that 10% GNP added to PLA increased thermal conductivity by 276%, while adding 10% BN lead to a 70% increase. Scanning electron microscopy (SEM) revealed that fusion between deposited filaments was optimized when extruded filaments were warmer, which demonstrates the need for high thermal conductivity to allow greater heat transfer in printing materials. Furthermore, SEM images showed that the nanoparticles were oriented in the same direction as the filaments, which may explain the large increases in thermal conductivity relative to the amount of additive in the nanocomposites (Fig. 3). Overall, adding graphene and boron nitride to 3D-printed materials leads to greatly improved thermal properties, helping to widen the scope of applications for FDM printing.

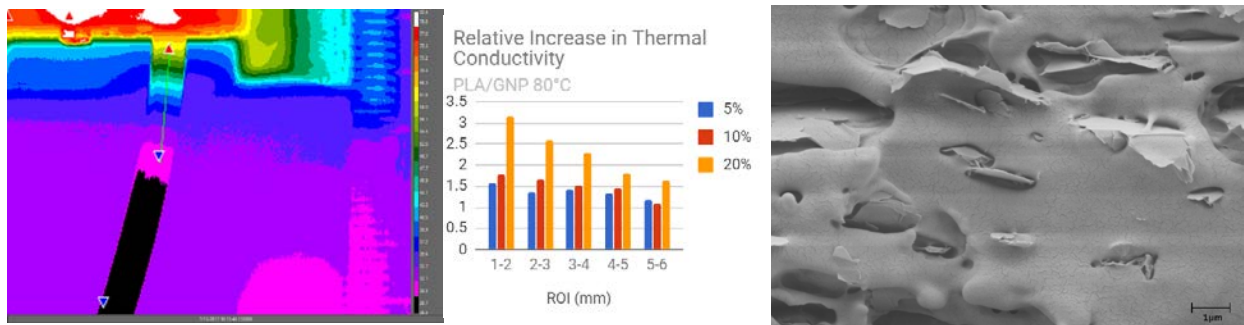


Figure 1. IR imaging of pure PP at 80°C. **Figure 2.** Thermal conductivity of PLA/GNP nanocomposites at varying concentrations. **Figure 3.** SEM imaging of oriented nanoparticles in a printed sample.

¹Wendel, B., Rietzel, D., Kühnlein, F., Feulner R., Hülde, G., & Schmachtenberg, E. (2008). Additive Processing of Polymers. *Macromolecular Materials and Engineering*, 293 (10), 799-809. ²Sun, Q., Rizvi, G.M., Bellehumeur, C.T., Gu, P. (2008). Effect of processing conditions on the bonding quality of FDM polymer filaments, *Rapid Prototyping Journal*, 14 (2), 72--80.

Thermal Enhancement of PBAT/Graphene Composites by Applying PLA as Second Phase Controller

Jinghan Tang¹, Marc Gottlieb², Rahat Ulah³, Yichen Guo³, Yuan Xue³, Xianghao Zuo³, Miriam Rafailovich³

¹Mater Dei High School, Santa Ana, CA 92707, ²Cooper Union, Manhattan, NY 10003, ³State University of New York at Stony Brook, Stony Brook, NY 11794

Heat management has been the main threshold in the fabrication of integrated electronics. In the industry of electronic devices, such as light emitting diodes, heat transfer has become an urgent project that needs to be solved immediately. With the excellent thermal properties, graphene is usually regarded as a significant additive for polymers nanocomposites to help enhancing the thermal stability of polymers.¹ Heat transfer, one of the most important projects in materials science, has been studied for decades. Since polymers have poor ability to transfer heat, we considered graphene can improve the thermal conductivity if well exfoliated in polymer matrix.

In this project, we used a twin-screw extruder (C.W. Brabender) to mix PLA (Poly lactic Acid)/PBAT (polybutyrate adipate terephthalate) blends with different concentrations of graphene (H-5 and H-25) to test the variation of thermal conductivity. A hot pressure was used to mold the specimen for thermal conductivity and mechanical tests. Then, thermal conductivity of the samples was tested using Unitherm™ Model 2022 Thermal Conductivity Instrument. Instron 5542 (Instron Co., Grove City, PA) was used to advance the tensile properties test; this instrument was used in compliance with ASTM D-638, type M. Monitor/Impact Testing Machines Inc. is used to carry on Izod impact tests. The Izod impact tests are according to ASTM D-256 test method.

Previous studies have shown that PLA and PBAT are immiscible.² It was hypothesized that PLA as a second phase can cause better arrangement of graphene in PBAT phase. The results of the thermal conductivity test shows that PBAT/PLA/graphene system will obtain higher heat conduct coefficient than PBAT/graphene composites, which is shown in Fig 1. The TEM

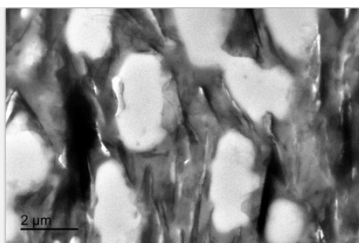


Fig 2. TEM image of PBAT/PLA/20H5

image of PBAT/PLA with 20% H-5 graphene (Fig 2.) shows that PBAT becomes the continuous phase when the ratio of PBAT and PLA is 3:1 and meanwhile graphene can form a continuous path in PBAT matrix, which is also proved by the thermal conductivity data since higher loading of graphene filling in PBAT phase will help building a tight arrangement to transfer heat.

Fig 3. shows the contact angle image, a small piece of polymers were put on graphene layers. The contact angle of PLA droplets on graphene layer is 73.03 while the contact angle of PBAT droplets on graphene is 19.72, which is much smaller. The contact angle indicates that the better intercalation of graphene in PBAT phase than PLA phase.

In conclusion, greatly improvement of thermal conductivity was obtained when graphene added in to polymers. PLA is helpful to help construct the graphene path in PBAT phase. Thus, PBAT/PLA blend is a well-worked system to enhance the thermal conductivity.

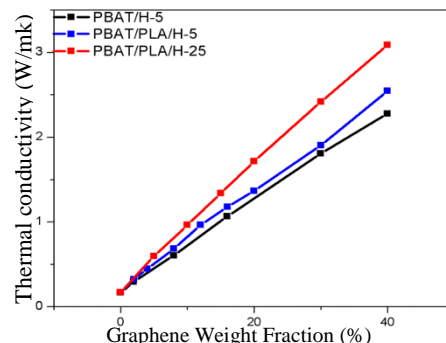


Fig 1. PBAT/Graphene Thermal conductivity

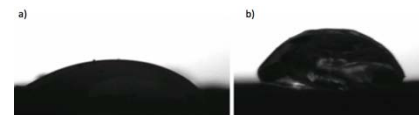


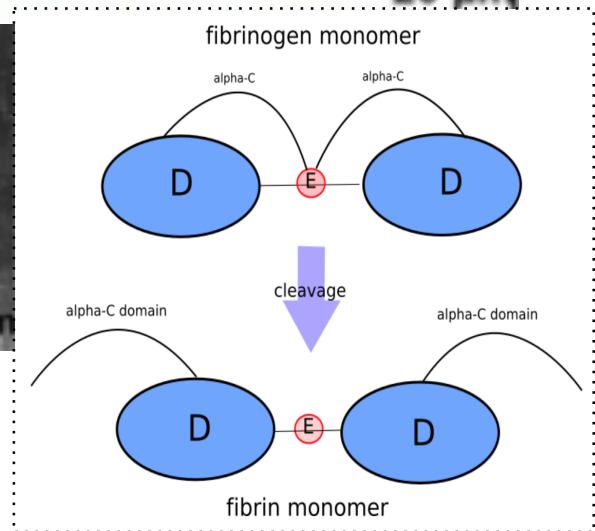
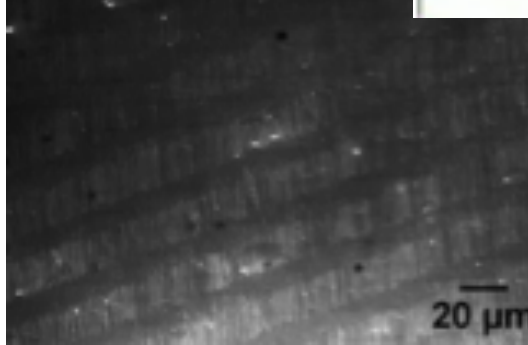
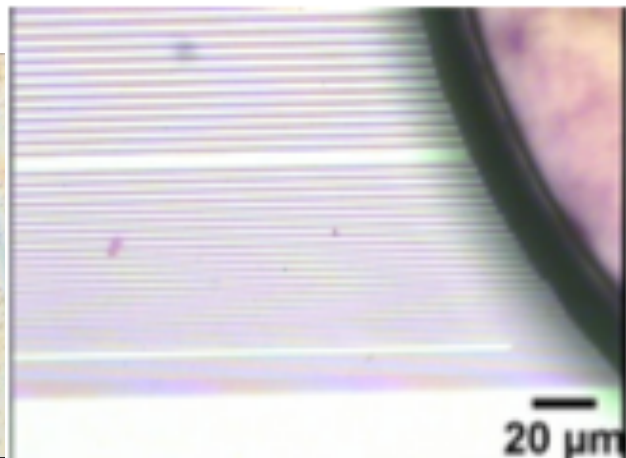
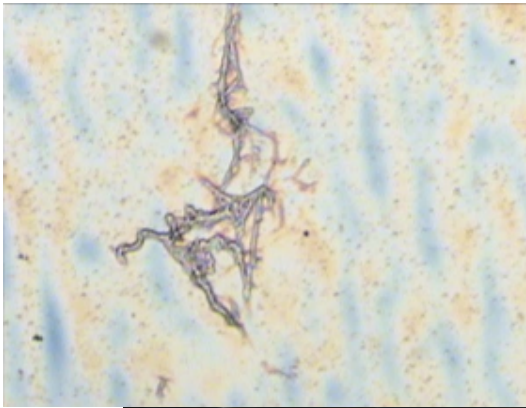
Fig 3. Contact Angle:
a) PBAT on H5 b) PLA on H5

¹Yichen Guo, Shan He, Kai Yang, Yuan Xue, Xianghao Zuo, Yingjie Yu, Ying Liu, Chung-Chueh Chang, Miriam H. Rafailovich, Enhancing the Mechanical Properties of Biodegradable Polymer Blends Using Tubular Nanoparticle Stitching of the Interfaces. ACS Appl. Mater. Interfaces 2016, 8, 17565–17573.

²Wanyoung Jang, Zhen Chen, Wenzhong Bao, Chun Ning Lau, Chris Dames, Thickness-Dependent Thermal Conductivity of Encased Graphene and Ultrathin Graphite. Nano Lett. 2010, 10, 3909–3913.

Session IV: DNA and Proteins on Surfaces

**Graduate Student Mentors:
Donald Liu, Kao Li**



Utilizing microwells and microchannels to improve the efficiency of lithographic enzymatic fragmentation of surface-adsorbed DNA for use in Next Generation Sequencing (NGS)

Albert Tian¹, Dana Waitman², Aaron Singer³, Donald Liu⁴, Christy Siu⁴, Dr. Jonathan Sokolov⁴,
Dr. Miriam Rafailovich⁴

¹Ward Melville High School, NY, 11790, ²The Frisch School, NJ, 07652, ³Davis Renov Stahler Yeshiva High School for Boys, NY, 11598, ⁴Dept. of Materials Science and Engineering, Stony Brook University, Stony Brook, NY

The government-funded Human Genome Project cost over three billion dollars and took over ten years¹ to sequence an entire human genome. However, advances in the field of DNA sequencing, such as Next Generation Sequencing, make it possible to process a larger amount of DNA in a shorter amount of time using massively parallel sequencers. These sequencers require large inputs of fragmented DNA. A significant limitation of all current sequencing methods is the need to fragment DNA into small pieces for analysis. They have to be assembled into the full contiguous sequence from the fragments. The fragmentation is done randomly, with positional order being lost, greatly complicating the assembly process. A newly developed method² of cutting DNA while not disturbing the order involves coating the surface of a polydimethylsiloxane (PDMS) stamp with DNase enzyme and placing the stamp onto linearized DNA adsorbed onto a poly methyl methacrylate (PMMA) coated silicon wafer.³ Experiments were conducted to find a way to get DNase enzyme into microwells and channels transferred to a PDMS stamp using a silicon master. The two methods that were considered were using a vacuum-assisted method to pump DNase through microchannels in the PDMS and slowly dipping and removing the PDMS in a DNase solution, allowing the liquid to remain only in the microwells/channels. Silicon master molds were used to produce soft-lithography stamps. Molds were spin-coated in a solution of PMMA. PDMS was poured onto the (now PMMA coated) silicon wafer. The stamps were left overnight to cure on a hot plate. To test if liquid was going where intended during the first stages of our experiments, different dyes with contact angles similar to that of DNase solutions were used. Using optical and confocal microscopes, it was determined that dye was successfully pumped through the PDMS using the vacuum. As seen in figure 1, channels of various thicknesses were filled with dye by vacuuming the air surrounding a sample. It seems that the vacuum method is effective in filling channels from 4 to 15 micrometers wide with the aforementioned dye. However, when dipped stamps were used to cut lambda DNA, it was confirmed that the surface of the stamp, not the channels, was cutting the DNA (figure 2). In the near future, we hope to vary the dipping conditions in order to preferentially fill the microwells and channels.

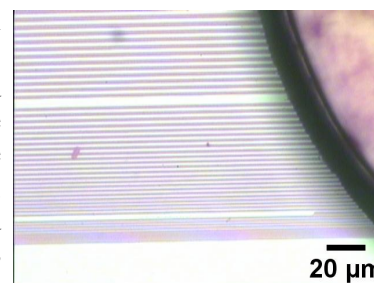


Fig. 1 Optical microscope image of dye running through PDMS channels

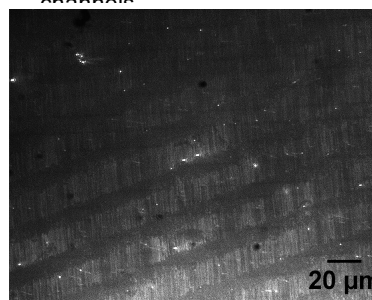


Fig. 2 Confocal images showing linear cuts made using the dipping method

¹ Gitlin, Jonathan Max. "Calculating the Economic Impact of the Human Genome Project." *National Human Genome Research Institute (NHGRI)*, www.genome.gov/27544383/calculating-the-economic-impact-of-the-human-genome-project/.

² Auerbach, Alyssa; Budassi, Julia; Shea, Emily; Zhu, Ke; Sokolov, Jonathan. Controlled enzymatic cutting of DNA molecules adsorbed on surfaces using soft lithography. American Physical Society, APS March Meeting 2013, March 18-22, 2013, abstract #R44.002

³ Auerbach, Alyssa; Budassi, Julia; Shea, Emily; Zhu, Ke; Sokolov, Jonathan. Controlled enzymatic cutting of DNA molecules adsorbed on surfaces using soft lithography. American Physical Society, APS March Meeting 2013, March 18-22, 2013, abstract #R44.002

Synthesis of a water-soluble thin-film for absorption of DNA and subsequent removal

Anthony Del Valle¹, Donald Liu², Christy Siu², Morty Grunseid², Jonathan Sokolov²

¹Ward Melville High School, New York, 11790, ²Dept. of Material Sciences and Engineering, Stony Brook University

The efficient and accurate sequencing of DNA has important applications in biology and medicine. This was the driving force behind projects such as the Human Genome Project in the 1990's. While DNA sequencing has come a long way in terms of technology, further research is required in order to improve current methods with respect to speed, cost and accuracy. The sequencing platforms widely used today involve random cutting of DNA into small fragments (typically 200 to 1000 bases long), followed by sequencing of the fragments and the "assembly" of the fragments into long contiguous

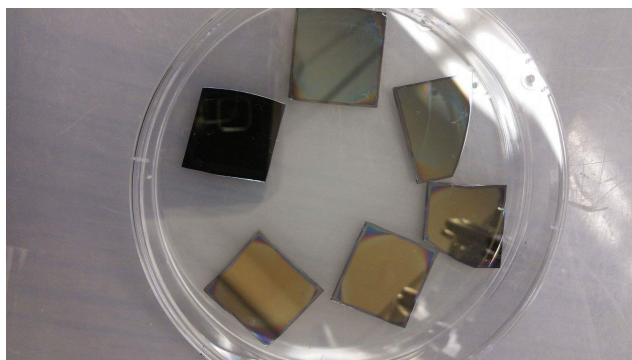


Fig.1 Silicon wafers coated with 5% PAA

sequences. The assembly step could be greatly simplified if the original order of the fragments is preserved. A new method² of DNA fragmentation involved cutting surface immobilized DNA has been developed which has the potential to preserve the order. The DNA must be stretched in a very flat surface (such as a coated silicon wafer), cut, and then taken off in order to be sequenced in a sequencer, such as Pacific Biosciences II But, it is difficult to remove the DNA from the silicon. In order to bypass this, we used a method of adding a sacrificial layer of a water-soluble thin film¹. We also had to make sure that the layer which was coating the silicon was compatible with DNA, as it could easily be damaged or denatured. This led to us creating a solution of poly(acrylic acid) (PAA), Sodium Hydroxide (NaOH) & water, since these substances did not cause the DNA any harm and created a viable water-soluble thin-film. We had to create a solution which could to be spin casted, which meant our solution needed to have a pH of around 7.5. In order to free the solution of any particulates or residue, we filtered it using a .5 micron filter. After this, we scribed and cut the silicon wafers which were to be used in the experiment. We made them around 2cm X 2cm and after treating them to an acid and base cleaning, we put them under vacuum to make sure they were free from contamination. Consequently, we heated the samples to 150 C in order to make sure the film properly adhered to the surface. It was treated with a calcium chloride (CaCl₂) bath to make the film insoluble. Although this apparently worked, its effects were significantly decreased after an hour of being away from the CaCl₂ bath. We tested it the thin-film by adding water to the surface. The surface still showed signs of the film after being thoroughly washed by water as seen in figure 1. After being tested, we deposited lambda DNA onto the film and viewed it using a fluorescence microscope to make sure the DNA was intact. Since we added a droplet of DNA coated in Sybr gold onto the silicon wafer instead of the traditional method of dipping the wafer into the DNA, we didn't see the standard "rain" pattern of DNA. Further work will be done to vary buffer pH and type in order to optimize the DNA absorption.

[1] Linder, V., et al. "Water-Soluble Sacrificial Layers for Surface Micromachining." *Small*, vol. 1, no. 7, 2005, pp. 730-736, SCOPUS, www.scopus.com, doi:10.1002/smll.200400159.

[2] Sokolov, Jonathan; McCombie, Richard, William; Zhu, Ke; Budassi, Julia; Goodwin, Sara; Cho, NaHyun "Fragmentation of surface absorbed and aligned DNA molecules using soft lithography for Next-Generation Sequencing"

Investigating the Viability of PCL and xSIBS As Polymers for Heart Valves and Blood Vessels Through the Use of Fibrin

Emma Johnston¹, Anyerlin Mora², Nathan Sandler³, Kao Li⁴, Miriam Rafailovich⁴, Dennis Galanakis⁵

¹Harborfields High School, Greenlawn, NY 11740, ²Suffolk County Community College, Selden, NY 11784, ³Tufts University, Medford, MA 02155, ⁴Department of Materials Science & Engineering, Stony Brook University, Stony Brook, NY 11794, ⁵Stony Brook University Hospital, Stony Brook, NY

Valve stenosis, valve regurgitation, and leaky valves are just some of many issues that can cause the need for a heart valve replacement. Additionally, blood vessel replacement can be essential in cases of obstruction or destruction. Unfortunately, tissue replacements received from donors are prone to rejection if the tissue that is being used does not closely match the molecular composition of the recipient's tissues therefore risking that the tissue may be attacked and destroyed by the recipient's own immune system. It is for this reason that a new mechanical replacement must be found.

Unfortunately, current mechanical replacements are still very susceptible to complications such as thrombosis and embolism, both of which can cause a clogged artery or vein and possibly a need for further surgical intervention¹. Due to this, any novel polymers that have the mechanical properties necessary for a heart valve, such as styrene isoprene butadiene, or a blood vessel, such as polycaprolactone, must be examined thoroughly to test how prone they are to fiber formation when thin films of the polymer come into contact with fibrin solutions [Figure 1].



Figure 1. A fiber that formed overnight on a thin film of xSIBS.

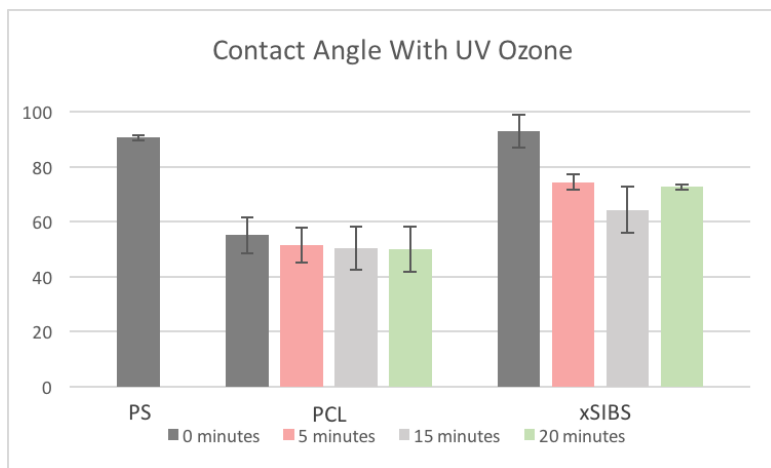


Figure 2. This chart shows the average contact angle of DI water on various polymers after they are exposed to UV ozone for varying periods of time.

Additionally, previous studies have shown that fibrinogen fibers do not form on hydrophilic surfaces². It is for this reason that we also investigated the impact of UV ozone on fiber formation, as UV ozone has been shown to increase the hydrophilicity of a polymer thin film³ [Figure 2]. If the effects of UV ozone can be modified so that they have increased longevity, this method could render the polymerstransplantable as they will not be as likely to cause clotting complications in patients as current technologies do.

In order for either xSIBS or PCL to be used as biocompatible materials, a rapid screen must be developed to test if clotting will occur. This study is the beginning of the development of that screening.

¹ Khan, S. S., et. al. "Twenty-year comparison of tissue and mechanical valve replacement." *The Journal of Thoracic and Cardiovascular Surgery* 122.2 (2001): 257-69. Web.

² Zhang, Liudi, et. al. "The influence of surface chemistry on adsorbed fibrinogen conformation, orientation, fiber formation and platelet adhesion." *Acta Biomaterialia* 54 (2017): 164-74. Web.

³ Clark, Theotis, et. al. "A New Application of UV-Ozone Treatment in the Preparation of Substrate-Supported, Mesoporous Thin Films." *Chemistry of Materials* 12.12 (2000): 3879-884. Web.

Examining the Effect of Varying Surface Chemistries and Its Influence on the Growth of Fibers

Nupur Dave¹, Yingyue Liu², Nathan Sandler³, Anyie Mora⁴, Kao Li⁵, Miriam Rafailovich⁵, Dr. Dennis Galanakis⁶

¹John Foster Dulles High School, Sugar Land, TX 77479, ²General Douglas MacArthur High School, Levittown, NY 11756, ³Tufts University, Medford, MA 02155, ⁴State University of New York at Stony Brook, Stony Brook, NY, 11794 ⁵Department of Material Science and Engineering, State University of New York at Stony Brook, Stony Brook, NY, 11794, ⁶ Stony Brook Blood Bank, Stony Brook, NY, 11794

Heart disease, such as coronary artery disease (CAD), has become one of the most fatal and recurrent medical conditions worldwide¹. Currently, drug eluting stents (DES) are implanted into the clogged artery and an anti-restenosis drug is released slowly over the time period of 1-2 years until the plaque slowly degrades². Recently, doctors have been investigating the use of biodegradable stents (BDS), which made out of biodegradable polymers, such as polylactic acid (PLA), that deteriorate after 2 years, leaving the artery working naturally. PLA is a common polymer used to make various biomedical devices due to its thermoplastic characteristics and biological inertness. However, stent thrombosis is still a pressing issue that affects about 2-3% of all CAD patients³. Thrombosis occurs when foreign materials are implanted in the body, causing blood clots in vessels and thus a disruption in the circulatory system. Fibrinogen, an important protein monomer, cleaves into fibrin molecules that eventually form fibers. Fibrinogen is an integral component in the hemostasis and coagulation. When foreign materials are implanted, fibrinogen monomers often clot together and adhere onto the stent, consequently obstructing the circulatory system which could be fatal. In this research, we investigate fibrinogen growth while changing surface chemistry on PLA to prevent stent thrombosis.

Solutions of pure PLA ($M_w=60k$) and manufactured PLA ($M_w=50k$) were dissolved in chloroform while PMMA ($M_w=120k$) and PS ($M_w=200k$) were dissolved in toluene to create polymer solutions of 15 mg/mL concentration.

The solutions were then spin casted onto silicon substrates of Miller Index [100] and annealed overnight.

Additionally, a PLA mold was created by molding pure PLA into small cylinder molds through the hot press. Furthermore, a stent structure out of pure PLA was 3D printed to test the fibrinogen growth. To alter the surface chemistry, some samples were then tested in the UV Ozone for various amounts of time. PLA and PMMA

samples were tested in the UV Ozone for 1, 4, 10, 15, 30, 45 minutes, and then the contact angles were measured using the goniometer to test for increased hydrophilicity.

The optimal time was determined to 20 minutes, as the contact angle dropped by 6° (PLA spin casted), 17° (PLA molded) and 15° (PMMA) (Fig 1). This shows that the hydrophilicity was induced the most by the UV Ozone. The controls were designated as the wafer that was coated with PS, without any UV Ozone, to study *in vitro* growth of fibrinogen. The wafers were then submerged in fibrinogen solution (donated by the SBU Blood bank) for 8 hours for full fiber development. We tested p17, a solution with high concentration of fibrinogen, and 50p, normal concentration of fibrinogen. The samples were characterized using optical microscopy (Fig 2) and the atomic force microscope.

The p17 high fibrinogen solution was first tested on PS and PLA spin casted samples, but minimal fibers were shown, ~0.74%. This lead to the conclusion that with high fibers, the fibrinogen monomers attach to the surface but the fully formed fibers never attached. The 50p solution formed fully formed fibers on our PS and PLA controls, so that was used for future experiments. The fiber area from the PS control was 40.75%. On the PLA spin casted, fibers and clots made up 19.41% of the sample and the mold was 1.14%. On the non-UV Stent, there were significant amounts of fiber growth, showing that *in vivo* (Fig 3), PLA attracts fibrinogen monomers despite its bio-friendly properties. The surface chemistry after treating our samples in the UV Ozone for 20 minutes, the percentage dropped to 0.006% (PLA Spincasted) and 0.04% (PLA molded). After 30 minutes, it rose back up to 0.128% (PLA Spincasted) (Fig 4). The induced hydrophilicity prevented the fibrinogen monomers from attaching onto the surface, preventing full grown fibers from forming. For future study, antibodies will be placed on the PLA, PMMA and PS samples to observe the fibrinogen monomer distribution and orientation on the substrate. Furthermore, endothelial cells should be placed to test cell adhesion onto the different polymer surfaces and stent surface chemistries.

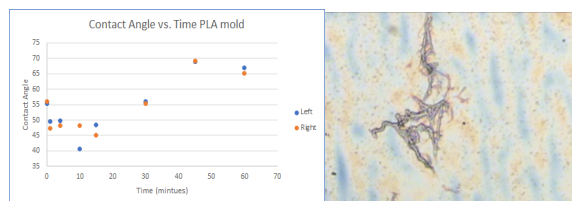


Fig 1. Graph comparing contact angle vs time on PLA mold sample. Shows the lowest angle is found at 15 min. Fig 2. Optical Microscope images of 50p normal fiber concentration solution on PLA film coated on silicon substrate.

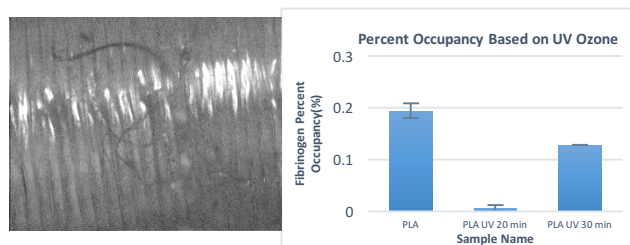


Fig 3. Optical Microscope image of fully grown fiber on pure PLA stent surface. Fig 4. Bar graph showing fiber occupancy (area of fibers/area of samples) compared by UV Ozone/ surface chemistry.

¹Byrne, R. A., Joner, M., & Kastrati, A. (2015). Stent thrombosis and restenosis: what have we learned and where are we going? The Andreas Gruntzig Lecture ESC 2014. *European Heart Journal*, 36(47), 3320-3331.

²Drug-Eluting Stents - Part I." *Drug-Eluting Stents I*. N.p., n.d. Web. 06 Aug. 2017

³Iakovou, Ioannis. "Thrombosis After Stent Implantation: How Much of a Problem Is There?" *Medscape*. N.p., n.d. Web. 06 Aug. 2017.

P12 Peptide's Effects on Inhibiting Fibrinogen Fiber Formation in Blood Coagulation and Application of Machine Learning in Fiber Counting

Thomas Chen^{1*}, Kevin Gao^{2*}, Alexander Wang^{3*}, Kao Li⁴, Anyie Mora⁴, Nathan Sandler⁵, Dennis Galanakis⁴, Miriam Rafailovich⁴

¹Mission San Jose High School, Fremont, CA 94539, ²Amador Valley High School, Pleasanton, CA 94566, ³Dougherty Valley High School, San Ramon, CA 94582, ⁴Department of Materials Science and Engineering, Stony Brook University, Stony Brook, NY 11794, ⁵Tufts University, Medford, MA, 02155

*These authors contributed equally to this work

Fibrinogen is a glycoprotein that plays a key role in blood coagulation, an essential process in wound healing. Usually, it cannot form fibers or clots without first being cleaved by thrombin, as shown in Figure 1. However, recently it has been shown that fibrinogen monomers can adsorb onto hydrophobic surfaces via their hydrophobic D and E regions¹, thus exposing their alpha-C domains for other monomers to attach to. As more monomers attach, the resulting chain of monomers can become a large fiber that provides the structural support for blood clots¹. However, blood clotting can prove harmful when

hyper/hypotension, clogged arteries, or surgeries induce clotting within blood vessels. This condition, called thrombosis, clogs arteries, which leads to strokes, heart attacks, and organ failure. P12 is a recently discovered fibronectin derived peptide consisting of 14 amino acids² that has been shown to reduce erythrocyte aggregation in burn wounds³. In this study, we further show that both linear and circular P12 reduces fibrinogen fiber formation by blocking the alpha-C domains from recruiting other monomers. We spuncast monodispersed polystyrene (200k molecular weight) and poly(methyl methacrylate) onto silicon wafers and annealed the wafers. We plated three purified fibrinogen-fibrin solutions—P17 (fibrin-rich), 50P (fibrin-moderate), and 50S (fibrin-poor)—onto the wafers. For each solution, we had two wafers for control, two for linear P12, and two for circular P12. Samples were allowed to grow for 10 minutes, 1 hour, or 8 hours and were cleaned before optical and atomic-force microscopy. ImageJ and Machine Learning were utilized to count the area covered by fibers. Our results demonstrate that the addition of P12 inhibits the formation of fibrinogen fibers. After 8 hours, our control fibrin-rich (P17 and 50P) samples had fully developed fibers and clots whereas both LP12 and CP12 samples had no clots. Using ImageJ analysis, we determined quantitatively that the fiber density on the substrate surface decreased by almost 10 times upon adding either CP12 or LP12. Furthermore, our control results with fibrin-poor 50S show that the presence of fibrin molecules on protofibrils are necessary for clot formation. That is, fibrinogen molecules alone can form a fibrinogen monolayer but no fibers or clots. Antibodies were used to fluorescently label certain sites on the fibrinogen molecules to conclusively show that P12 specifically inhibits the alpha-C domains on fibrinogen molecules, thereby preventing long fibers from forming.

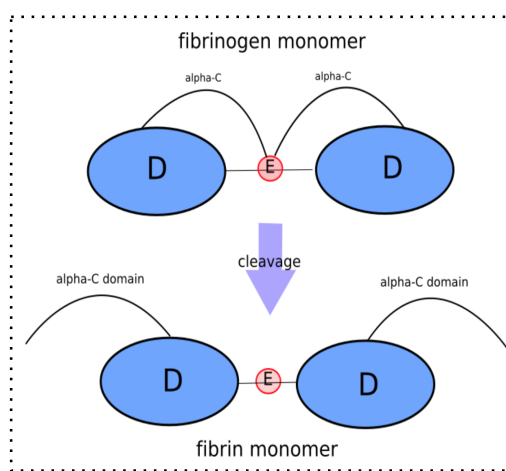


Fig. 1 - Fibrinogen monomer being cleaved into a fibrin monomer

¹ Zhang, L., Casey, B., Galanakis, D. K., Marmorat, C., Skoog, S., Vorvolakos, K., Simon, M., Rafailovich, M. H. (2017). The influence of surface chemistry on adsorbed fibrinogen conformation, orientation, fiber formation and platelet adhesion. *Acta Biomaterialia*, 54, 164-174. doi:10.1016/j.actbio.2017.03.002

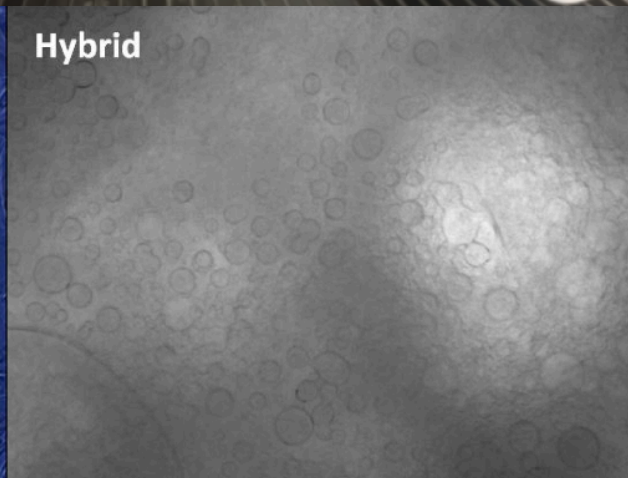
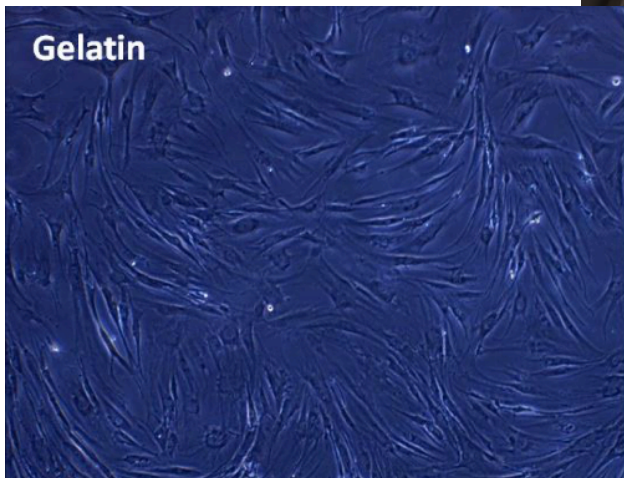
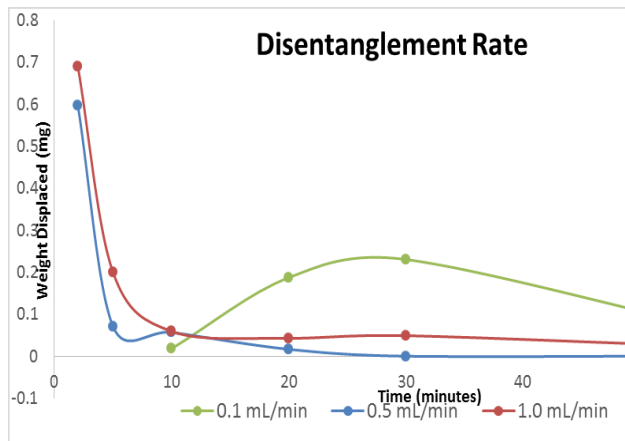
² Ohashi, Tomoo. "A Fibronectin-Derived Cell Survival Peptide Belongs to a New Class of Epiviosamines." *Journal of Investigative Dermatology*, vol. 134, no. 4, Apr. 2014, pp. 882-884., doi:10.1038/jid.2013.470.

³ Asif, Bilal, et al. "Blood Vessel Occlusion in Peri-Burn Tissue Is Secondary to Erythrocyte Aggregation and Mitigated by a Fibronectin-Derived Peptide That Limits Burn Injury Progression." *Wound Repair and Regeneration*, vol. 24, no. 3, 28 Apr. 2016, pp. 501-513., doi:10.1111/wrr.12430.

Session V: Hydrogels

Graduate Student Mentor:

Clement Marmorat



Examining the Integrity of Pluronic[®] F127 for use in Drug Delivery

Atif Akhter¹, Bharvi M. Chavre², Brandon Weiss², Levy Sominsky³, Clement Marmorat⁴, Miriam Rafailovich⁴

¹St. Mary's High School, 51 Clapham Ave, Manhasset, NY 11030

²G.W. Hewlett High School, 60 Everit Ave, Hewlett, NY 11557

³Vanderbilt University, 2201 West End Ave, Nashville, TN 37235

⁴Stony Brook University Department of Materials Science, 100 Nicolls Rd, Stony Brook, NY 11794

Pluronic[®] F127 is a block copolymer comprised of poly(ethylene oxide)-poly(propylene oxide)-poly(ethylene oxide) (PEO-PPO-PEO)^[1]. Pluronic[®] contains micelles, which are aggregates of molecules in a solution. This unique micelle structure gives Pluronic[®] increased solubility and stability, which allows it to have many biomedical applications. Presently, Pluronic[®] is used to deliver anti-cancer drugs to target areas of the body^[5]. In addition, it is being tested for use in the spinal cord for post-surgical treatment^[3]. However, a current problem with hydrogels is finding the correct balance of micelle interaction in a gel for long term drug delivery.

To determine the integrity of the Pluronic[®] gel and its effectiveness when surrounded by physiological fluids, flow tests were conducted utilizing a 3D printed chamber. Three different concentrations of F127 (30%, 27.5%, 25%) were tested at three different flow rates (0.1 mL/min, 0.5 mL/min, 0.9 mL/min) at 37 °C (to mimic conditions in the human body). The flow-through, the resulting liquid at the end of the flow test, was collected in a Falcon[™] tube at the end of the 6 minute test.

UV-Visible Spectrophotometry was conducted to investigate the properties of the gels and the flow-throughs. We found that, in general, at lower flow rates, there is a greater diffusion of Pluronic[®] gel (Figure 1).

PEG, polyethylene glycol, is a polyether compound with many medicinal applications^[4]. It has even been seen to improve nerve impulse connection^[2]. Varying concentrations of 300K and 4000K PEG were combined with 25% F127. We saw that there was some significant increase in the elastic modulus of the Pluronic[®] gel when combined with PEG compared to regular 30% Pluronic[®] gel (Figure 2).

Future works may include in vivo experimentation in mice, which would allow us to see how the gel is affected by different proteins and acids found in the body.

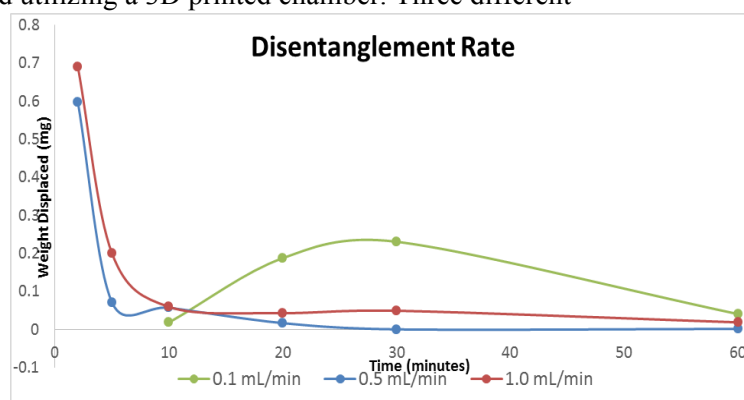


Figure 1: Rate at which 30% Pluronic[®] gel disentangles at different flow rate. Data was compiled from UV-Vis analysis.

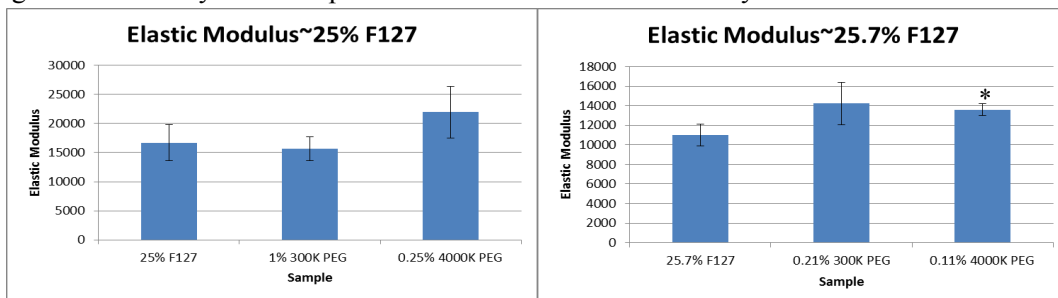


Figure 2: Elastic modulus of different Pluronic[®] gels from rheology. * indicates significance (p-value <0.5)

[1] Akash, M. S. H., & Rehman, K. (2015). Recent progress in the biomedical applications of Pluronic (PF127): Pharmaceutical perspectives. *Journal of Controlled Release*, 209, 120-138. <https://doi.org/10.1016/j.jconrel.2015.04.032>

[2] Borgens, R., Shi, R., & Bohnert, D. (2002). Behavioral recovery from spinal cord injury following delayed application of polyethylene glycol. *Journal of Experimental Biology*, 205, 1-12.

[3] Kabanov, A., Batrakova, E., & Alakhov, V. (2002). Pluronic block copolymers as novel polymer therapeutics drug and gene delivery. *Journal of Controlled Release*, 82, 189-212.

[4] Karaman, S., Karaipckli, A., Sari, A., & Bicer, A. (2011). Polyethylene glycol (PEG)/diatomite composite as a novel form-stable phase change material for thermal energy storage. *Solar Energy Materials & Solar Cells*, 95, 1647-1653.

[5] Raval, A., Pillai, S., Bahadur, A., & Bahadur, P. (2017). Systemic characterization of Pluronic micelles and their application for solubilization and in vitro release of some hydrophobic anticancer drugs. *Journal of Molecular Liquids*, 230, 473-481. <https://doi.org/10.1016/j.molliq.2017.01.06>

The Integration of Graphene Oxide and Reduced Graphene Oxide to Strengthen and Expand Elastic Modulus in F-127 Pluronic Acid Gels

Nicholas Williams¹, Roshan Reddy¹, Rebecca Isseroff¹, Clement Marmorat², Miriam Rafailovich²
Lawrence High School, 2 Reilly Road, Cedarhurst, NY, 11516, Dept of Materials Science and Chemical Engineering, Stony Brook University, Stony Brook, NY, 11794

Recent developments in biomedical technology and surgical procedures have led to the investigation of hydrogels as biocompatible gels for use as filaments in the human body. Following procedures which involve the removal or replacement of bones, structures, or spinal fluids, biocompatible hydrogels may be able to fill in for such parts of the body¹. The intrigue in pluronic hydrogel research is due to their unique structure. Pluronic F-127 gels are created through the formation of micelles resulting from the hydrophobic and hydrophilic characteristics of the PEO and PPO polymer structures which create each individual pluronic chain. The hydrophilic characteristics of PEO cause it to be attracted to water around it, while the hydrophobic characteristics of PPO cause it to retract from any contact with water. These conflicting characteristics in the pluronic chains create the micelle structure, where the hydrophobic PPO segments form the center of the micelles while the hydrophilic PEO segments of the pluronic chains “branch” out from the center of the micelle structures. These micelles form an FCC structure (Face Center Cubic) with the micelles acting as the vertices of the cube. Overall, this gelling property of pluronic F-127 at the same temperature as the normal human body is what brings such potential to the gel when combined with drug delivery and surgical procedures.

Issues surrounding the use of pluronic gels involve its reactions with excess amounts of water and its overall elastic modulus as a gel. For example, for implementation as a substitute for spinal fluid, the pluronic gel must be able to withstand the constant motion of the spinal cord. Furthermore, the gel must have a large elastic modulus so that it does not break or dissipate as the subject moves. In addition, the presence of excess amounts of water in the human body cause the micelle configurations in the gel to break apart, as the PEO intermolecular bonds are not very strong (having only London Dispersion forces to hold them intact). To improve upon the elastic modulus of pluronic and allow it to withstand higher concentrations of water, graphene oxide (GO) and reduced graphene oxide (RGO) have been added to the gel in an attempt to create an intermediary connection between micelle groups which would strengthen the gel as a whole. Theoretically, the added graphene oxide and reduced graphene oxide would allow for the PEO polymer groups to create stronger intermolecular bonds with the functional groups attached to the GO or RGO. Despite such theories, the overall strength of the hybrid gel appeared to decrease in comparison to the pure pluronic gel². One possible explanation for this could be that the RGO and GO sheets within the hydrogel have caused the PEO structures of the pluronic to attach to the sheet as opposed to each other, which disrupted the micelle configuration, thus weakening the gel. Future work will explore alternate methods of crosslinking F-127.

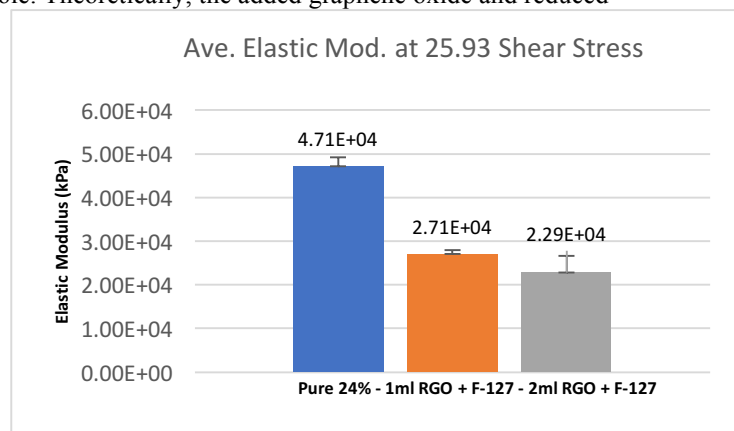


Figure 1: Data table showing elastic modulus of different concentrations of hybrid pluronic gels

1. Niloy Kundu, Arpita Roy, Debasis Banik, Jagannath Kuchlyan, and Nilmoni Sarkar*

Department of Chemistry, Indian Institute of Technology, Kharagpur 721302, WB, India
J. Phys. Chem. C, 2015, 119 (44), pp 25023–25035

DOI: 10.1021/acs.jpcc.5b05251

Publication Date (Web): October 12, 2015

Copyright © 2015 American Chemical Society

2. Sheng-Zhen Zu*† and Bao-Hang Han*†

National Center for Nanoscience and Technology, Beijing 100190, China, and Graduate School of Chinese Academy of Sciences, Beijing 100049, China

J. Phys. Chem. C, 2009, 113 (31), pp 13651–13657

DOI: 10.1021/jp9035887

Publication Date (Web): July 2, 2009

Copyright © 2009 American Chemical Society

Synthesis and Characterization of Gelatin and Pluronic® F127 Hybrid Hydrogels for Cell Barrier Layer Applications

Rachel Li¹, Jainil Sutaria², Chelsea Wang³, Clement Marmorat⁴, Adriana Pinkas-Sarafova⁴, Miriam Rafailovich⁴
¹Spackenkill High School, New York, NY 12603, ²Ardley High School, Ardsley, NY 10502, ³Fossil Ridge High School, Fort Collins, CO 80528, ⁴Department of Materials Science and Engineering, Stony Brook University, Stony Brook, NY 11794

Hydrogels are three-dimensional hydrophilic polymeric networks composed of natural or synthetic polymer chains. They are biocompatible and can be engineered to mimic the characteristics of naturally occurring gels. Hydrogels show promising biomedical applications as they provide separation of bio-layers, essential to prevention of scar tissue for post-operative recovery. Gelatin is a natural biopolymer derived from collagen. While commercially widespread and low cost, gelatin possesses poor mechanical strength and a high dissolution rate in physiological conditions^[1]. Pluronic® F127 is an amphiphilic, tri-block copolymer composed of PEO₉₉-PPO₆₇-PEO₉₉ chains^[2]. F127 has been widely explored for biomedical applications due to its unique self-assembling micellar structure and biocompatibility. In this study, gelatin-F127 hybrid hydrogels were synthesized to optimize mechanical properties and biocompatibility.

Hybrid gels were synthesized by mixing 10% w/v gelatin with 0%, 5%, 15%, and 20% w/v F127. Microbial transglutaminase (mTG) was added to crosslink the gelatin. Gel solutions were plated and incubated for 12 hours at 37°C. Rheological analysis revealed that the addition of F127 polymer chains in the gelatin matrix significantly increased the elastic modulus from 2.31 kPa for pure gelatin to 11.0 kPa for the 20% F127 hybrid, improving mechanical strength (Figure 1). To determine the stability of the hybrid hydrogels, elastic modulus was measured following a 2 hour swelling procedure with deionized (DI) water. No significant change in elastic modulus was observed before and after swelling (Figure 1), suggesting that F127 polymer chains remained entrapped within the gelatin mesh network through physical or chemical interactions.

To further characterize structural interactions between F127 polymer chains and the gelatin mesh network, DI water was used to swell hybrid gels with varying mesh sizes composed of either 7.5% or 15% w/v gelatin and 20% w/v F127 at 30 minute intervals. Gel thickness at each interval was measured, indicating that the 7.5% w/v gelatin hybrids contracted to approximately half the thickness of the 15% w/v gelatin hybrids after two swelling intervals (Figure 2). This suggests that the gelatin mesh network, independent of the initial mesh size, equilibrates to a constant mesh size with the lowest enthalpy. UV-Vis spectrometry performed on excess liquid collected at each interval showed a higher rate of F127 diffusion out of gels with lower gelatin concentration (7.5% w/v) compared to gels with higher gelatin concentration (15% w/v) (Figure 3).

To analyze gel degradation in physiological conditions, sterile gels were swelled with DI water, PBS, and DMEM. No significant change was observed in the elastic modulus of the gels swelled with different solutions, demonstrating the stability of the gels in physiological conditions. Human dermal fibroblast (HDF) cells were plated onto gelatin control gels and hybrid gels. Cell attachment was assessed using optical microscopy. After 7 days of culture, cells attached and proliferated on the gelatin control gel, while no cells were present on the hybrid hydrogels (Figure 4). The inability of HDF cells to attach on the hybrid gels suggests that gelatin-F127 hybrid hydrogels possess promising characteristics to serve as viable cell barrier layers.

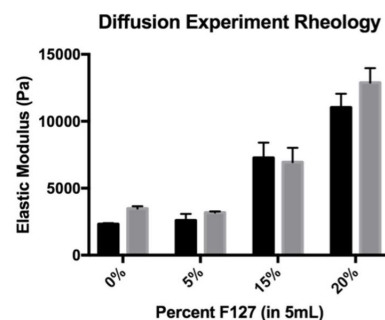


Figure 1: Rheological analysis of hybrid gels

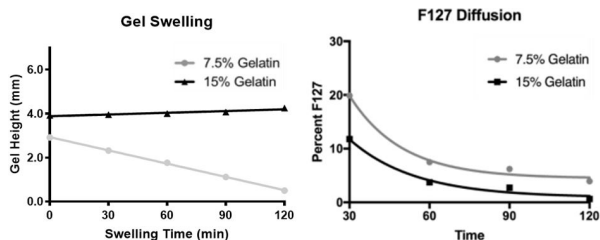


Figure 2: Gel swelling and contraction

Figure 3: F127 diffusion out of hybrid gels

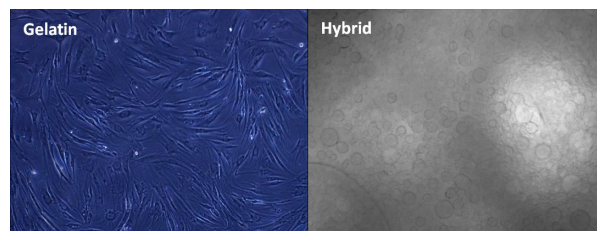


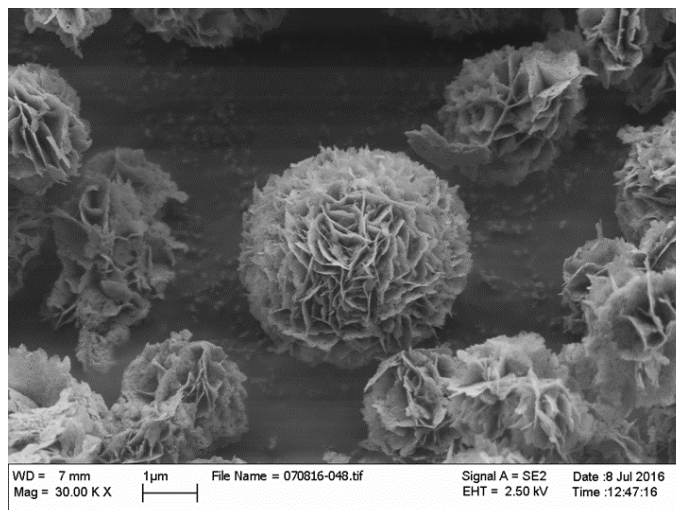
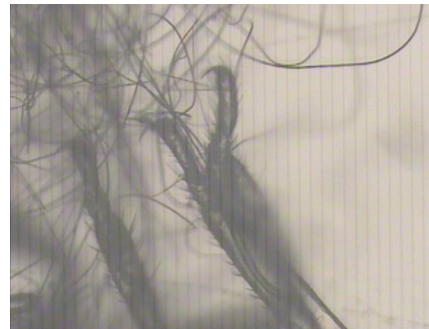
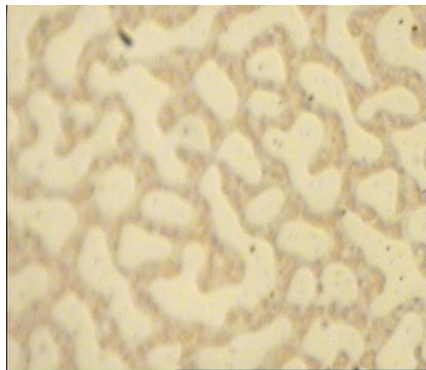
Figure 4: Cell attachment on gelatin and hybrid after 7 days of culture

[1] Tatini, D., et al. (2015). Pluronic/gelatin composites for controlled release of actives. *Colloids and Surfaces B: Biointerfaces*, 135, 400-407. doi:10.1016/j.colsurfb.2015.08.002

[2] Bhatnagar, D., et al. (2013). Rheological Characterization of Novel HA-Pluronic Thermoreversible Hydrogels. *Journal of Chemical and Biological Interfaces*, 1(2), 93-99. doi:10.1166/jcibi.2013.1015

Session VI: Sensors and Detectors

**Mentors: Vincent Ricotta, Fan Yang ,
John Luckner Jerome, Stephen Walker,
Michael Vaccariello**



Developing a Prototype Home Automation System Using Arduino Microcontrollers

Taylor Pedley¹, Indeeep Singh², Vincent Ricotta³, Miriam Rafailovich³

¹Smithtown High School East, Saint James, NY;

²Stony Brook University Department of Mechanical Engineering, Stony Brook, NY;

³Stony Brook University Department of Materials Science and Engineering, Stony Brook, NY

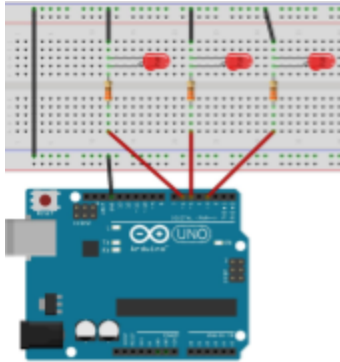


Figure 1: Three LEDs are connected to digital ports 3, 5, and 6. Diagram made with Fritzig.

Dr. Brooke Ellison, a Director of Ethics and Education at Stony Brook University, is paralyzed from the neck down as a result of a car crash she endured at 11 years old. For her and other people with quadraplegia, home automation is more than a convenience, it is a means to gain independence. She currently uses a Tongue Activated Communications Controller, a 9-button remote worn in the mouth like a retainer¹, to operate her wheelchair. The focus of this project was to integrate a joystick into this existing technology, thus allowing her greater control of appliances, namely lights, in her household via Bluetooth.

An Arduino Uno R3, a low-cost computer board that can process simple inputs and outputs, was the base of this project. Arduino and other open-source electronics companies develop specialized boards, called “shields,” to expand the Uno’s capabilities¹. The Uno was programmed in C++ using the Arduino IDE. A breadboard, 22 gauge wire, LEDs, and 330Ω resistors were used to create the circuit that the Uno would control.

The complete, 3-LED circuit used for all tests is shown in Figure 1.

The Uno was first interfaced with a Seeedstudio Bluetooth Shield, allowing it to communicate with a Bluetooth SPP, an application available to most iOS and Android devices. The user could then send numbers to the board via a bluetooth serial. One program responded to 1, 2, or 3, and would turn one of the three LEDs on or off when its respective number was entered. Another responded to numbers 1 through 9, and could adjust a single LED to 9 different levels of brightness. However, in order for quadraplegics to operate the system, devices that can be operated with a tongue, such as a button or joystick, must be connected to it.²

The first joystick programmed was on a PS3 remote with built in bluetooth capabilities. The PS3 remote was not compatible with the Bluetooth Shield connected to the phone, so instead, an Arduino USB Host Shield and CosTech Bluetooth Dongle were used to connect the Uno and remote wirelessly. Software was designed that could turn an LED on when its respective button was clicked. Then, the user could manipulate the joystick to gradually increase or decrease its brightness. In this system, over 200 brightness levels could be selected, as opposed to the 9 available when using a phone. Though less complex than operating a phone, the video game remote was designed for hands, so it is too big to be used within the mouth.

A device the size of the tip of a finger was used next. By utilizing all three of Papilio Platform Micro-Joystick Wing’s axes, a complete lighting system could be operated. Pushing it left and right changed which LED was selected. Clicking it like a button turned the currently selected light on or off, and pushing it up and down gradually brightened or dimmed the selected LED. Unlike the phone and PS3 remote, the joystick is not a bluetooth device, so in the future, a board that includes both the joystick and a bluetooth antenna will be designed.

¹ Fortune, Daniel, et al. *Tongue Activated Communications Controller*. 15 Apr. 1993.

² Badamasi, Yusuf Abdullahi. “The Working Principle of an Arduino.” *2014 11th International Conference on Electronics, Computer and Computation (ICECCO)*, 2014.

Utilizing Natural Patterns from Polymer Blend Phase Separation with Argon Etching to Create Gold Patterned Silicon Wafers

Daniel Seligson¹ Emily Wang² Savannah Lo³ Maira Khan⁴ John Jerome⁵ Miriam Rafailovich⁶

¹Ramaz Upper School, New York, NY 10075 ²The Wheatley School, Old Westbury, NY 11568 ³South Side High School, Rockville Centre, NY 11570 ⁴Harvard University, Cambridge, MA 02138 ⁵Suffolk Community College, Selden, NY 11784

⁶Stony Brook University Department of Materials Science & Engineering, Stony Brook, NY 11794

The phase separation that occurs when two insoluble solutions are combined often allows for the mixed solution to retain the properties of the individual polymers. In addition to altering the chemical properties of the solution, when the the solution is used as a coating, the coating can demonstrate different surface morphologies that can be useful in the fields of electronics and biotechnology¹. This technique of phase separation was used as a template to create gold nanopatterns on silicon wafers.

Current methods of creating gold nanopatterns on silicon wafers utilize costly techniques such as electron beam lithography and focused ion beam². The use of phase separation combined with Argon etching offers a more cost efficient method of producing patterned silicon chips.

In this experiment, polymer blend solutions of ethylene vinyl acetate (EVA), Polymethyl methacrylate (PMMA), Polystyrene (PS), PBrS, and monodispersed PMMA were created in toluene. These two-polymer blend solutions were then spin casted onto silicon wafers with a 50 nanometer thick gold coating. After annealing the samples at 24 hours, 48 hours and 72 hours, it was found that combinations of EVA and PMMA, EVA and PS, EVA and PBrS, and PMMA(md) and PBrS showed the clearest phase separations between the two solutions when viewed under an optical microscope (figure 1) and an atomic force microscope (AFM).

To etch the surfaces of the coated wafers, a low power argon beam was used to remove the polymer coatings. Based on comparisons made between the before and after etching AFM and optical microscope pictures, it was shown that the gold around the bumps (which resulted from the phase separation) was noticeably reduced.

Future studies utilizing these different gold patterned silicon wafers include examining their electrical conductivity and using the wafers as a scaffold to examine stem cell proliferation.

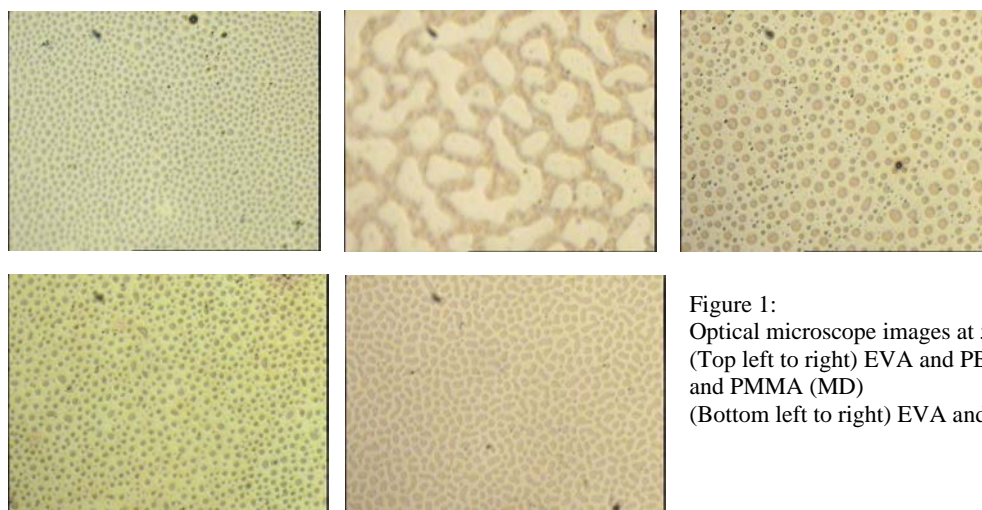


Figure 1:
Optical microscope images at 50X of:
(Top left to right) EVA and PBrS; EVA and PMMA; EVA and PMMA (MD)
(Bottom left to right) EVA and PS; PMMA (MD) and PBrS

¹ Xue, L., Jilin Zhang, & Han, Y. (n.d.). *Phase separation induced ordered patterns in thin polymer blend films*. Retrieved from <http://www.sciencedirect.com/science/article/pii/S0079670011001067>

² Mendes, P. M., Jacke, S., Critchley, K., Plaza, J., Chen, Y., Nikitin, K., . . . Fitzmaurice, D. (n.d.). *Gold Nanoparticle Patterning of Silicon Wafers Using Chemical e-Beam Lithography*. Retrieved from http://myukk.org/SM2017/sm_pdf/SM844.pdf

Properties of Bismuth Oxyhalides when Exposed to Light¹

Daniel Seligson¹ Emily Wang² Savannah Lo³ Nathan Sandler⁴ Maira Khan⁵ John Jerome⁶ Miriam Rafailovich⁷

¹Ramaz Upper School, New York, NY 10075 ²The Wheatley School, Old Westbury, NY 11568 ³South Side High School, Rockville Centre, NY 11570 ⁴Tufts University, Medford, MA 02155 ⁵Harvard University, Cambridge, MA 02138 ⁶Suffolk Community College, Selden, NY 11784 ⁷Stony Brook University Department of Materials Science & Engineering, Stony Brook, NY 11794 ⁸Department of Oral Biology and Pathology, School of Dental Medicine, Stony Brook, NY

Current solar cell technologies are limited by the accumulation of dust, hindering light penetration and decreasing its efficiency, thus creating the need for a self cleaning solar cell that would not only increase its longevity but improve its overall performance as well. Such a cell would need a coating with anti-bacterial and hydrophobic properties.

Bismuth oxyhalide particles, which were found to release hydroxide that break down organic matter¹ and kill bacteria² when exposed to sunlight, were chosen to be the active ingredient in the coating. Four types of Bismuth oxychloride particles which differed by chloride count, doping, and the inclusion of bromine, were tested to see their effects on gram positive and gram negative strains of bacteria.

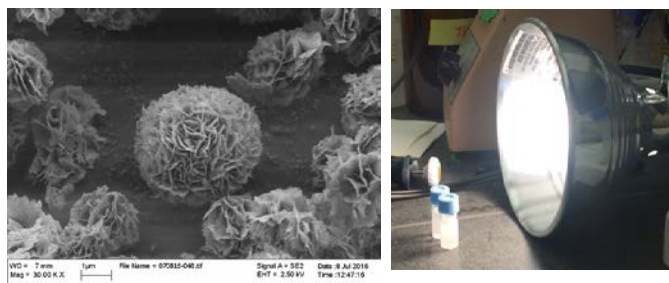


Figure 1: (left) SEM image of Bismuth Oxyhalide Particle; $\text{BiOCl}_{0.80}\text{Br}_{0.20}$ (2895.8 ± 887.2 nm); scale bar is one micron. (right) Exposure procedure: The two experimental vials were exposed to the plant light for 20 minutes, being shaken every 2 min to keep the particles from settling on the bottom

Various solutions with differing concentrations were initially made with bismuth oxyhalide suspended in either deionized water or phosphate buffered saline (PBS). Bismuth oxychloride with bromine was suspended in deionized H_2O and was added to *Staphylococcus aureus* and *Klebsiella pneumonia* suspended in phosphate buffered saline (PBS). Experimental vials of the bacteria were exposed to an 80 watt blue, plant light (fig.1) while control vials were wrapped in aluminum foil. The bacteria were plated on

petri dishes and incubated overnight. The number of bacteria colonies found on the dishes, though being significantly lower than expected, were similar among all of the samples. Future experiments can be done using different light sources for different lengths of time, different variations of the bismuth oxyhalide particles, and different concentrations of the particle.

¹ Hani Gnayem, Vladimir Uvarov, Ofer Lahad and Yoel Sasson. *Hybrid bismuth oxyhalides@gypsum as selfcleaning composites: novel aspects of a sustainable photocatalytic technology for solar environmental cleanup*. RSC Adv., 2015, 5, 66650

² Ilana Sherman, Yoram Gerchman, Yoel Sasson, Hani Gnayem and Hadas Mamane. *Disinfection and Mechanistic Insights of Escherichia coli in Water by Bismuth Oxyhalide Photocatalysis*. Photochemistry and Photobiology, 2016, 92: 826–834

Examining the Digestion of Polystyrene by *Tenebrio molitor*

John Pennisi¹, Harry Shan He², Michael Vaccariello³, Miriam Rafailovich²

¹South Side High School, Rockville Centre, NY 11570

²Department of Materials and Science and Chemical Engineering Stony Brook University, Stony Brook, NY 11794

³Sachem High School East, Farmingdale, NY 11738

Polystyrene (PS) is a leading global contaminant affecting our ecosystems and the health of planet. The stiff and durable configuration of PS make it extremely resilient to biodegradation. An estimated 8 metric tons of plastic end up in the oceans every year¹. The larvae of *Tenebrio molitor*, commonly known as mealworms, have been cited as being able to digest polystyrene using the microorganisms in their digestive tracks². This concept could potentially be used as an agent to recycle these materials back into the environment. The focus of this study was to identify the metabolites produced by mealworms after digesting polystyrene foam. Three trials of mealworms were made, each trial contained three groups as shown in Fig. 1. Mealworms were fed various food sources such as bran (control), polystyrene foam, aluminum foil, and polyurethane. Every other day the mealworms were rotated between their respective feeding dish and an empty waste collection dish. During the experiment the weights of the mealworms and food source were recorded Fig. 1. Over the course of the experiment waste was slowly accumulated and collected to be used for the testing. The waste was then put under Fourier transform infrared spectroscopy and X-ray fluorescence to determine its composition and toxicity. The purpose of this study is to determine if mealworms would be a feasible solution for this environmental crisis. If the waste products produced by the mealworms are less harmful to the environment then, the microorganisms responsible for the digestion could be harnessed in mass quantities and used to aid in removing pollution.

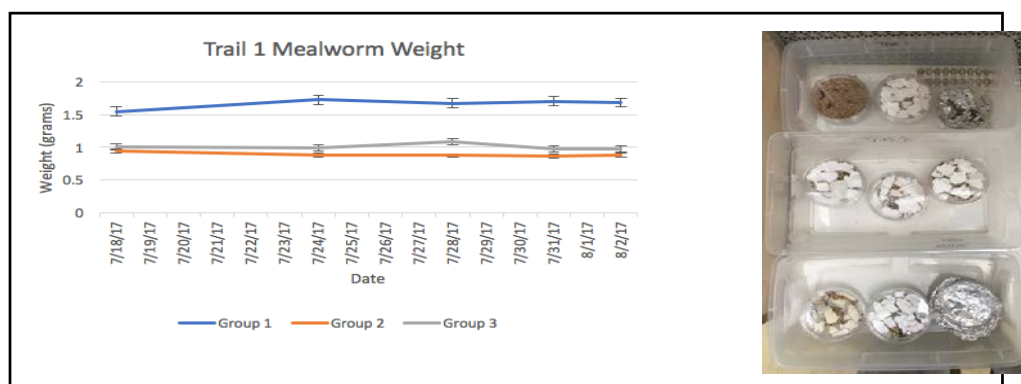


Figure 1: Left: fluctuating weight of mealworms over the course of 15 days

¹Sifferlin, Alexandra. "Here's How Much Plastic Ends Up In the World's Oceans." *Time*. Time, 12 Feb. 2015. Web. 04 Aug. 2017.

²Yang, Yu, Jun Yang, Wei-Min Wu, Jiao Zhao, Yiling Song, Longcheng Gao, Ruifu Yang, and Lei Jiang. "Biodegradation and Mineralization of Polystyrene by Plastic-Eating Mealworms: Part 1. Chemical and Physical Characterization and Isotopic Tests." *Environmental Science & Technology* 49.20 (2015): 12080-2086. *Environmental Science & Technology*. Web. 4 Aug. 2017.

Optimizing and Testing the Specificity and Accuracy of a Bio Sensor by Finding the Saturation Concentration of Thiols

Neil Appel, Rambam Mesivta, Lawrence, NY, 11559

Vincent Ricotta and Miriam Rafailovich, Dept. of Materials Science and Chemical Engineering, Stony Brook University, Stony Brook, NY, 11794

With the Zika endemic on the rise, there is an increased demand for more efficient ways of detecting the virus, because of the similarity of its symptoms to the common flu and the dengue virus. Although there are other methods of detecting Zika besides for bio sensing, bio sensors provide the fastest results. Therefore, optimizing this method would be the most beneficial.

To create a bio sensor, you must coat a silicon wafer in 50 nm thick gold film, cut the wafer into strips with dimensions of 0.8 by 2 cm, rinse with absolute ethanol followed by DI water, punch a 0.6 cm diameter hole into a strip of Teflon tape, cover the sensor but leave the space where you punched a hole and a thin strip of gold on top exposed.

To find the saturation concentration you must use titration along with process of elimination to narrow down the possible concentrations. First test the bare Au as a control, then imprint with 0.1, 1.0, 10, and 100 μM concentration solutions and then test the saturation using CV (cyclic voltammetry) using a potentiostat. After conducting these experiments, we concluded that the saturation concentration must be between 1 and 10 μM . Then we tested a concentration of 5 μM and deduced that the concentration has to be between 5 and 10 μM . And finally, we tested concentrations of 8 and 9 μM and finalized the saturation concentration to be between 9 and 10 μM . We didn't narrow this data down any further because it would make a negligible difference if we got a more specific measurement.

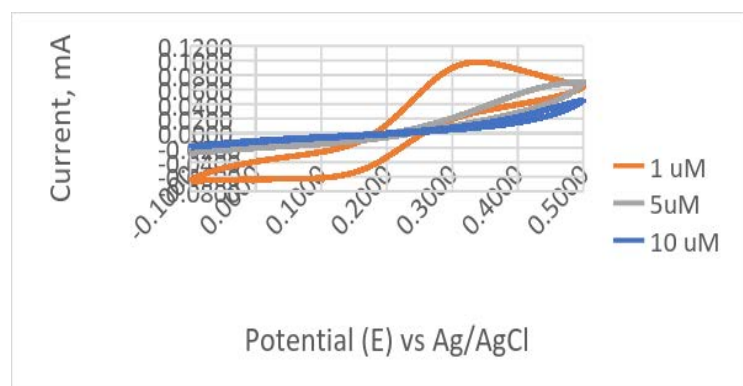


Figure 1. Cyclic Voltammograms of AuSi sensors : CV of bare Au vs sensors with concentrations of 0.1, 1.0, 10, and 100 μM solutions of thiols.

1. Y. Yu, Q. Zhang, C. Chang, Y. Liu, Z. Yang, Y. Gao, Y. Wang, D. Galanakis, K. Levon and M. H. Rafailovitch, Analyst 2016, DOI: 10.1039/C6AN01157H. 2. Mathur A, Blais S, Goparaju CMV, Neubert T, Pass H, et al. (2013) Development of a Biosensor for detection Detection of Pleural Mesothelioma Cancer Biomarker Using Surface Imprinting. PLoS ONE 8(3): e57681. doi:10.1371/journal.pone.0057681

2. Mathur A, Blais S, Goparaju CMV, Neubert T, Pass H, et al. (2013) Development of a Biosensor for detection Detection of Pleural Mesothelioma Cancer Biomarker Using Surface Imprinting. PLoS ONE 8(3): e57681. doi:10.1371/journal.pone.0057681

Engineering electrospun microfibers capable of trapping termites

Julia Pandolfo¹, Michael Vaccariello², Harry Shan He³, Miriam Rafailovich³

¹South Side High School, Rockville Centre, NY

²Sachem High School East, Farmingville, NY

³Department of Material Science & Chemical Engineering, Stony Brook University, Stony Brook NY

It is estimated that over 600,000 homes in the United States become infested with termites each year. Many of these homes become subject to fumigation, a process that releases chemicals into the home that are often harmful to both human and environmental health¹. The goal of our research is to create an effective, environmentally safe, and toxin-free method of trapping and killing termites. We achieved this by using the electrospinning process to create microfibers from recycled polystyrene (PS), a non-biodegradable polymer found in Styrofoam products. We worked in cooperation with FiberTrap, a company that had originally manufactured similar microfibers intended to trap bedbugs.

Electrospinning is the process of creating thin fibers using charged polymers sprayed onto a collecting plate. The electrospinning apparatus, composed of a high voltage power supply, a container for fluid storage, and an electrode collector, uses a strong electrical field to draw polymer fluid into fine filaments². To begin this process, we created a 15% PS solution of high viscosity by allowing .75 mg of a Styrofoam DART coffee cup to dissolve in 2.5 mL of tetrahydrofuran (THF) and 2.5 mL of dimethylformamide (DMF) overnight. The electrospinning of the solution resulted in three groups of microfibers, which were subsequently used in experimentation.

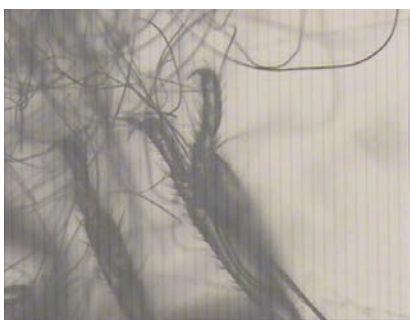


Figure 1. Termite leg, approximately 15 μm , caught in microfibers.

For the fibers to be effective, their diameter must equal the distance between the setae (bristles) on the insect's leg. As the insect struggles inside the fibers, it becomes further trapped (Fig. 1). We ran two trials, each involving three groups of ten termites. In the first trial,

the termites in Group 1 were used as a control group. Group 2 termites were placed on top of the microfibers in a petri dish containing moist wood. Group 3 termites were placed adjacent to the microfibers in a petri dish containing moist wood. While initially observing the three groups, we saw that termites interacting with the fibers had become trapped. We left the experiments untouched for twenty-four hours, and discovered the following morning that many of the termites had been able to escape the fibers. We repeated the experiment, removing the moist wood from the petri dishes containing the fibers. In twenty-four hours, we had a 100% success rate in trapping and killing all of the termites in Groups 2 and 3. We concluded that a dry environment is needed to ensure that the fibers retain their shape and effectiveness.

The next problem identified was that of drawing the termites away from their food source and into the microfiber traps. The chemical 2-phenoxyethanol, commonly used as a drying agent in ballpoint pens, was identified as a pheromone mimic³. In future studies later this summer, we plan to test microfiber traps incorporating small volumes of the chemical in order to give the termites a motive for interacting with the fibers.

¹ "Termite Statistics." *Termites.com*, Orkin, www.termines.com/information/statistics/.

² Fang, Jian, Xungai Wang, and Tong Li. "Functional Applications of Electrospun Nanofibers." *Nanofibers - Production, Properties and Functional Applications* (2011): n. pag. Web. 19 July 2017.

³ National Center for Biotechnology Information. PubChem Compound Datatbase; CID=31236, <https://pubchem.ncbi.nlm.nih.gov/compound/31236> (accessed Aug. 6, 2017).

Kasim Wagar, Nether Sandler, Alpha Chen, Oliver Xu, Margaret Sui, Brandon Weiss, Richard Zhu, Luke, Lisa, Mia Pandoro, Alex Wang, Aaron Singer, Grace, Savannah Lo, Siobhan Milan, Chelsea Wang, Sabrina, Albert, Neil Appel, Jan Hsu, Roshan Reddy, Andy Wang, Helen Zhang, Konstantina Angara, Karena Etwaru, Nichol Williams, yingyue Liu (maggie), Rishi Patel, Zffy Tang, Paul, Jaimil, Anthe, Phil, Prist, Emily Ma, Taylor, Moira, Leela, Eunice Yang, Muzee, Dane, Zffy Tang, Paul, Jaimil, Anthe, Phil, Prist, GEMMA SCHNEIDER, Vedant Singh, MAX PORTER, Helen Zhang, Konstantina Angara, Karena Etwaru, Nichol Williams, yingyue Liu (maggie), Rishi Patel, Zffy Tang, Paul, Jaimil, Anthe, Phil, Prist, CAROLYN WONG

The Garcia Research Program students and staff gratefully acknowledge the support of The National Science Foundation and the Morin Foundation Trust